The Bis-Salphen Zn(II) Unit: A Versatile Building Block for Self-Assembled Heteroleptic Coordination Cages

Leonardo Donaggio, Kristian Schweimer, Frank W. Heinemann, Janosch Hennig, Hannah Kurz*

Contents

1. General information

Solvents and chemicals: Unless otherwise specified, all starting materials, reagents and solvents were used as supplied and without further purification (TCI Pharmaceutical Standards, BLDpharm, Fisher Scientific, Sigma Aldrich).

NMR spectroscopy: Room-temperature (^{1}H, HMBC, ^{13}C, J-mod, ^{1}H-^{1}H-COSY) NMR spectra were recorded with a 500 MHz Avance III HD NMR spectrometer from Bruker. Diffusion-ordered spectroscopy (DOSY) experiments to obtain translational diffusion coefficients were performed on a 600 MHz Avance II+ Bruker spectrometer. HSQC experiments were performed on a 300 MHz Avance Bruker spectrometer. Gradient strength was calibrated using a doped water sample (2 mM $CuSO_4$, 1 % H_2O in D_2O) assuming a diffusion coefficient of $1.90 \cdot 10^{-9}$ m^2/s at a calibrated temperature of 298 K using either a 1D ^{1}H pulse gradient stimulated echo with bipolar gradients[1] or a double stimulated echo for convection compensation[2]. The integrated signal intensity was observed as a function of increased gradient strength, and analysed according to $S(Q) = S(0) * \exp\{-\Delta Q\}$ with $Q = \gamma^2 g^2 \delta^2 (\Delta - \delta/3 - \tau/2)$ (γ = gyromagnetic ratio, g = gradient strength, δ = gradient pulse length, Δ = diffusion delay, τ = gradient recovery delay[3].

Chemical shifts (δ) are given in parts per million (ppm) from low to high field and referenced using the residual solvent signal (^{1}H, ^{13}C). The multiplicity is given using the following abbreviations: singlet (s), doublet (d), broad (br). Coupling constants (J) are reported in Hertz (Hz).

Elemental analysis: CHN analyses were measured with an Unicube from Elementar Analysen Systeme. The samples were prepared in a tin boat, sulfanilamide was used as standard and the samples measured at least twice. The values were given as an average of the two measurements.

Mass spectrometry: Low-resolution electrospray time-of-flight (ESI-TOF) mass spectra of the complexes were obtained from a Waters Micromass LCT Premier mass spectrometer. High-resolution electrospray measurements of the cages were performed on an ESI-TOF MicroTOF II spectrometer from Bruker. Signals were reported in m/z units.

Single crystal X-ray diffraction: The single crystal X-ray structure determination of cage **1** was performed at 100 K using Mo*K*α radiation (λ = 0.71073 Å). Data was collected on a Bruker Kappa IμS Duo PHOTON2 diffractometer equipped with QUAZAR focusing Montel optics. The absorption correction was performed based on multiple scans using SADABS2016/2 (Bruker. SADABS; Bruker AXS Inc., 2016/2). The structures were solved by direct methods using SHELX XT 2014/5[4] and refined on F^2 by full-matrix least-squares techniques using SHELXL 2019/3.[5] Molecular structures were represented using Mercury 2022.2.0. All non-hydrogen atoms were refined with anisotropic displacement parameters. Hydrogen atoms were placed in positions calculated for optimized geometry, their isotropic displacement parameters were tied to those of the corresponding carrier atoms by a factor of either 1.2 or 1.5.

UV-vis spectroscopy: Absorbance spectra were obtained using an Agilent UV-Vis spectrophotometer Cary 60 (Agilent Technologies, USA) operating in a spectral range of 190–1100 nm. All spectra were conducted in quartz cells with 1 cm lightpath (Hellma, Germany).

Photoluminescence spectroscopy: Measurements were conducted on a FluoTime 300 spectrometer from PicoQuant using the software EasyTau2. A 300 W Xe lamp was used for the emission and excitation experiments. Quantum yields were determined at room temperature using a 78mm integrating sphere and a 300 W Xe lamp as excitation source. The emission data was corrected against the absorbance at the respective excitation wavelength. Please note that the fluorescence excitation spectra were corrected against the intensity of the powerdiode to correct against lamp intensity fluctuations at the respective wavelength. Time correlated single photon counting (TCSPC) spectra were performed using a 355 nm laser (VisUV, PicoQuant).

2. Synthesis and characterization

2.1. Synthesis of bis-Zn(II)-salphen complex Zn_2L

Bis-Zn(II)-salphen complex **Zn_2L** was synthesized *via* a modified literature procedure[6]. 1,2,4,5-benzenetetramine tetrahydrochloride (200 mg, 0.678 mmol, 1 eq) and 3,5-di-*tert*-butylsalicylaldehyde (723 mg, 4.07 mmol, 6.0 eq) were stirred in 30 mL MeOH at room temperature for 18 h. The reaction yielded a yellow-orange precipitate that was collected by filtration and washed with 5 mL MeOH. The obtained solid was resuspended in 30 mL MeOH and $Zn(OAc)_2 \cdot 2H_2O$ (828 mg, 3.77 mmol, 5.5 eq) were added. The reaction mixture was stirred at room temperature for 18 h. Red precipitate was collected on a frit filter and washed with 5 mL MeOH and dried *in vacuo* (yield over two steps: 80%).

^{1}H-NMR (500 MHz, $(CD_3)_2CO$, 298 K): δ = 9.22 (s, 2H), 8.47 (s, 1H), 7.44 (d, 2H, ^4J = 2.6 Hz), 7.17 (d, 2H, ^4J = 2.6 Hz), 1.55 (s, 18H), 1.34 (s, 18H). **^{13}C-NMR** (126 MHz, $(CD_3)_2CO$, 298 K): δ = 172.36, 163.10, 142.50, 139.77, 130.03, 129.91, 119.48, 103.22, 36.32, 34.43, 31.83, 30.20. Elemental analysis calculated (%) for $C_{66}H_{94}N_4O_6Zn_2$ ($[Zn_2L(H_2O)_4]$) C 65.94, H 7.88, N 4.66; found C 65.79, H 7.46, N 4.38. MS (**LR-ESI-TOF**) m/z for $[M+Na^+]$ 1151.5.

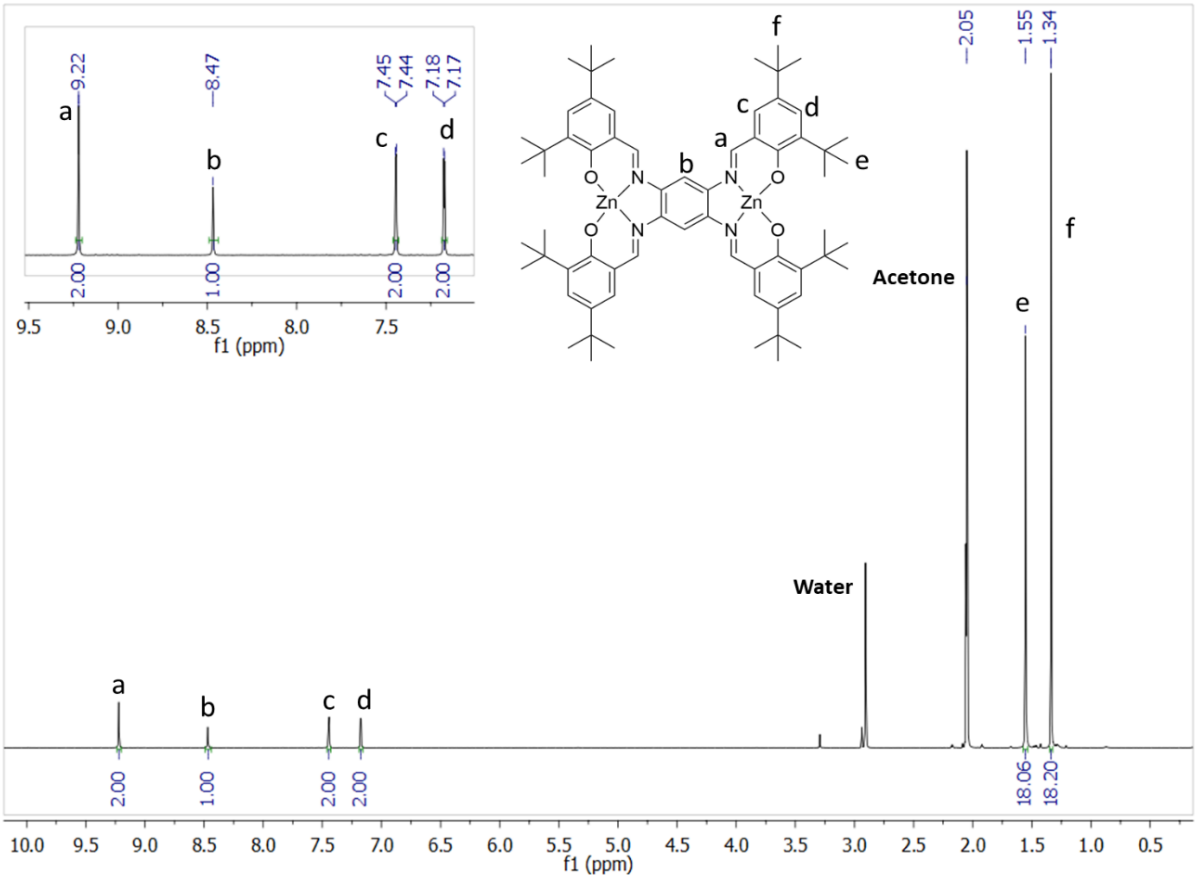

*Figure S1: ^{1}H NMR spectrum of **Zn_2L** (500 MHz, $(CD_3)_2CO$, 298 K).*

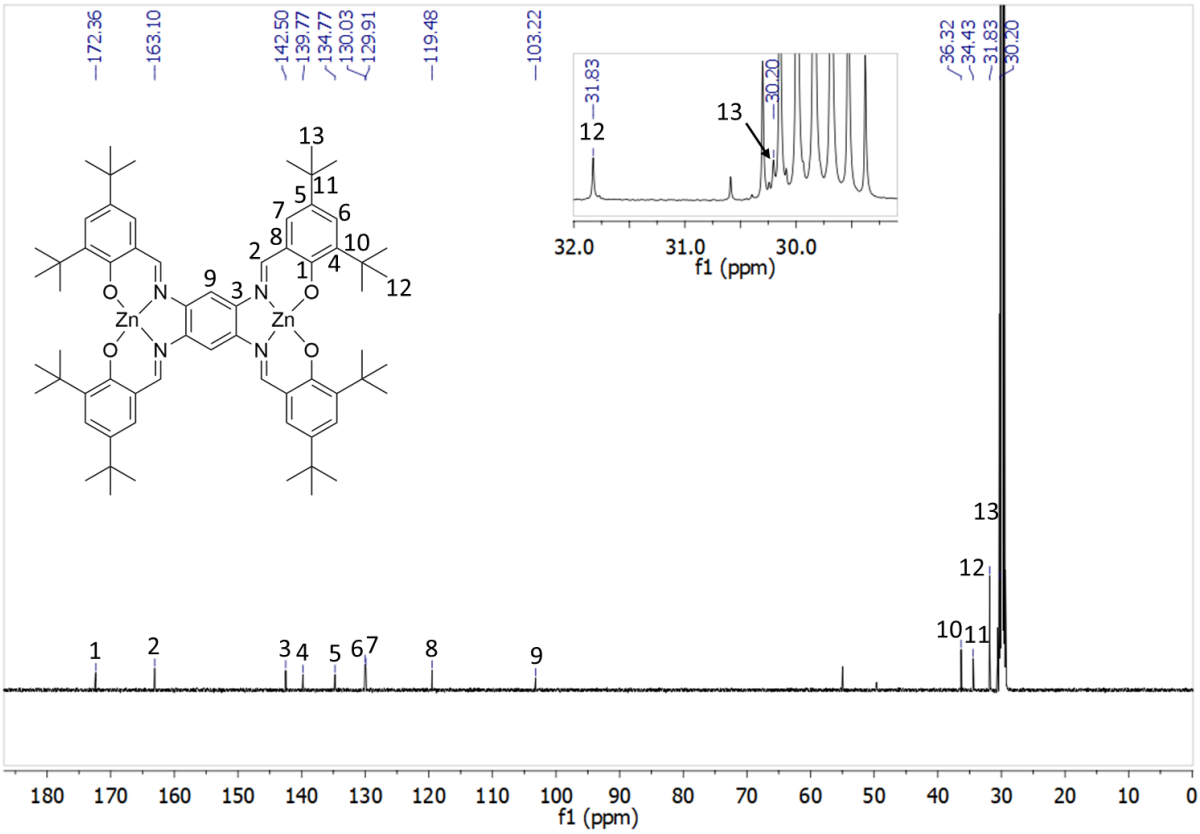

*Figure S2: ^{13}C NMR spectrum of **Zn_2L** (500 MHz, $CO(CD_3)_2$, 298 K).*

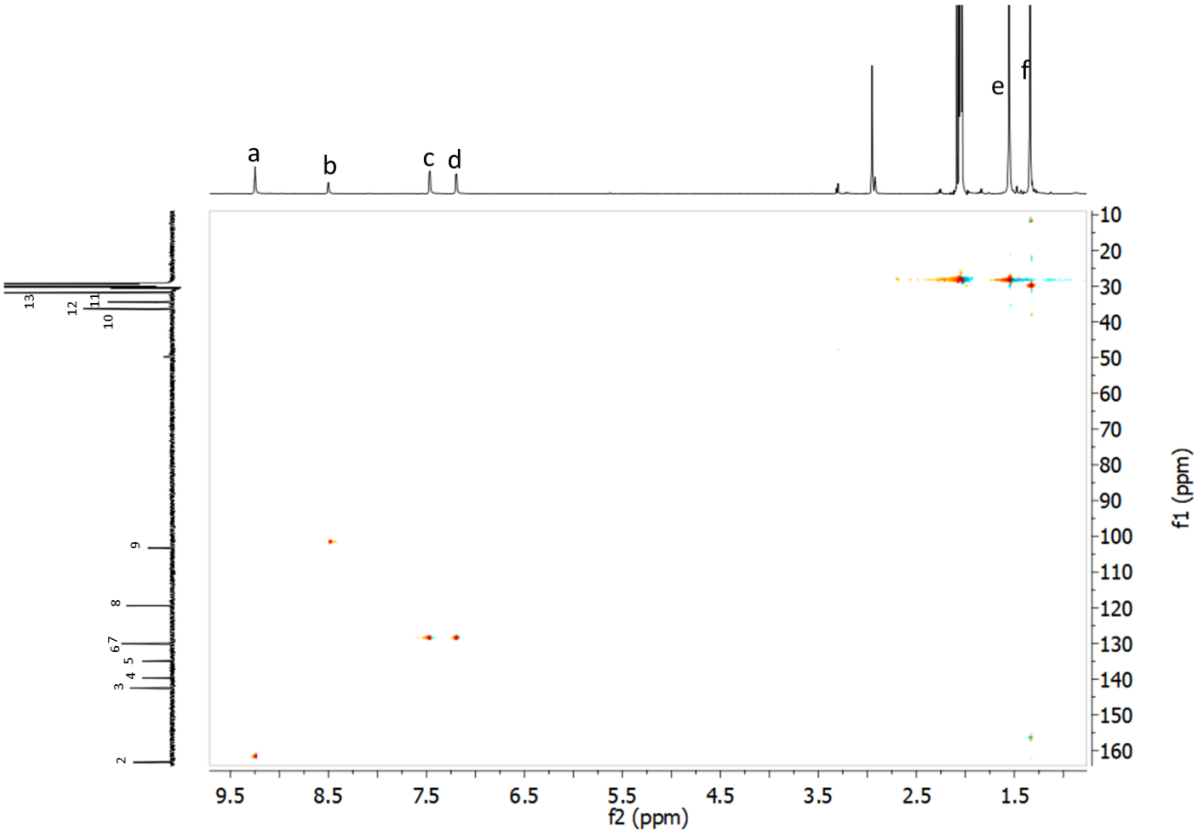

*Figure S3: ^{1}H-^{13}C HSQC NMR spectrum of **Zn_2L** (300 MHz, $CO(CD_3)_2$, 298 K).*

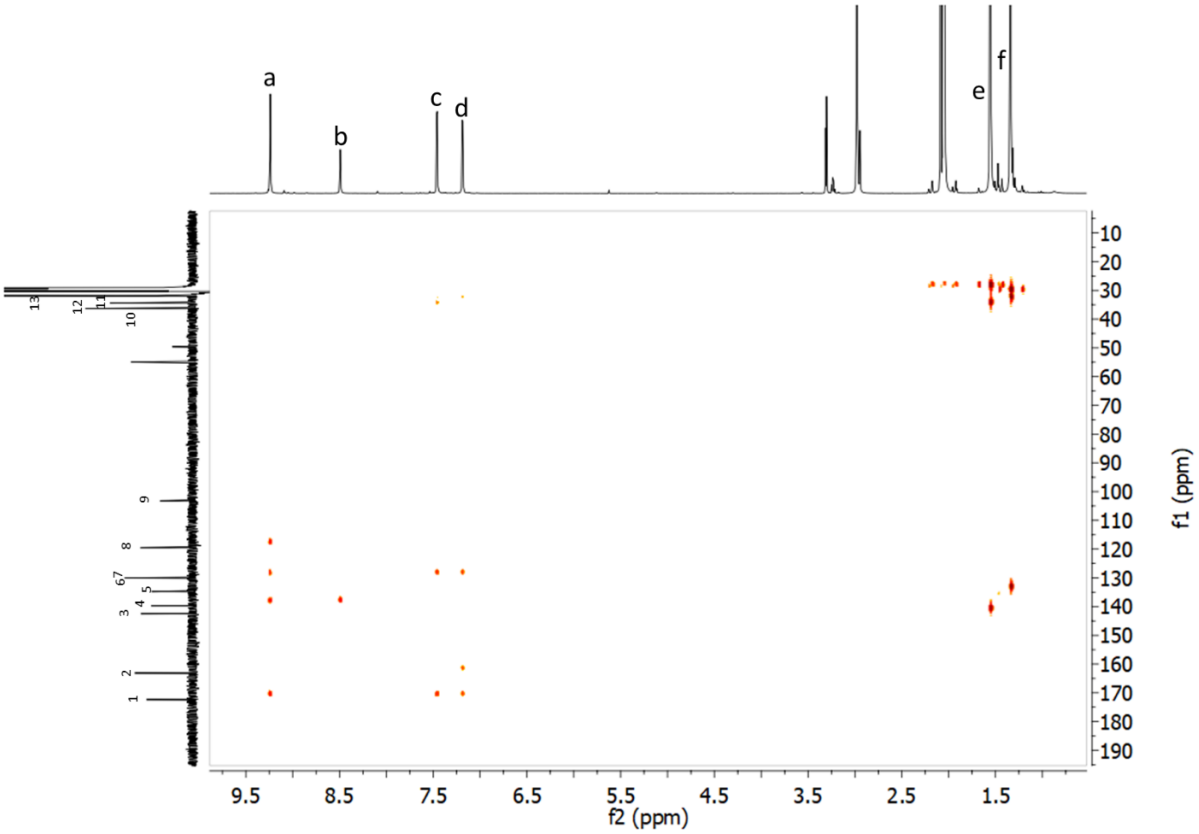

*Figure S4: ^{1}H-^{13}C HMBC NMR spectra of **Zn_2L** (500 MHz, $CO(CD_3)_2$, 298 K).*

2.2. Self-assembly of cage 1

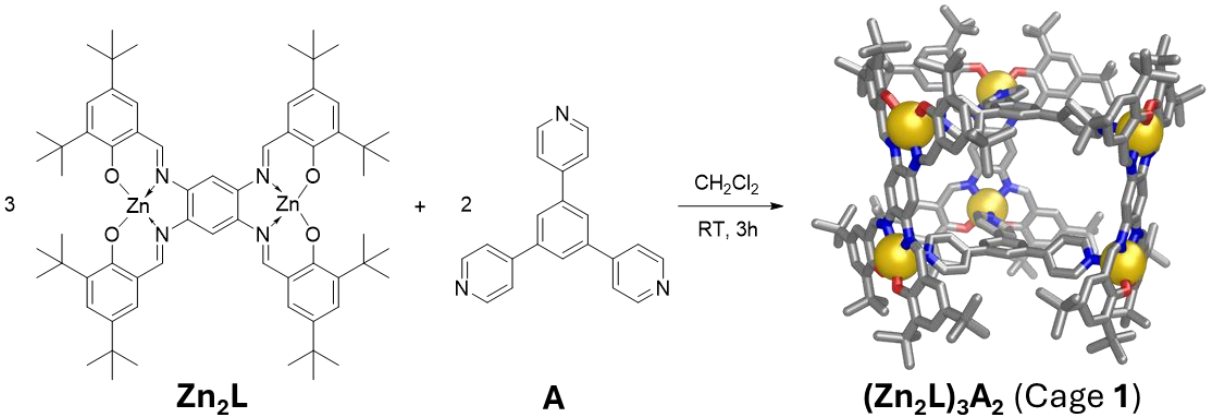

Zn_2L (16.4 mg, 14.6 µmol, 3.0 eq) and tris(4-pyridyl)-1,3,5-benzene **A** (3.0 mg, 9.7 µmol, 2.0 eq) were dissolved in 0.5 mL of DCM-d_2 and stirred for 3 h. Solvent was removed with rotary evaporation yielding cage **1** as an emissive bright red solid (19.4 mg, 4.8 µmol, MW = 4009.21 g/mol, yield = 100%).

^{1}H-NMR (500 MHz, CD_2Cl_2, 298 K): δ = 8.91 (s, 2H, a^1), 8.32 (d, ^{3}J = 4.9 Hz, 2H, b^1), 7.80 (s, 1H, c^1), 7.59 (s, 1H, d^1), 7.43 (d, ^{4}J = 2.5 Hz, 2H, e^1), 7.33 (d, ^{3}J = 5.3 Hz, 2H, f^1). 7.19 (d, ^{4}J = 2.5 Hz, 2H, g^1), 1.44 (s, 18H, h^1), 1.35 (s, 18H, i^1). **^{13}C-NMR** (126 MHz, CD_2Cl_2, 298 K): δ = 171.51, 162.18, 149.02, 148.47, 142.21, 139.11, 139.03, 134.73, 129.92, 129.13, 126.56, 122.40,

118.40, 102.51, 35.60, 33.89, 31.23, 29.37. **ESI-TOF:** 1127.5 [$\mathbf{(Zn_2L)_1A_0}$ + H^+], 1149.5 [$\mathbf{(Zn_2L)_1A_0}$ + Na^+], 1436.7 [$\mathbf{(Zn_2L)_1A_1}$ + H^+], 1458.6 [$\mathbf{(Zn_2L)_1A_1}$ + Na^+], 1767.8 [$\mathbf{(Zn_2L)_1A_2}$ + Na^+], 2585.2 [$\mathbf{(Zn_2L)_2A_1}$ + Na^+], and 2894.3 [$\mathbf{(Zn_2L)_2A_2}$ + Na^+].

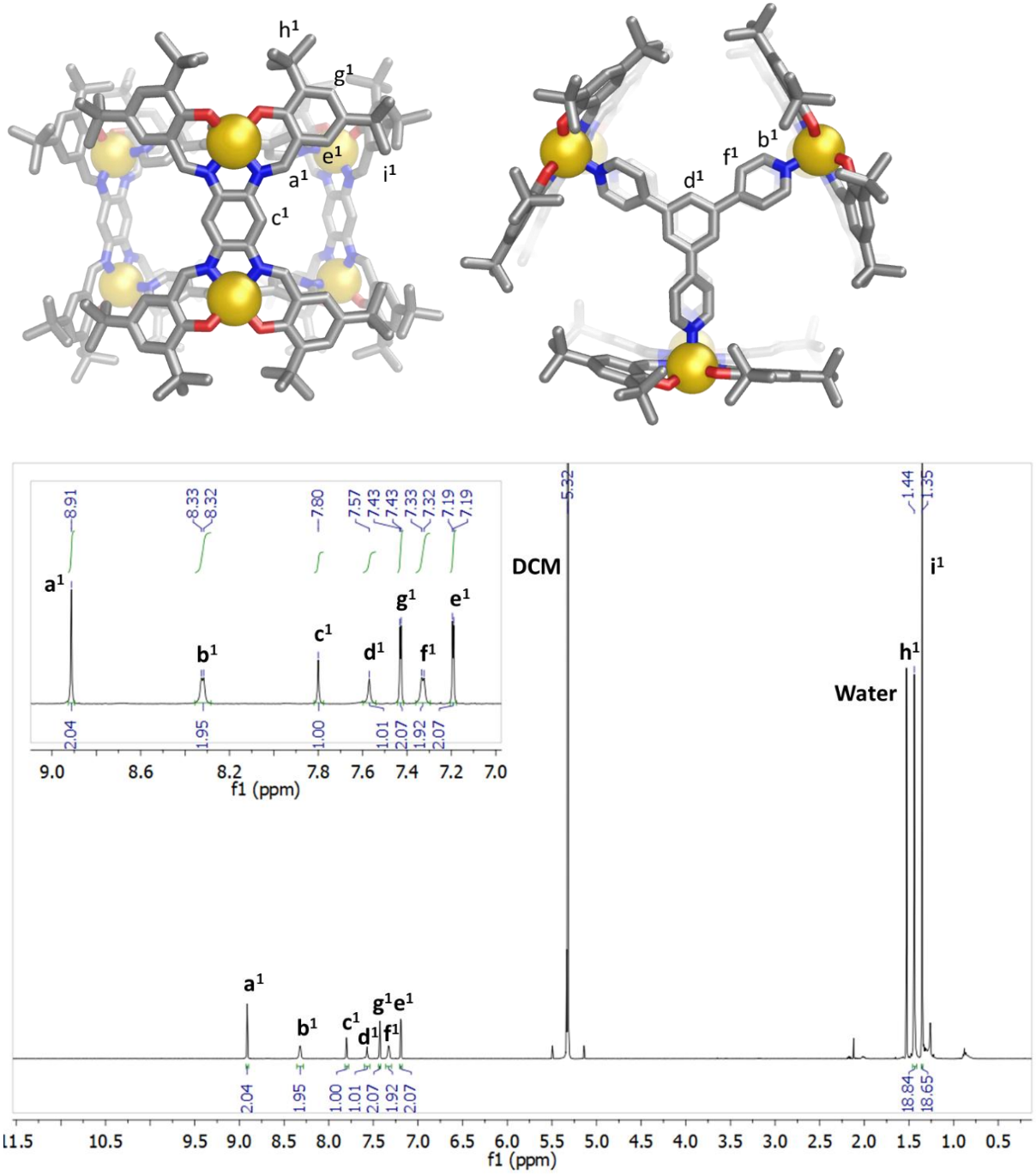

*Figure S5: ^{1}H NMR spectrum of cage **1** (500 MHz, CD_2Cl_2, 298 K).*

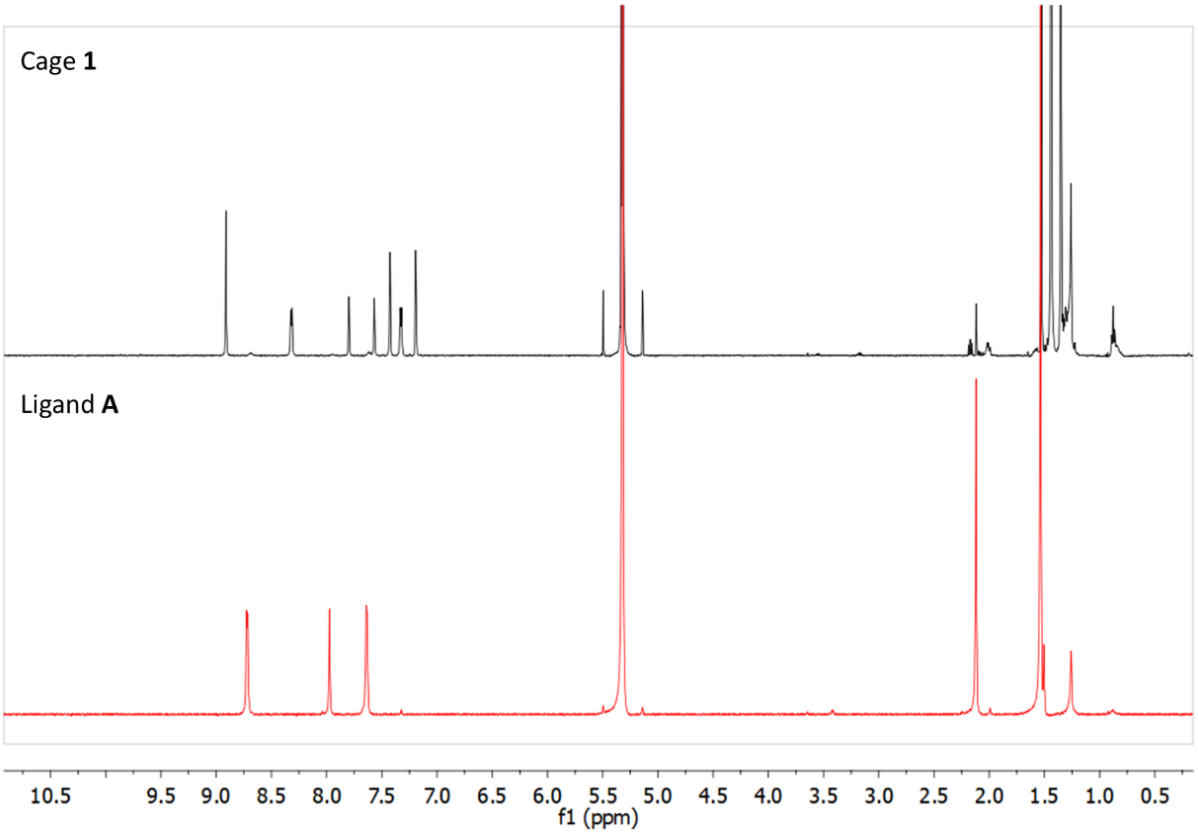

*Figure S6: Stacked ^{1}H NMR spectra of Cage **1** [0.25 mM] (top) and free ligand **A** (bottom) in CD_2Cl_2 (500 MHz, CD_2Cl_2, 298 K).*

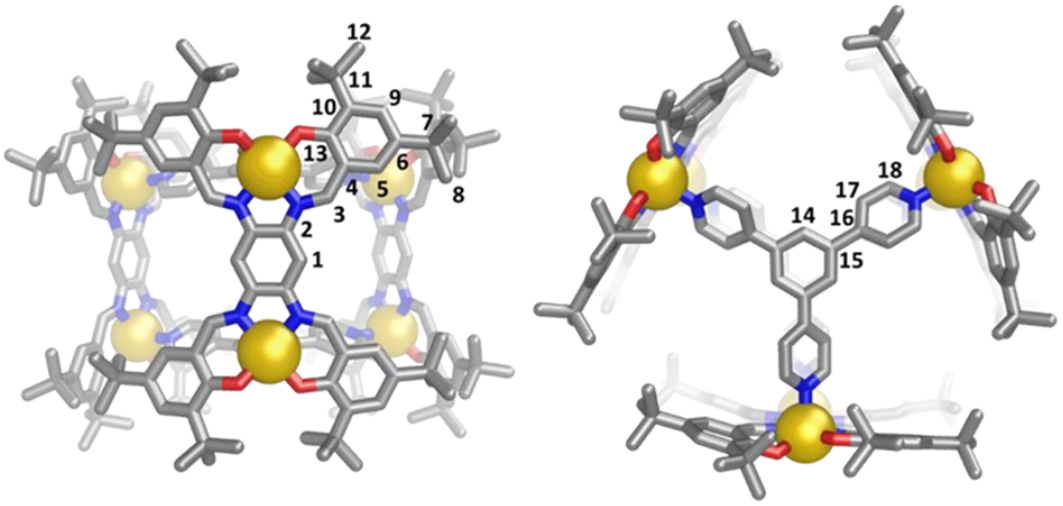

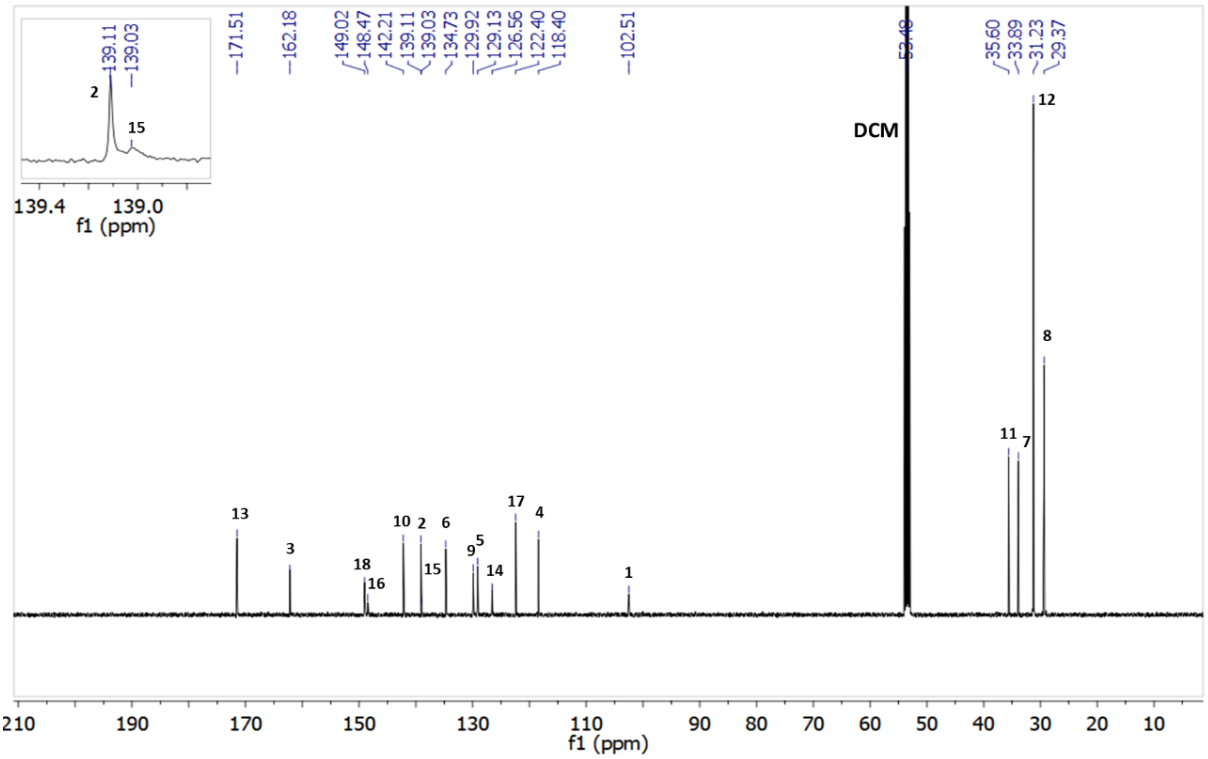

*Figure S7: ^{13}C NMR spectrum of cage **1** (500 MHz, CD_2Cl_2, 298 K).*

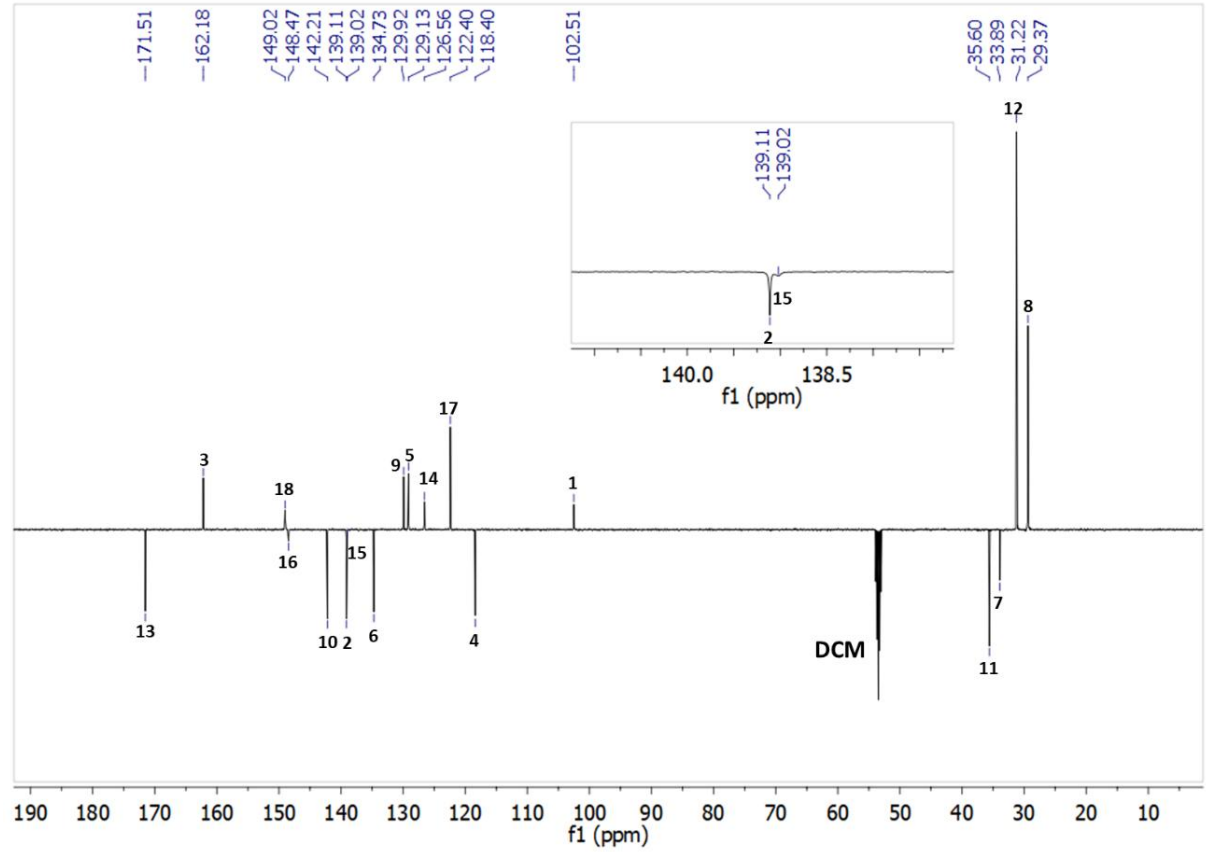

*Figure S8: J-modulated spin-echo NMR spectrum of cage **1** (500 MHz, CD_2Cl_2, 298 K).*

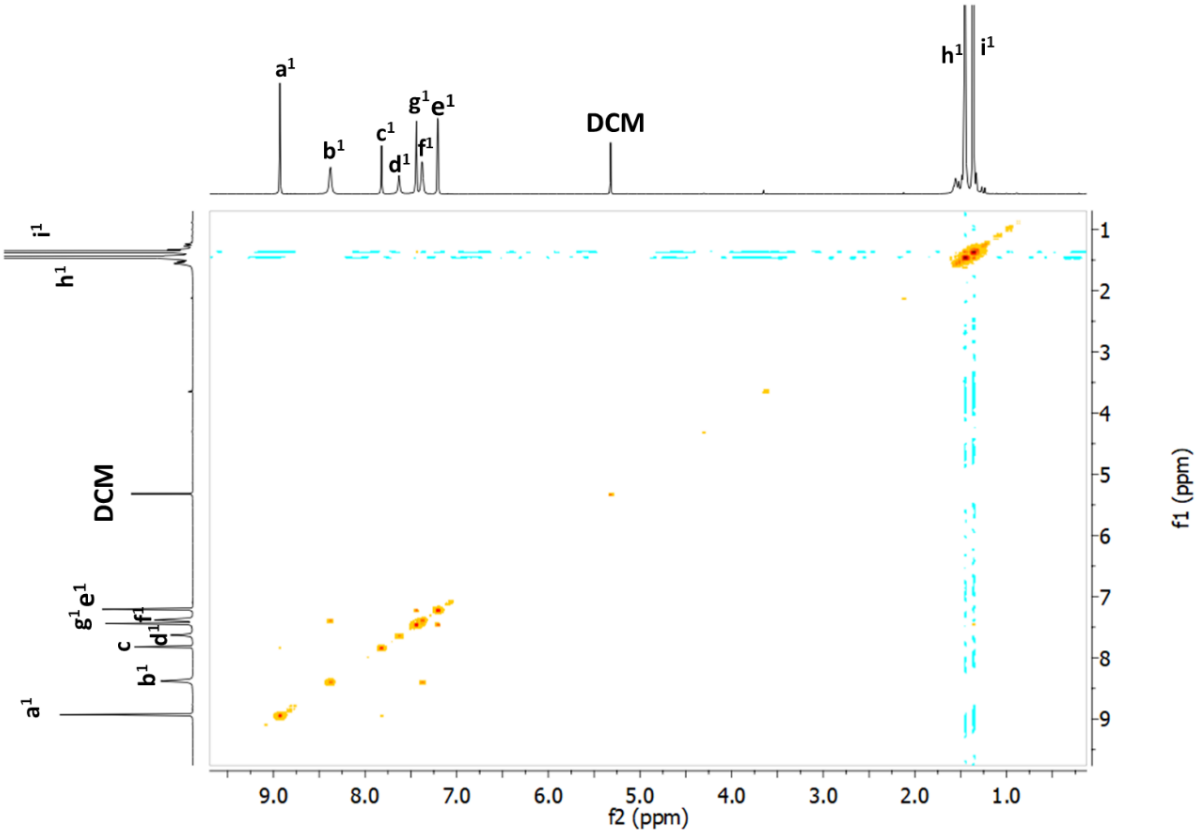

*Figure S9: ^{1}H-^{1}H-COSY NMR of cage **1** (500 MHz, CD_2Cl_2, 298 K).*

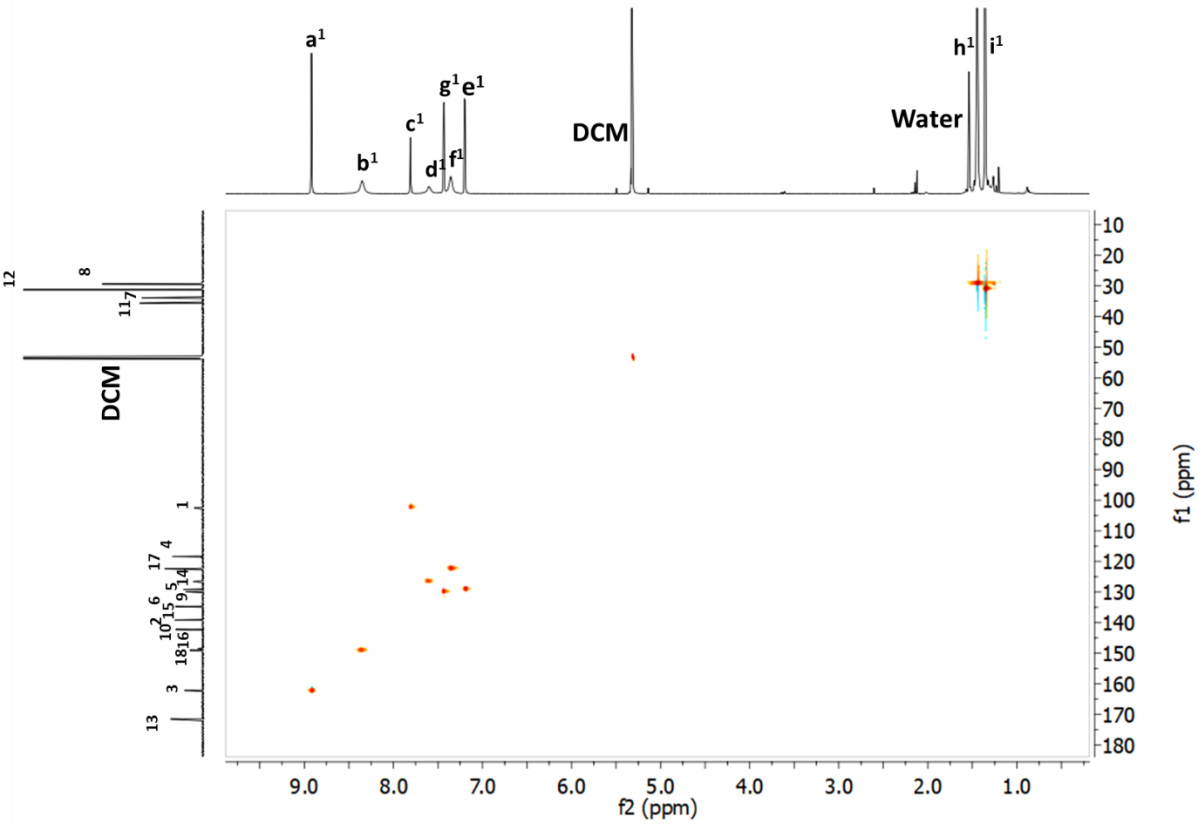

*Figure S10: ^{1}H-^{13}C HSQC spectrum of cage **1** (300 MHz, CD_2Cl_2, 298 K).*

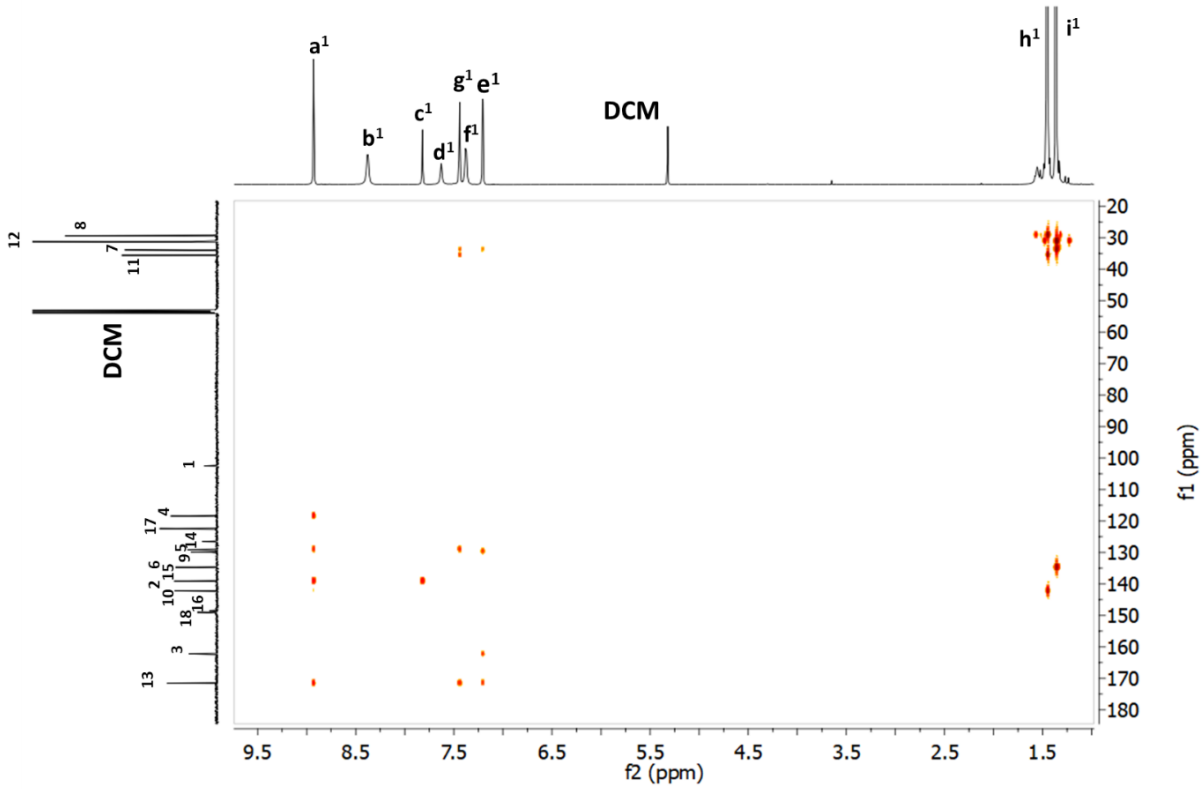

*Figure S11: ^{1}H-^{13}C HMBC NMR spectrum of cage **1** (500 MHz, CD_2Cl_2, 298 K).*

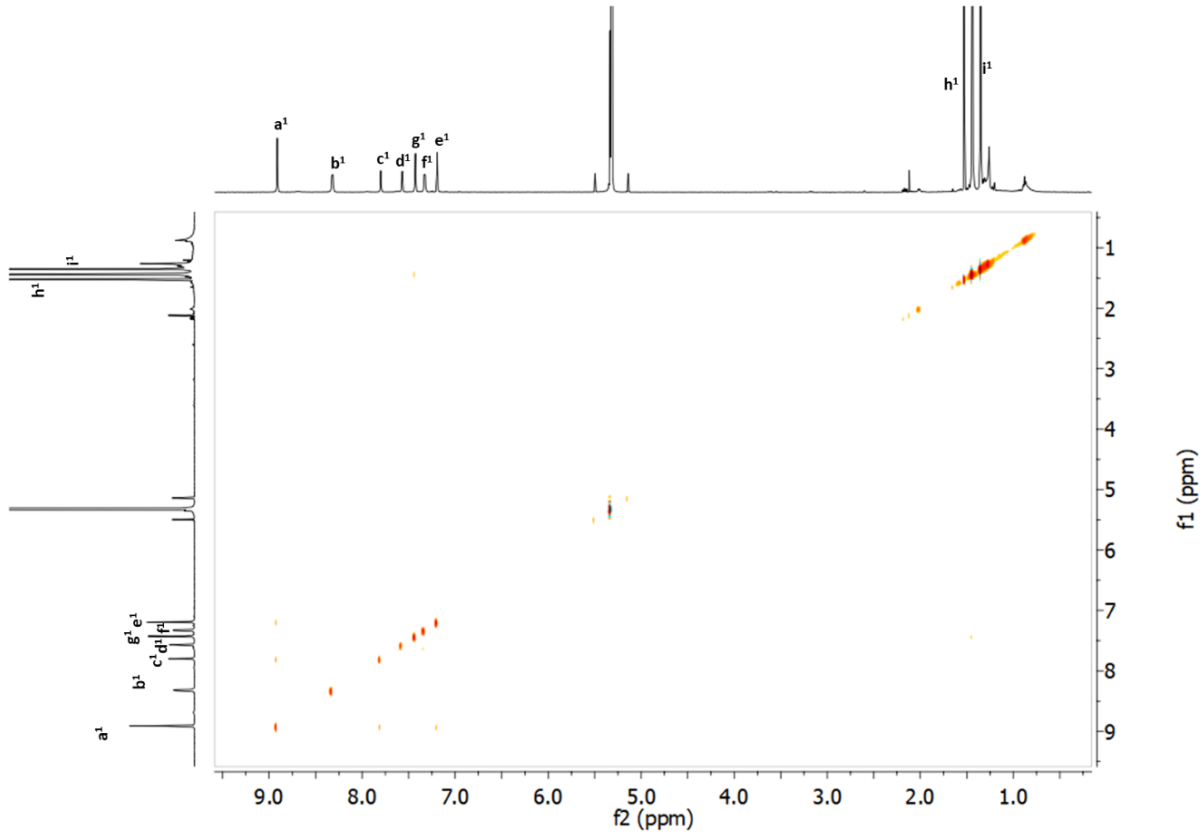

*Figure S12: ^{1}H-^{1}H NOESY NMR spectrum of cage **1** (500 MHz, CD_2Cl_2, 298 K).*

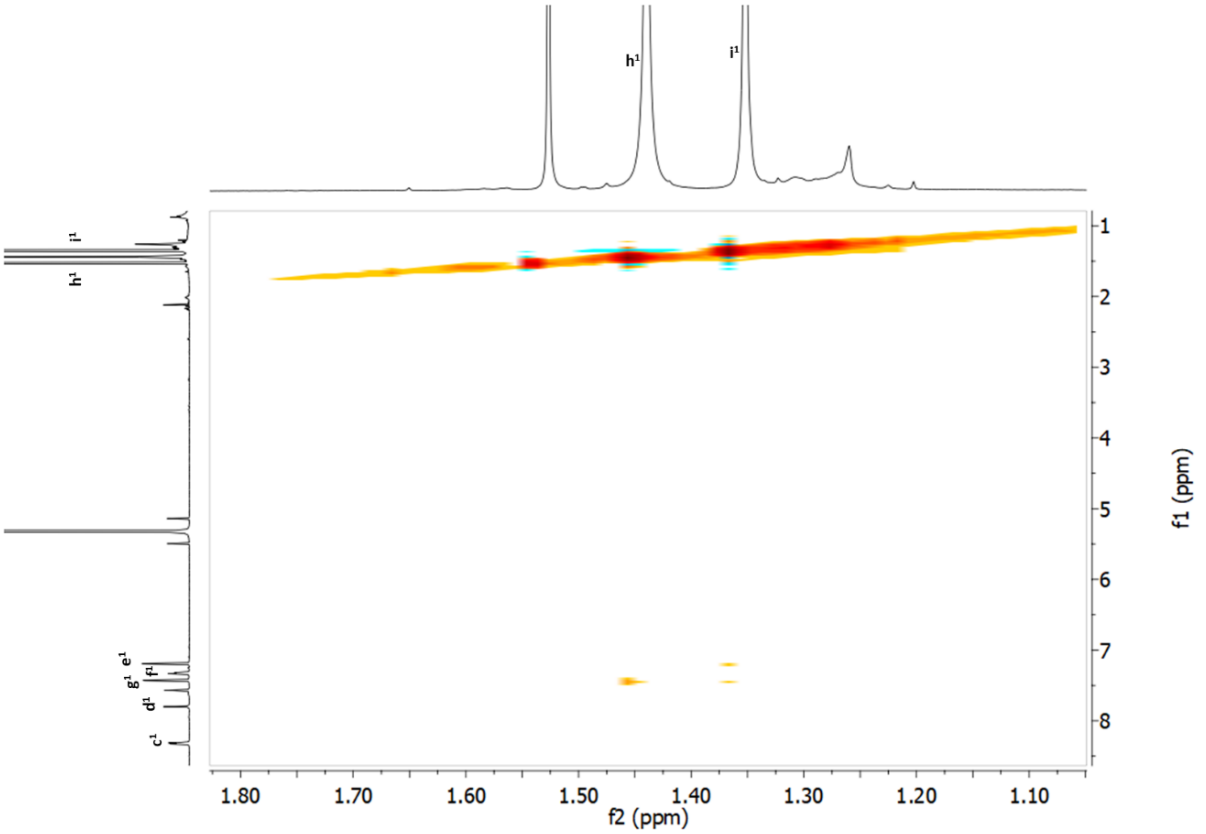

*Figure S13: ^{1}H-^{1}H NOESY NMR spectrum of cage **1** (500 MHz, CD_2Cl_2, 298 K).*

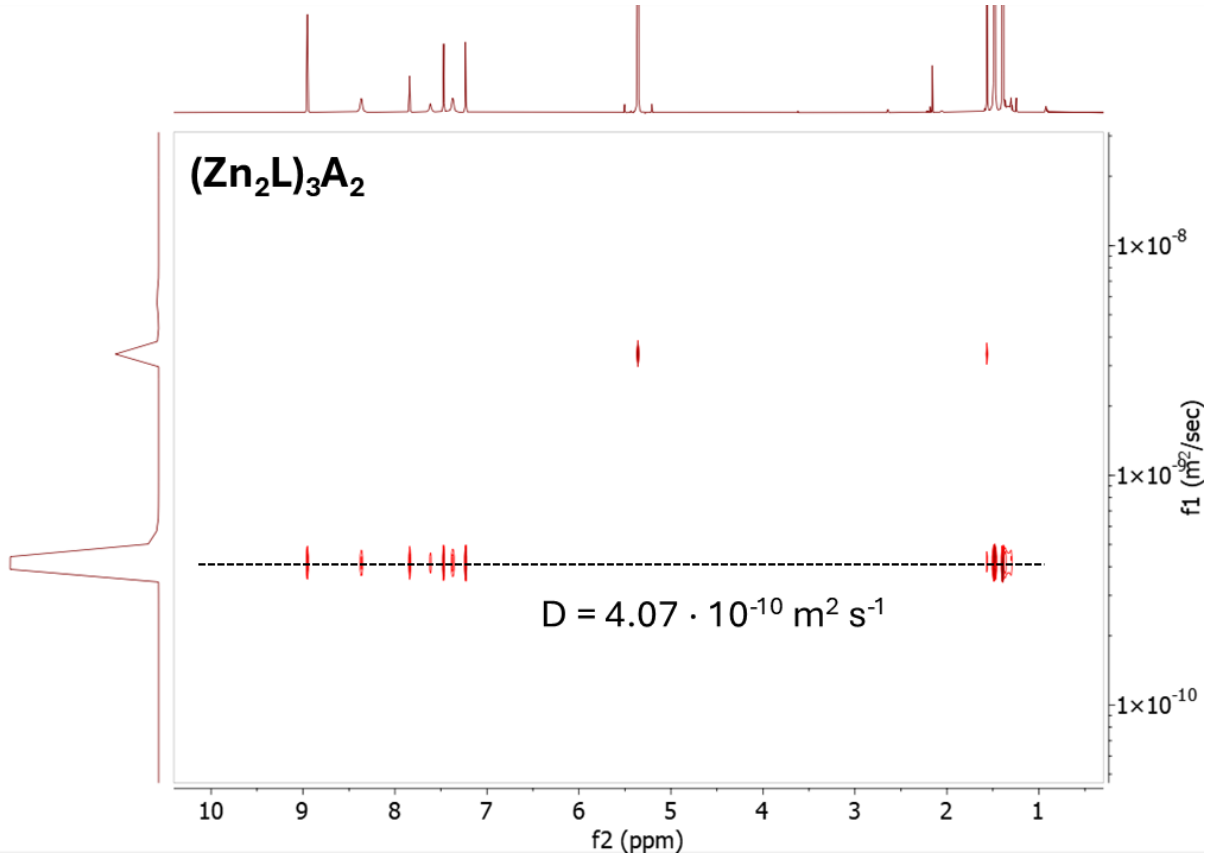

*Figure S14: ^{1}H DOSY NMR spectrum of cage **1** (600 MHz, CD_2Cl_2, 298 K).*

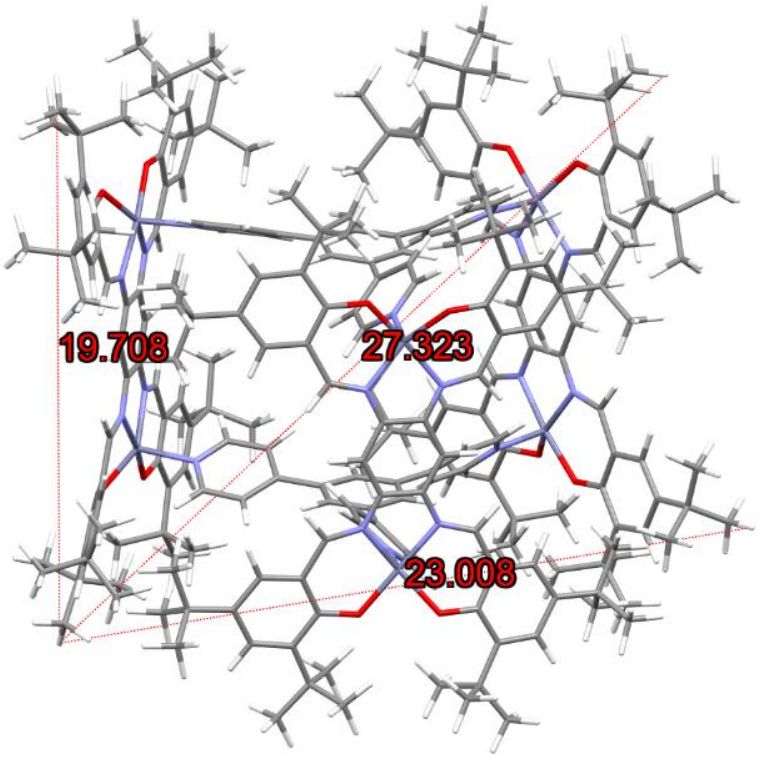

*Figure S15: Determination of the solvent-free diameter of cage **1** based on the MM2 model. The diameter was averaged from the three values to take the asymmetric nature of prismatic cage **1** into account.*

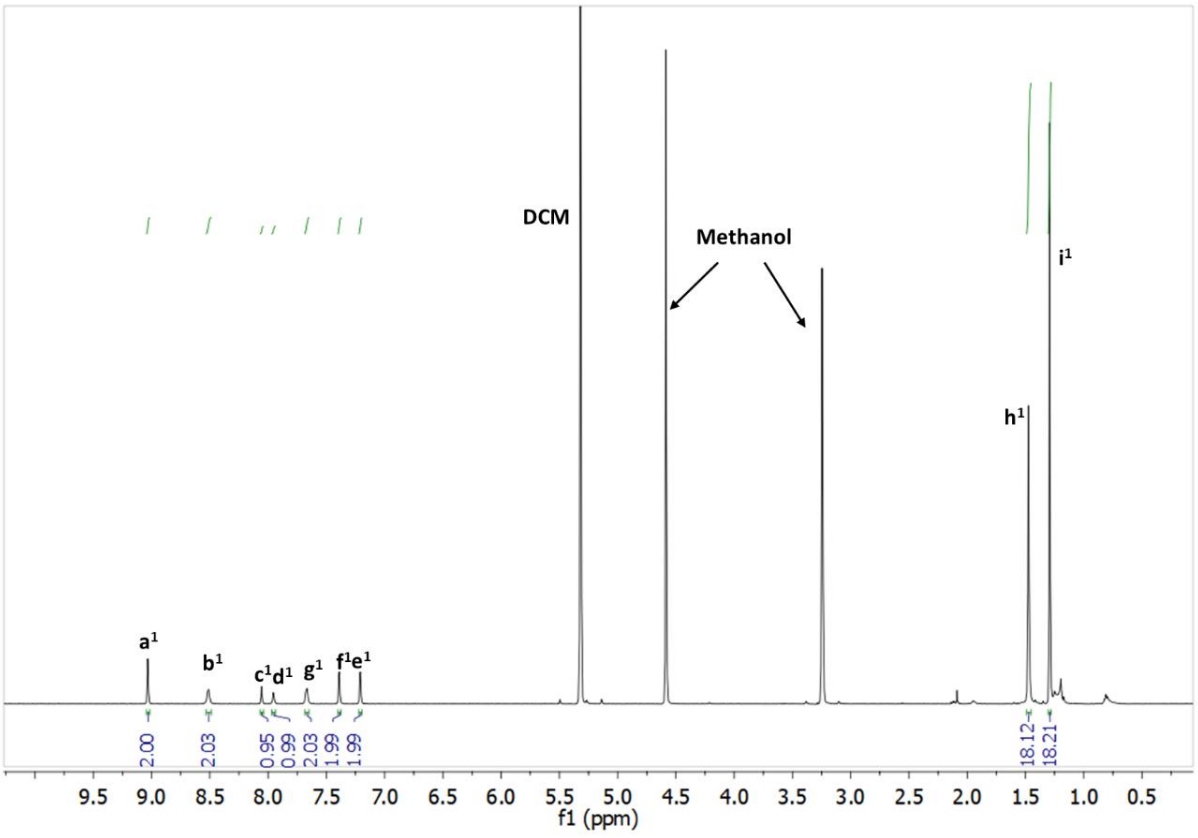

*Figure S16: ^{1}H NMR spectrum of cage **1** [0.5 mM] in a mixture of CD_3OD:CD_2Cl_2 in a 1:1 ratio (500 MHz, CD_2Cl_2:CD_3CD, 298 K).*

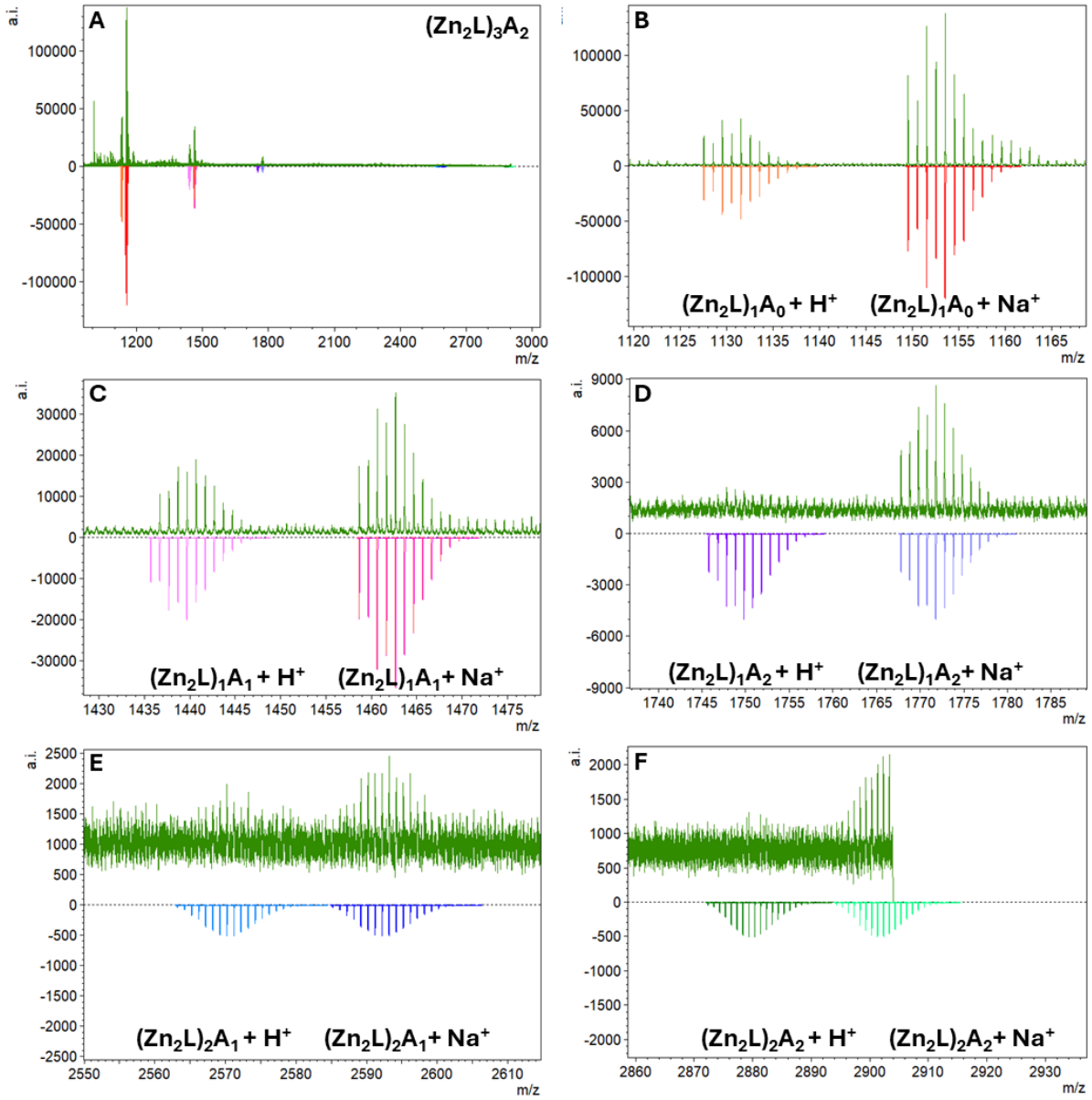

*Figure S17: Overview of the high-resolution ESI-MS spectrum of **1** (A) and zoom into ESI-MS signals (B-F). Please note, that only the following fragments have been observed: B: **$(Zn_2L)_1A_0$** + H^+ and **$(Zn_2L)_1A_0$** + Na^+; C: **$(Zn_2L)_1A_1$** + H^+ and **$(Zn_2L)_1A_1$** + Na^+; D: **$(Zn_2L)_1A_2$** + Na^+; E: **$(Zn_2L)_2A_1$** + Na^+; F: **$(Zn_2L)_2A_2$** + Na^+.*

2.3. Self-assembly of cage 2

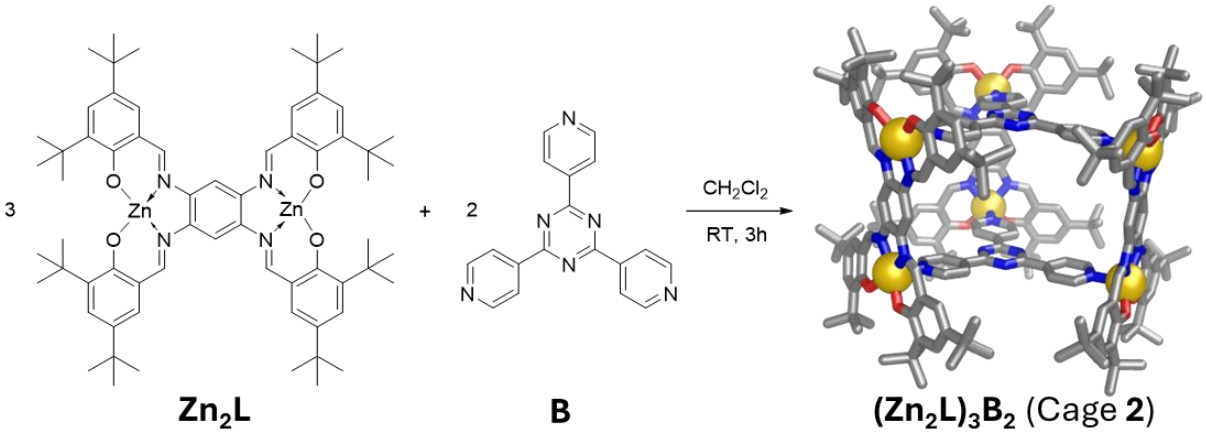

Zn_2L (16.3 mg, 14.4 µmol, 3.0 eq) and 2,4,6-tris(4-pyridyl)-1,3,5-triazine **B** (3.0 mg, 9.6 µmol, 2.0 eq) were dissolved in 0.5 mL of DCM-d_2 and stirred for 3 h. The product was obtained as a dark red solid after rotary evaporation (19.3 mg, 4.8 µmol, MW = 4015.65 g/mol, yield = 100%).

^{1}H-NMR (500 MHz, CD_2Cl_2, 298 K): δ = 8.92 (s, 2H, a^2), 8.39 (d, ^3J = 5.8 Hz, 2H, b^2), 8.03 (d, ^3J = 5.6 Hz, 2H, c^2), 7.80 (s, 1H, d^2), 7.46 (d, ^4J = 2.5 Hz, 2H, f^2), 7.27 (d, ^4J = 2.3 Hz, 2H, e^2), 1.38 (m, 38H, h^2). **^{13}C-NMR** (126 MHz, CD_2Cl_2, 298 K): δ = 171.70, 170.04, 162.54, 149.42, 143.65, 142.35, 139.18, 134.94, 129.99, 129.15, 122.97, 118.47, 103.03, 35.64, 31.36, 29.36. **HR-ESI-TOF**: 1127.5 [**$(Zn_2L)_1B_0$** + H^+], 1149.5 [**$(Zn_2L)_1B_0$** + Na^+], 1439.6 [**$(Zn_2L)_1B_1$** + H^+], 1461.6 [**$(Zn_2L)_1B_1$** + Na^+], 1773.7 [**$(Zn_2L)_1B_2$** + Na^+], 2566.2 [**$(Zn_2L)_2B_1$** + H^+], 2588.1 [**$(Zn_2L)_2B_1$** + Na^+], 2878.3 [**$(Zn_2L)_2B_2$** + H^+], and 2900.3 [**$(Zn_2L)_2B_2$** + Na^+].

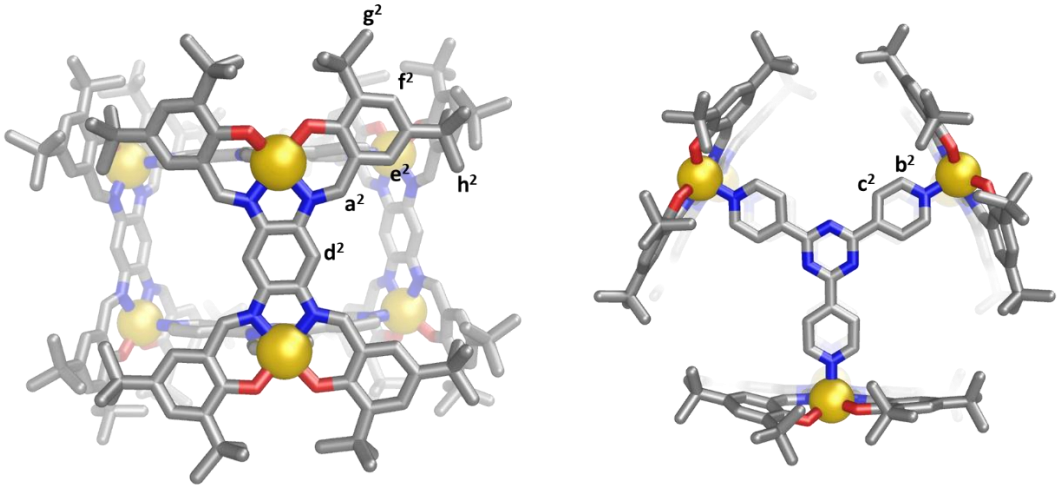

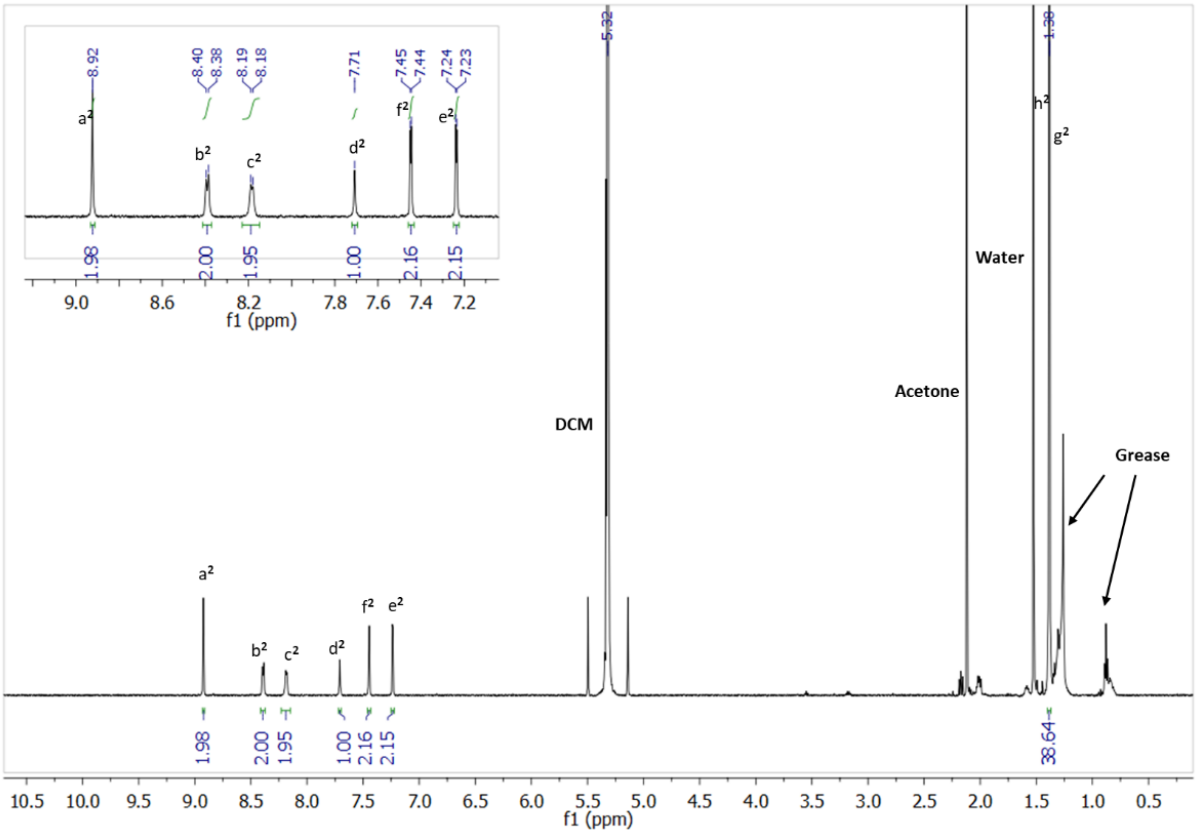

*Figure S18: ^{1}H NMR spectrum of cage **2** (500 MHz, CD_2Cl_2, 298 K).*

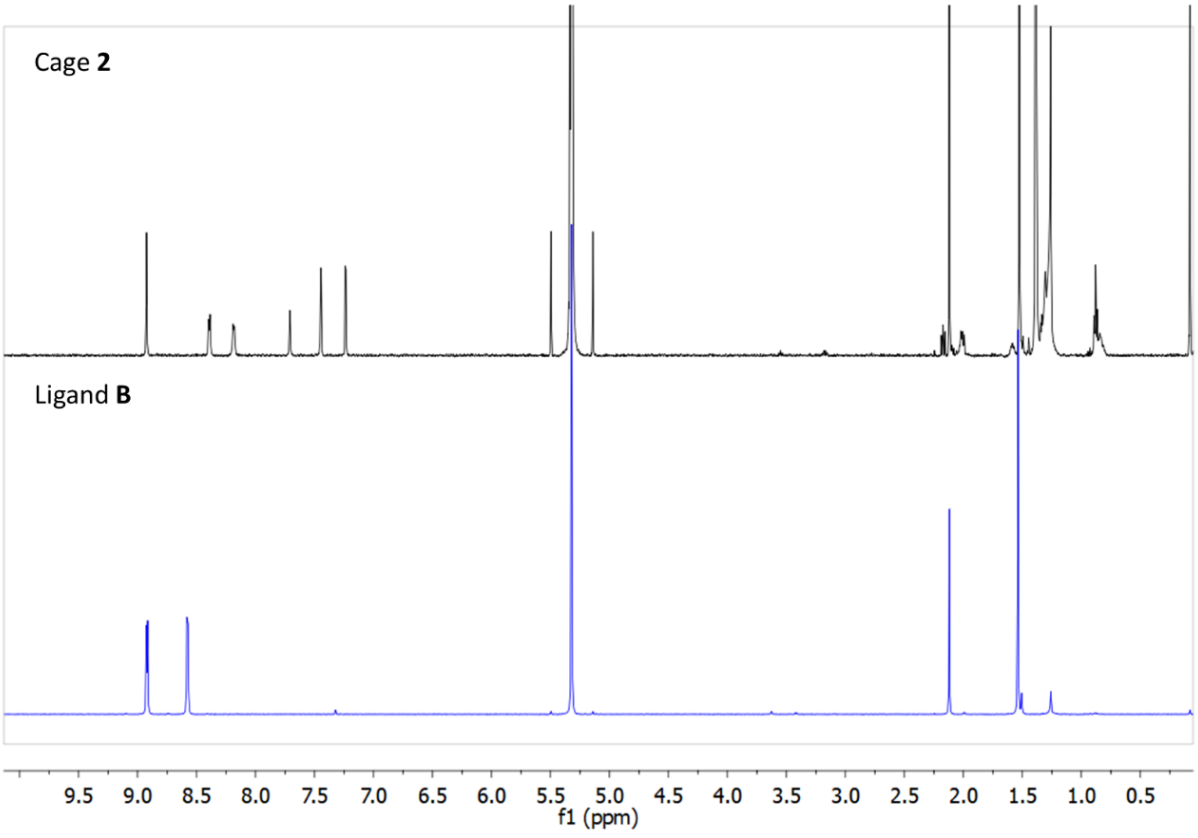

*Figure S19: Stacked ^{1}H NMR spectra of cage **2** [0.25 mM] (top) and ligand **B** (bottom) in CD_2Cl_2 (500 MHz, CD_2Cl_2, 298 K).*

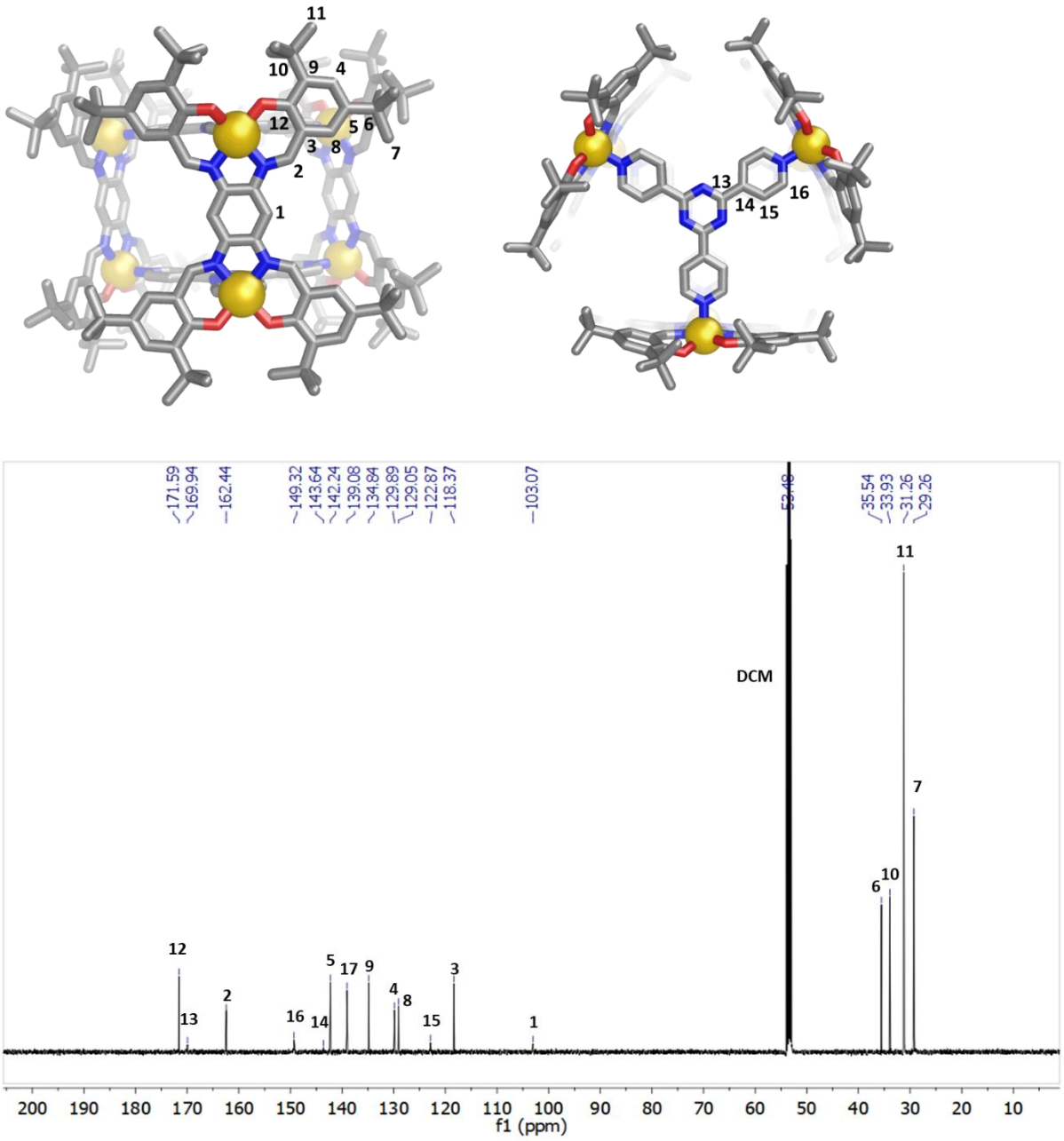

*Figure S20: ^{13}C NMR spectrum of cage **2** (500 MHz, CD_2Cl_2, 298 K).*

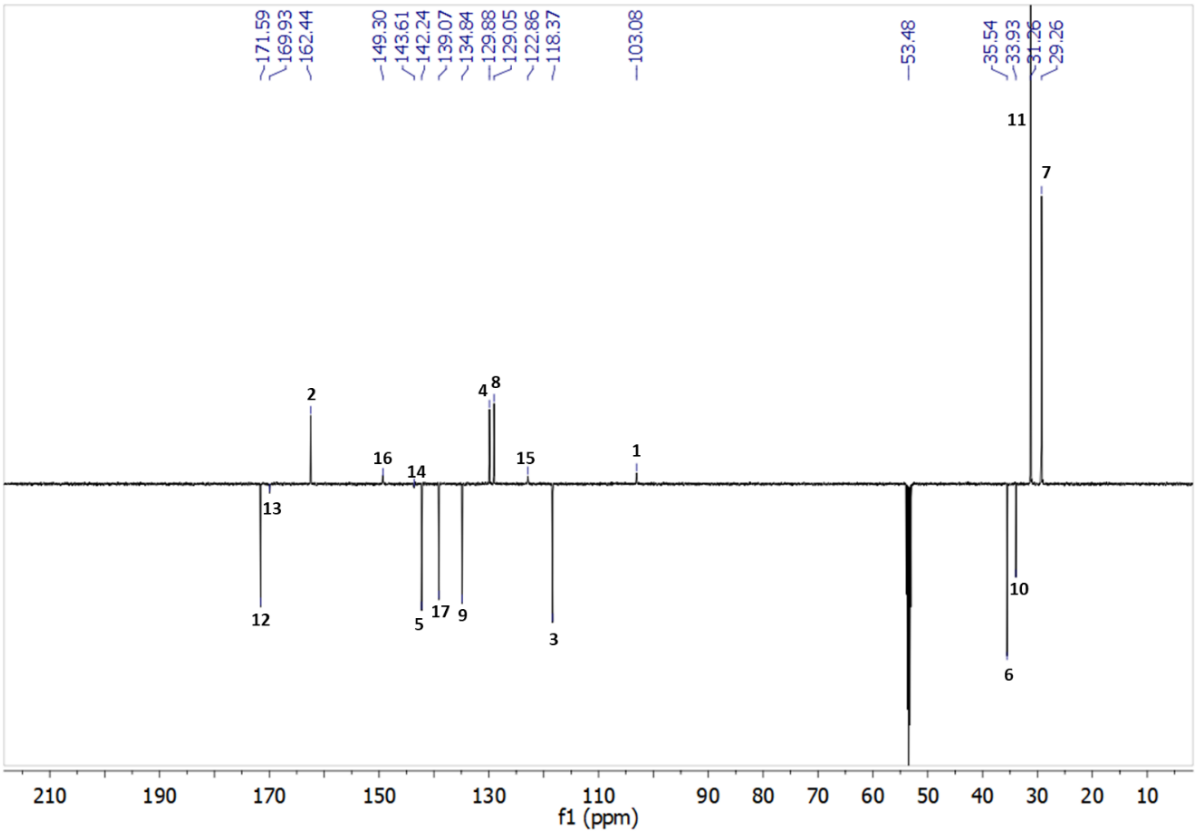

*Figure S21: J-modulated Spin-Echo NMR spectrum of cage **2** (500 MHz, CD_2Cl_2, 298 K).*

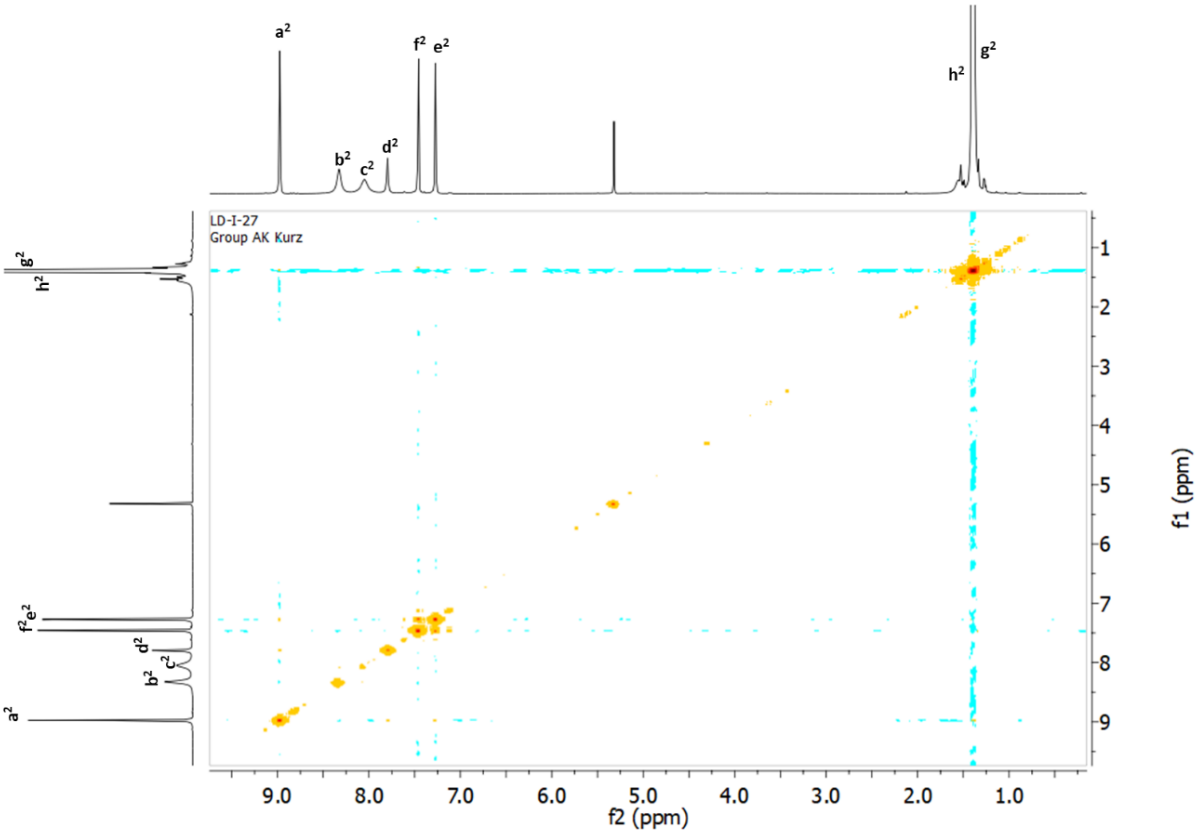

*Figure S22: ^1H-^1H COSY NMR spectrum of cage **2** (500 MHz, CD_2Cl_2, 298 K).*

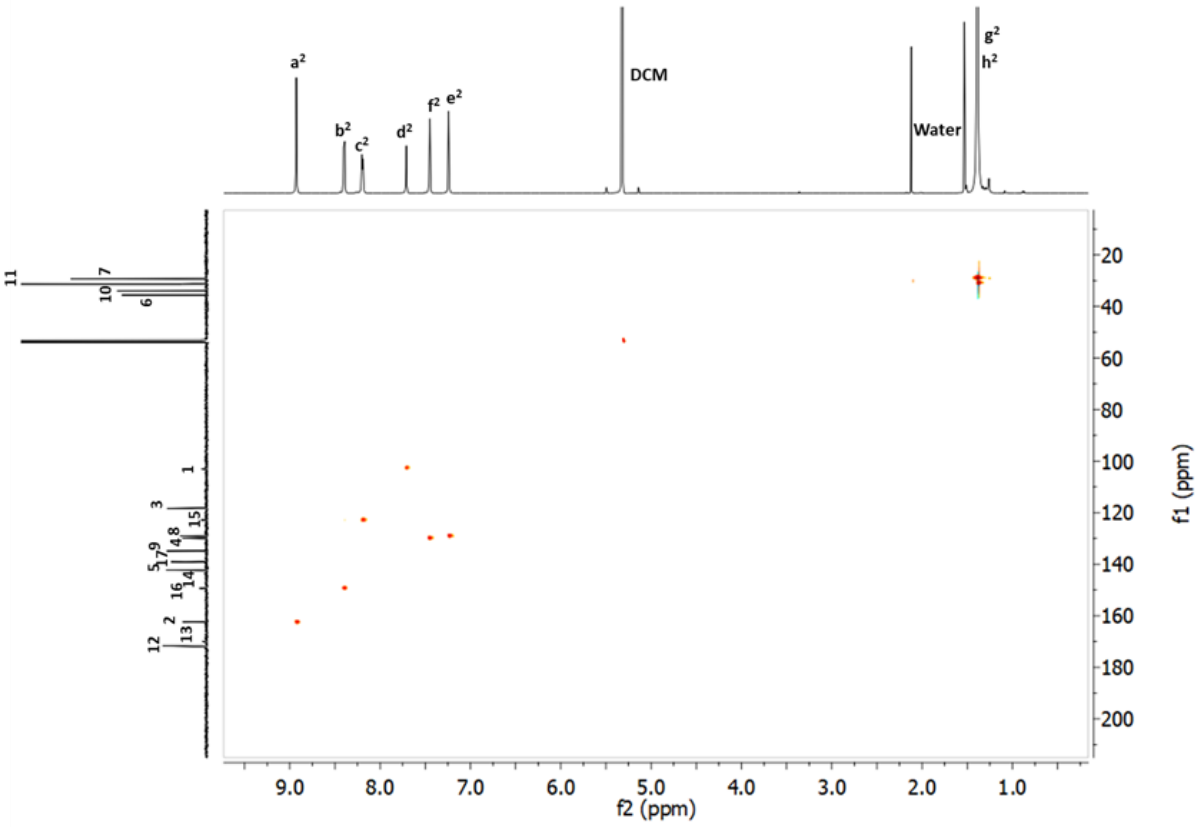

*Figure S23: ^{1}H-^{13}C HSQC NMR spectrum of cage **2** (300 MHz, CD_2Cl_2, 298 K).*

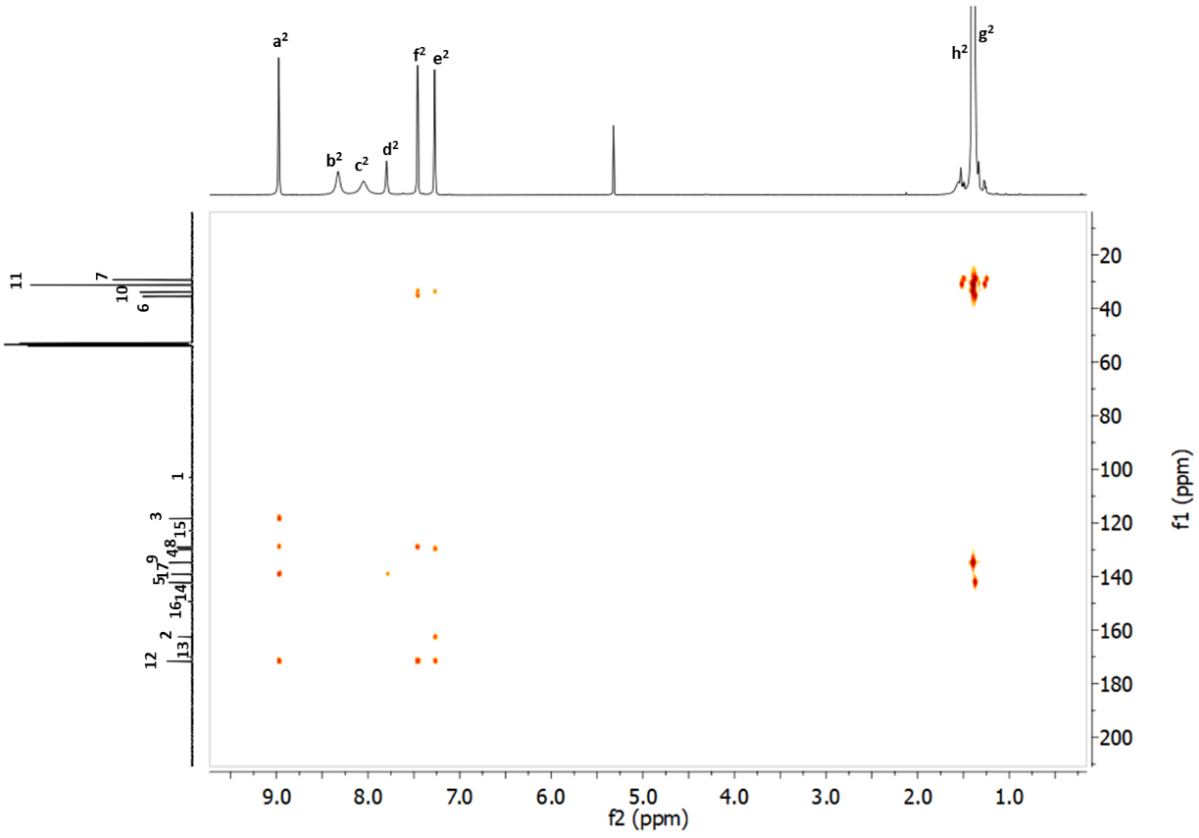

*Figure S24: ^{1}H-^{13}C HMBC NMR spectrum of cage **2** (500 MHz, CD_2Cl_2, 298 K).*

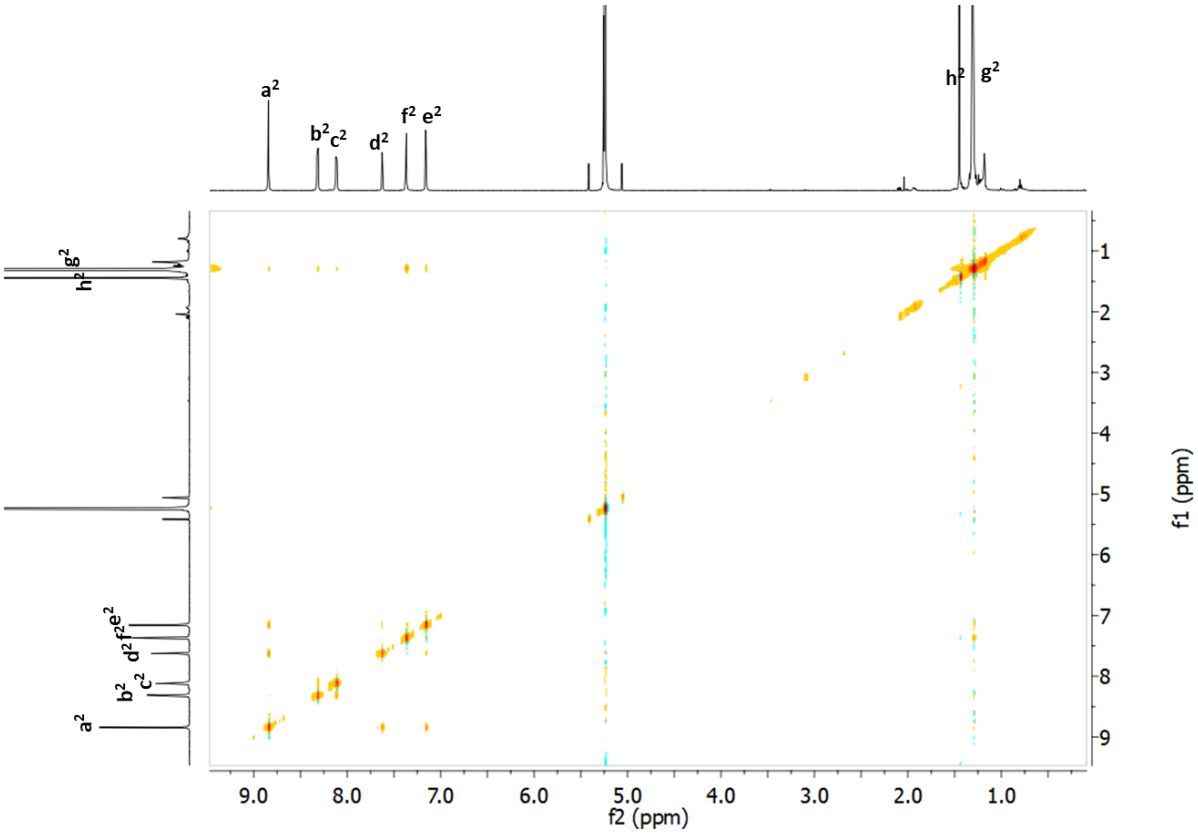

*Figure S25: ^{1}H-^{1}H NOESY NMR spectrum of cage **2** (500 MHz, CD_2Cl_2, 298 K).*

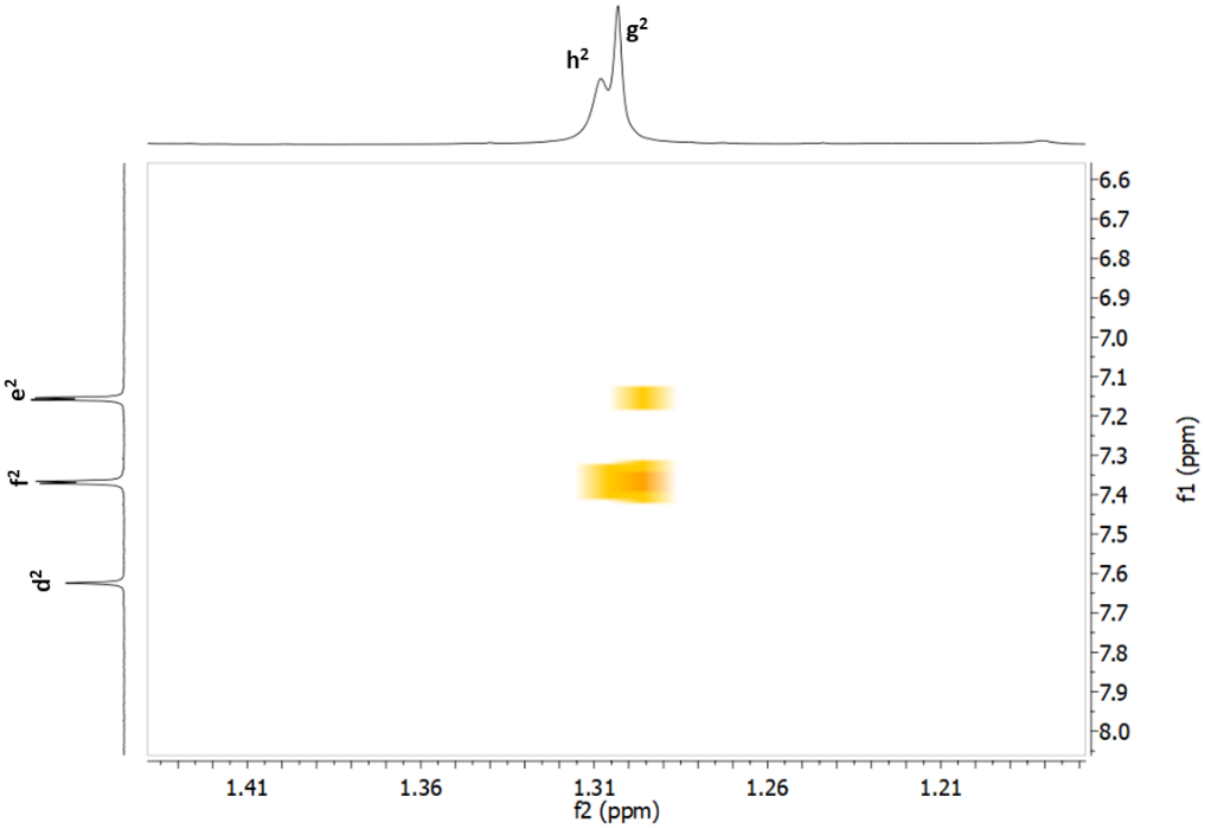

*Figure S26: ^{1}H-^{1}H NOESY NMR spectrum of cage **2** with focus on aromatic signals **f** and **e** with **g** and **h** (500 MHz, CD_2Cl_2, 298 K). To be noted that **g** couples with both **f** and **g** while **h** couples only with **f**.*

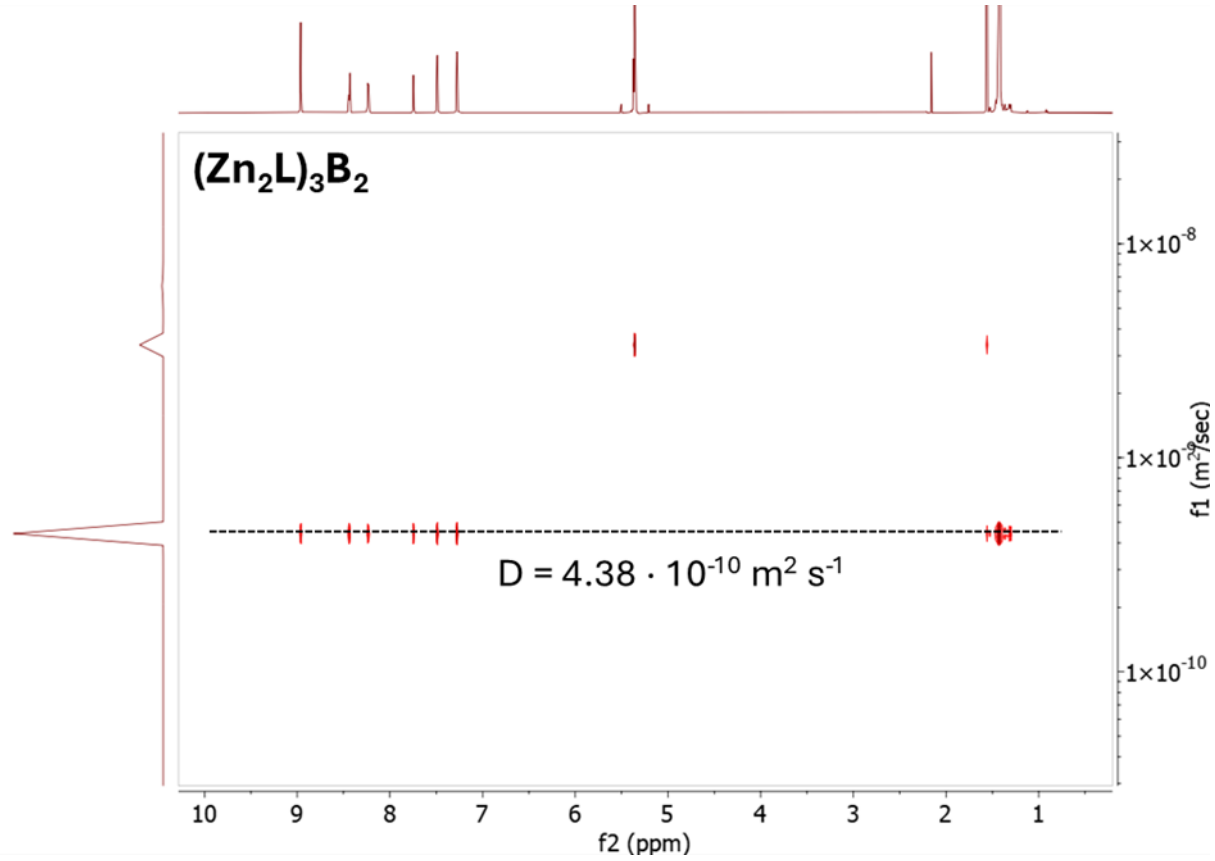

*Figure S27: ^{1}H DOSY NMR spectrum of cage **2** (600 MHz, CD_2Cl_2, 298 K).*

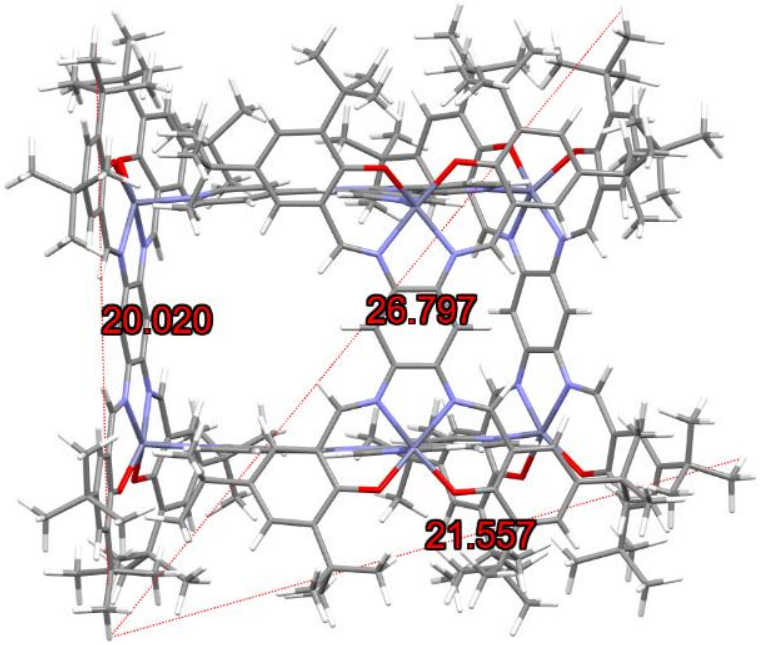

*Figure S28: Determination of the solvent-free diameter of cage **2** based on the MM2 model. The diameter was averaged from the three values to take the asymmetric nature of prismatic cage **2** into account.*

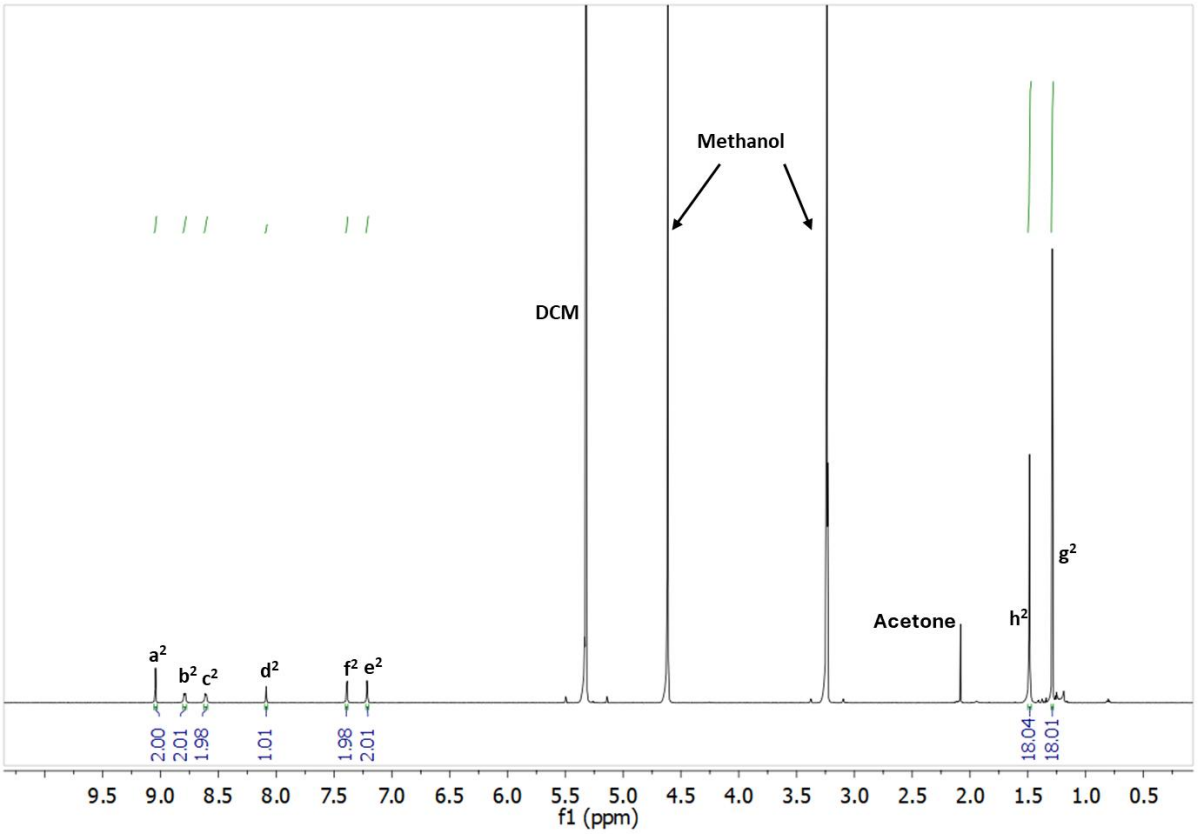

*Figure S29: ^{1}H NMR spectrum of cage **2** [0.5 mM] in a mixture of CD_3OD:CD_2Cl_2 in a 1:1 ratio (500 MHz, CD_2Cl_2:CD_3CD, 298 K).*

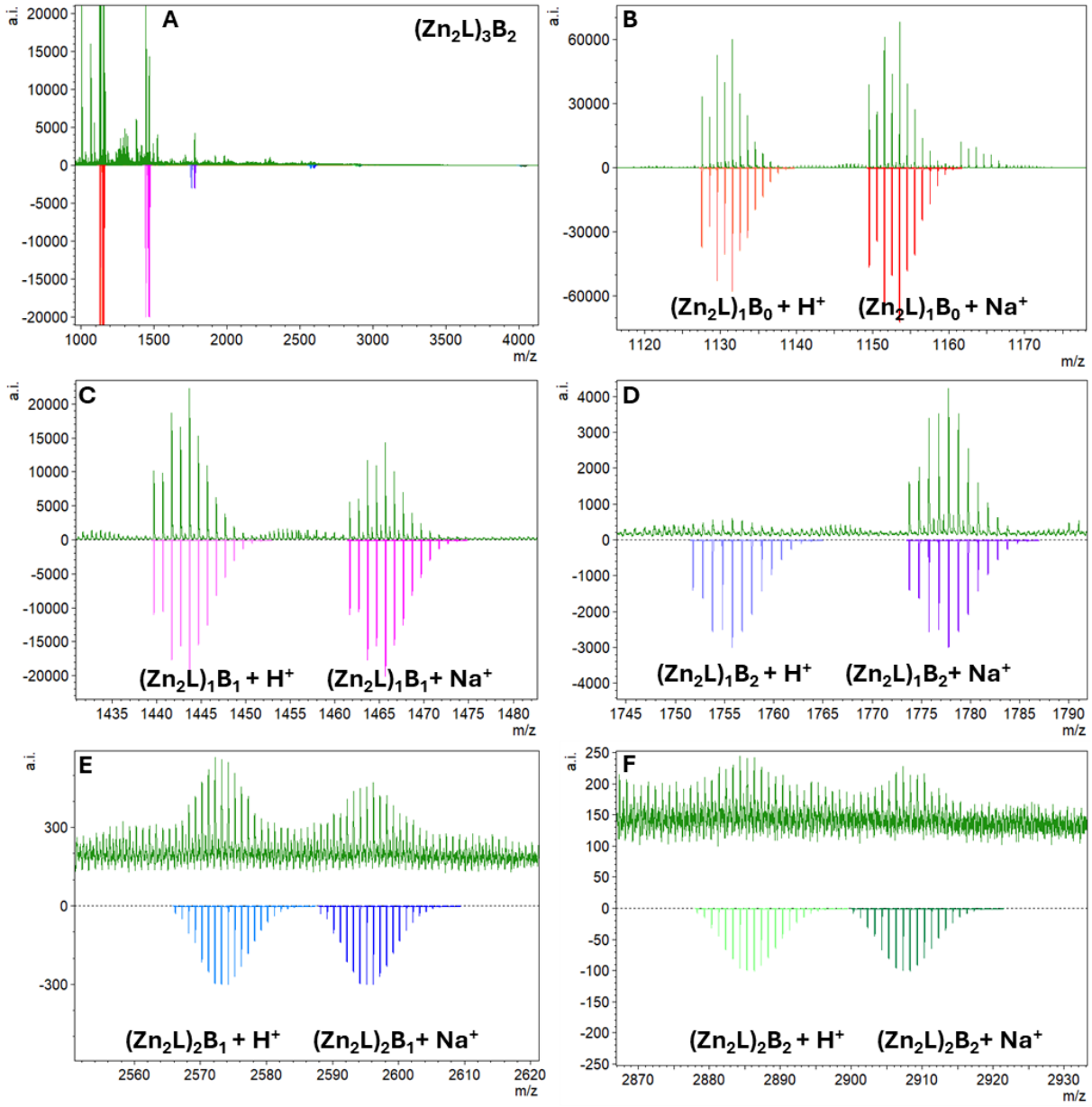

*Figure S30: Overview of the high-resolution ESI-MS spectrum of **2** (A) and zoom into ESI-MS signals (B-F). Please note, that only the following fragments have been observed: B: **$(Zn_2L)_1B_0$** + H^+ and **$(Zn_2L)_1B_0$** + Na^+; C: **$(Zn_2L)_1B_1$** + H^+ and **$(Zn_2L)_1B_1$** + Na^+; D: **$(Zn_2L)_1B_2$** + Na^+; E: **$(Zn_2L)_2B_1$** + H^+ and **$(Zn_2L)_2B_1$** + Na^+; F: **$(Zn_2L)_2B_2$** + H^+ and **$(Zn_2L)_2B_2$** + Na^+.*

3. Structure analysis

3.1. MM2 models

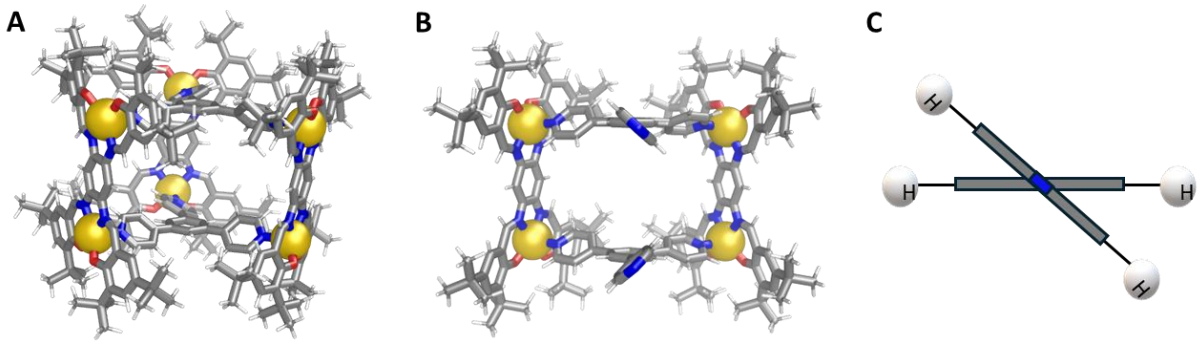

*Figure S31: MM2 model of cage **1** (**A**) with zoom into trigonal plane (**B**). Schematic illustration of the phenylic rings of ligand **A** to illustrate the twisting of the phenyl rings (**C**).*

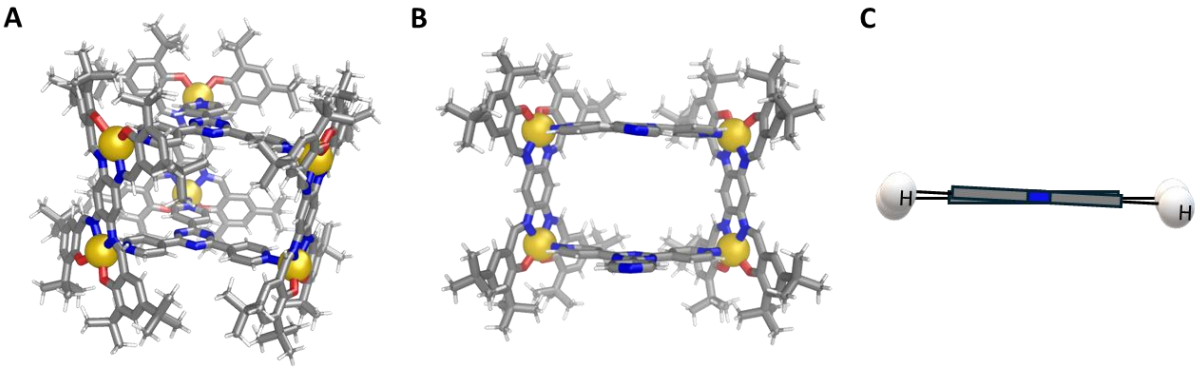

*Figure S32: MM2 model of cage **2** (**A**) with zoom into trigonal plane (**B**). Schematic illustration of the aromatic rings of ligand **B** to illustrate the planarity of the triazine ligand (**C**).*

3.2. Single-crystal X-ray structure determinations

Suitable crystals for single crystal X-ray diffraction of cage **1** $\mathbf{(Zn_2L)_3A_2}$ could be obtained from a low temperature liquid-liquid diffusion setup of CH_3CN into a DCM solution of cage **1**. All crystals of the sample diffracted only very weakly. This is a consequence of the large amount of solvent molecules included in the crystal lattice of this cage compound. Three of the *t*Bu substituents of the Zn_6 cage were disordered. Two alternative orientations each were refined and resulted in site occupancies of 50.1(14) and 49.9(14) % for the atoms C48 – C51 and C48A – C51A, of 28.2(19) and 71.8(19) % for the atoms C99 – C102 and C99A, C400 – C402, and of 46.3(11) and 53.7(12) % for the atoms C195 – C198 and C495 – C498, respectively. One *t*Bu_2Ph moiety of the ligand at Zn4 was disordered. Two alternative orientations each were refined and resulted in site occupancies of 81.5(15) and 18.5(15) % for the atoms C118 – C132 and C418 – C432, respectively. One of the pyridyl rings was disordered. Two alternative orientations each were refined and resulted in site occupancies of 54.7(13) and 45.3(13) % for

the affected atoms C211 – C214 and C412 – C414, respectively. A total of 25.63 molecules of MeCN and 4.54 molecules of CH_2Cl_2 could be identified and refined, some of which were also disordered. In these cases, again two alternative orientations were refined. Remaining solvent molecules were distributed randomly and caused only diffuse electron density. For this reason, the Squeeze routine was applied. A general RIGU restraint was applied to the atoms of all solvent molecules. Similarity and pseudo-isotropic restraints were applied in the refinement of the anisotropic displacement parameters of the disordered atoms. All hydrogen atoms were placed in positions of optimized geometry; their isotropic displacement parameters were tied to those of their corresponding carrier atoms by a factor of 1.2 or 1.5.

Suitable crystals for single crystal X-ray diffraction of Cage **2 $(Zn_2L)_3B_2$** could be obtained from a low temperature liquid-liquid diffusion setup of CH_3CN into a DCM solution of cage **2**. All crystals of the sample diffracted only very weakly. This obviously is a consequence of the large amount of unresolved solvent molecules included in the crystal lattice of this cage compound. A total of 8 molecules of MeCN and 4 molecules of CH_2Cl_2 could be identified and refined. Two of the identified CH_2Cl_2 locations were occupied by roughly 50% only. A large solvent accessible void was identified and obviously filled with randomly distributed solvent molecules. For this reason, the solvent mask routine in Olex2 was applied. A general RIGU restraint was applied to all identified non-hydrogen atoms of the crystal structure. Additional similarity and pseudo-isotropic restraints were applied in the refinement of the anisotropic displacement parameters of some atoms where necessary.

CCDC-x contains the supplementary crystallographic data for compounds cage **1** and cage **2**. The data can be obtained free of charge from The Cambridge Crystallographic Data Centre *via* www.ccdc.cam.ac.uk/structures.

*Table S1: Crystallographic data for cage **1** and cage **2**.*

	Cage **1 $(Zn_2L)_3A_2$**	Cage **2 $(Zn_2L)_3B_2$**
Formula	$C_{240}H_{285}N_{18}O_{12}Zn_6 \cdot 25.63(C_2H_3N) \cdot 4.54(CH_2Cl_2)$	$C_{234}H_{282}N_{24}O_{12}Zn_6 \cdot 8(C_2H_3N) \cdot 4(CH_2Cl_2)$
Sum formula	$C_{295.8}Cl_{9.1}H_{371.0}N_{43.6}O_{12}Zn_6$	$C_{254}H_{314}Cl_8N_{32}O_{12}Zn_6$
M / g·mol^{-1}	5443.71	4683.17
Crystal system	Triclinic	Triclinic
CCDC	2497733	2497723
Space group	*P-1* (Nr. 2)	*P-1* (Nr. 2)

Crystal description	Orange prism	Red prism
Crystal size / mm	0.16x0.21x0.30	0.22x0.23x0.30
a / Å	23.370(2)	23.8937(19)
b / Å	23.517(2)	23.9314(18)
c / Å	34.986(3)	36.662(3)
α / °	81.695(4)	86.198(4)
β / °	80.215(4)	72.187(4)
γ / °	60.768(3)	60.289(3)
V / Å^3	16493(3)	17243(2)
Z	2	2
$\rho_{calculated}$ / g·cm^{-3}	1.096	0.902
μ / mm^{-1}	0.560	0.519
F(000)	5763	4948
Θ_{range} / °	1.7 – 26.1	1.7 – 25.7
Radiation	Mo-K_α (0.71073 Å)	Mo-K_α (0.71073 Å)
T / K	100	100
Measured reflections	537300	456941
Independent reflections	64881	65347
Reflections with $I > 2\sigma(I)$	43703	41260
R_{int}	0.118	0.147
R_1 ($I > 2\sigma(I)$)	0.098	0.164
wR_2 (all data)	0.302	0.466
GooF (S)	1.03	1.71

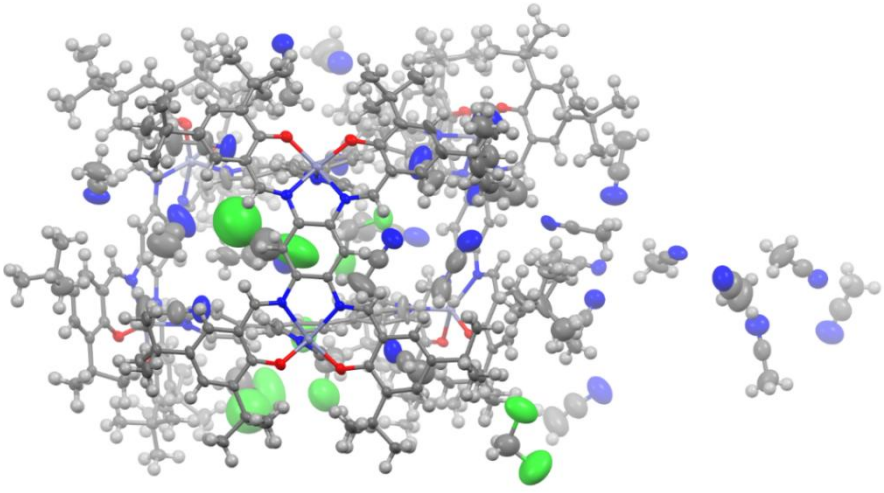

*Figure S33: Asymmetric unit of cage **1**. Displacement ellipsoids are given at 50% probability. Hydrogen atoms are illustrated as balls of arbitrary size. Colour code: carbon (grey), oxygen (red), nitrogen (blue), hydrogen (light grey), chlorine (green).*

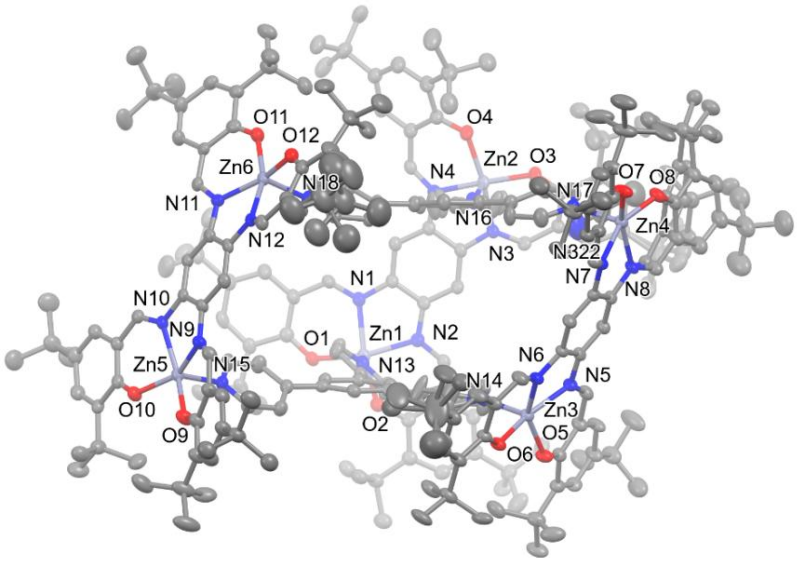

*Figure S34: Asymmetric unit of cage **1**. Hydrogen and solvent molecules are omitted for clarity. Displacement ellipsoids are given at 50% probability.*

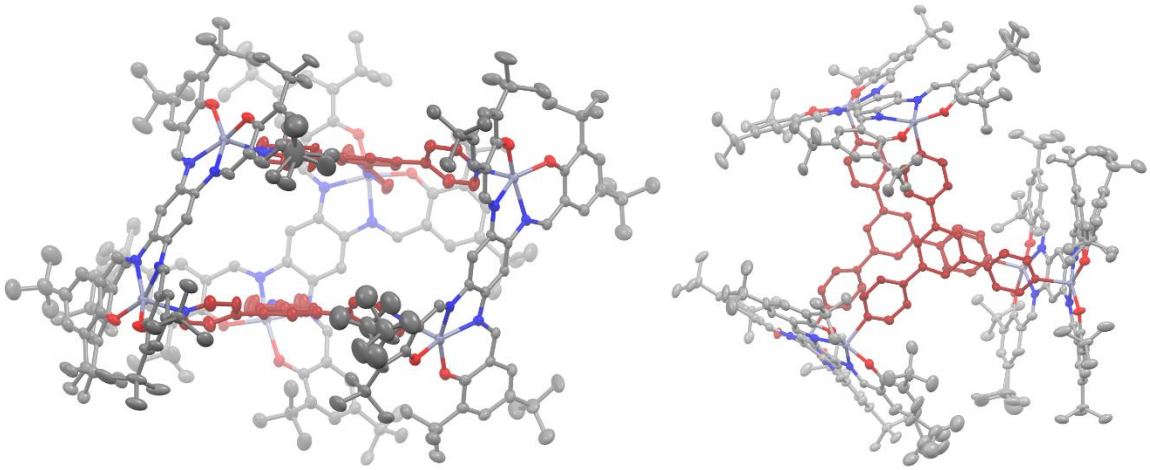

*Figure S35: Asymmetric unit of cage **1** from different angles (left: non-defined angle; right: along [001]). Hydrogens and solvent molecules are omitted for clarity. The tritopic ligands **A** are coloured dark red to illustrate the twisted nature of the cage within the crystal structure.*

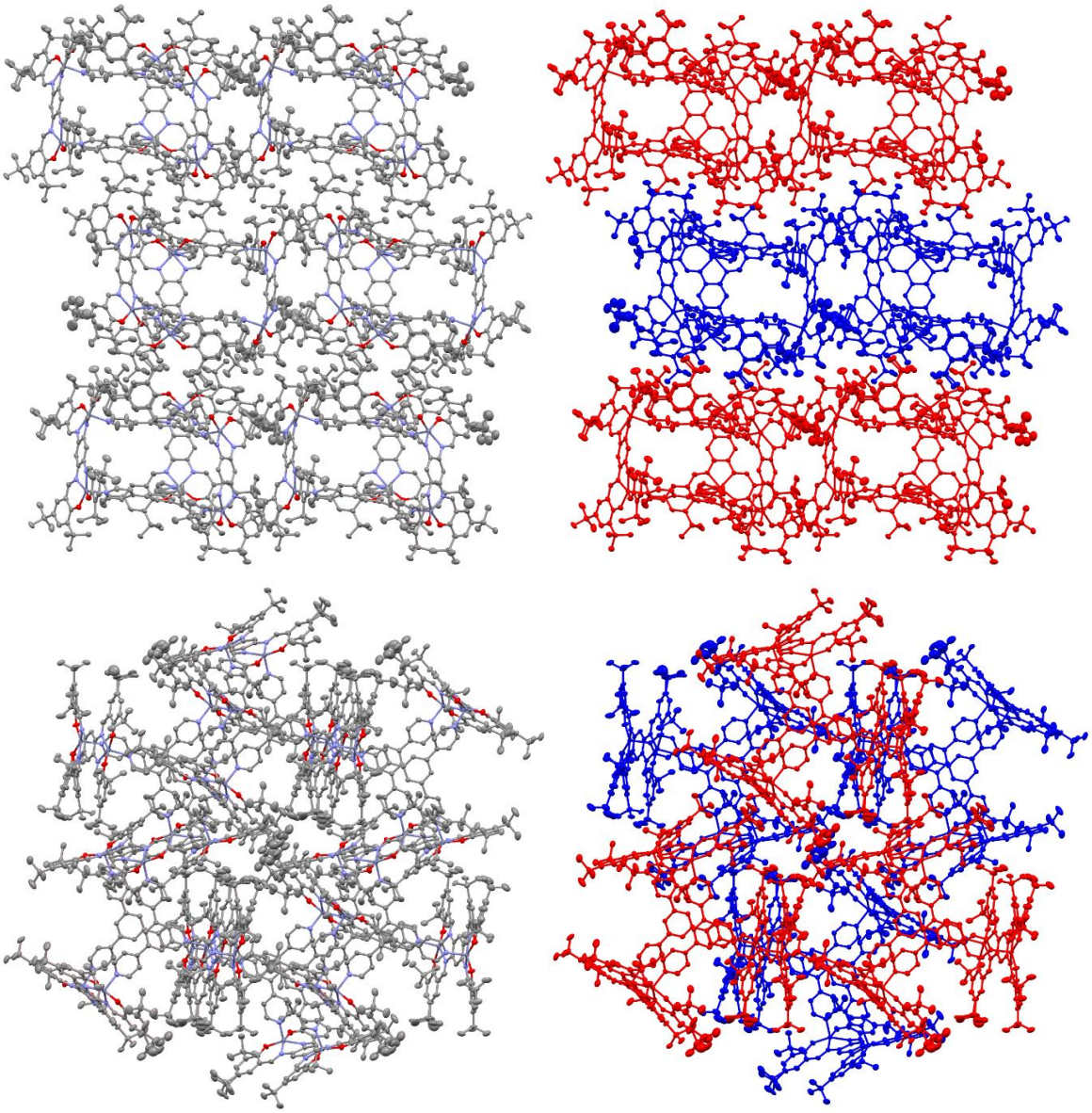

*Figure S36: Molecular packing of cage **1** along [100] (top) and [001] (bottom). Solvent molecules and protons were omitted for clarity.*

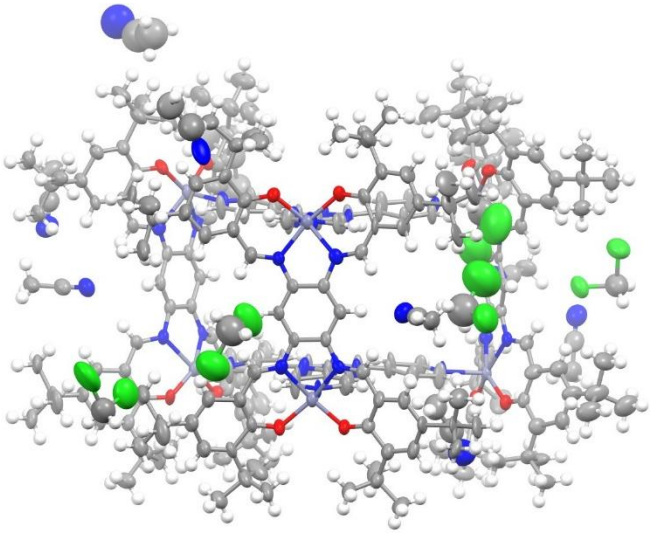

*Figure S37: Asymmetric unit of cage **2**. Displacement ellipsoids are given at 50% probability. Hydrogen atoms are illustrated as balls of arbitrary size. Colour code: carbon (grey), oxygen (red), nitrogen (blue), hydrogen (light grey), chlorine (green).*

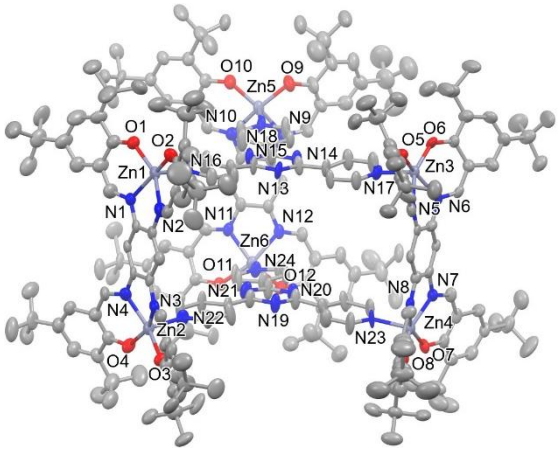

*Figure S38: Asymmetric unit of cage **2**. Hydrogen and solvent molecules are omitted for clarity. Displacement ellipsoids are given at 50% probability.*

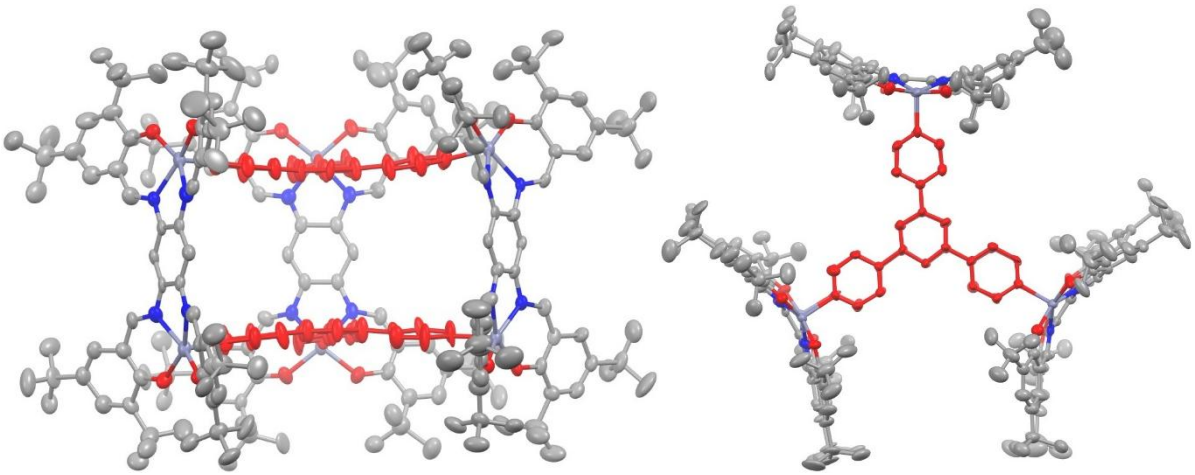

*Figure S39: Asymmetric unit of cage **2** from different angles (both: non-defined angles). Hydrogens and solvent molecules are omitted for clarity. The tritopic ligands **B** are coloured dark red to illustrate the twisted nature of the cage within the crystal structure.*

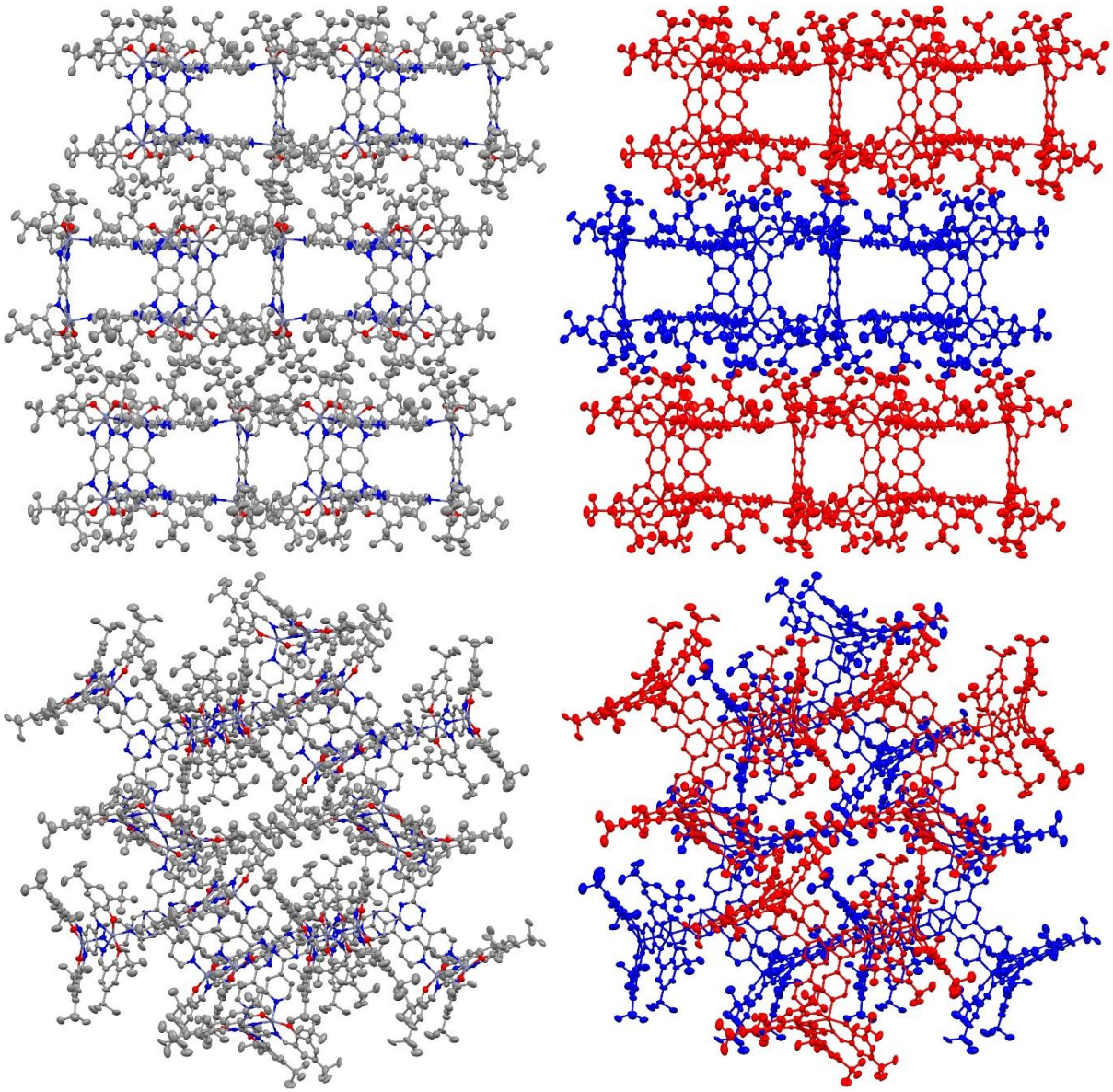

*Figure S40: Molecular packing of cage **2** along [100] (top) and [001] (bottom). Solvent molecules and protons were omitted for clarity.*

4. NMR dilution studies

Variable concentration ^{1}H NMR experiments were conducted by preparing 4 mM solution of the cage and diluting it by half after every measurement. Spectra samples with concentrations of 30 µM or lower were measured with 32 scans.

4.1. Dilution series cage 1

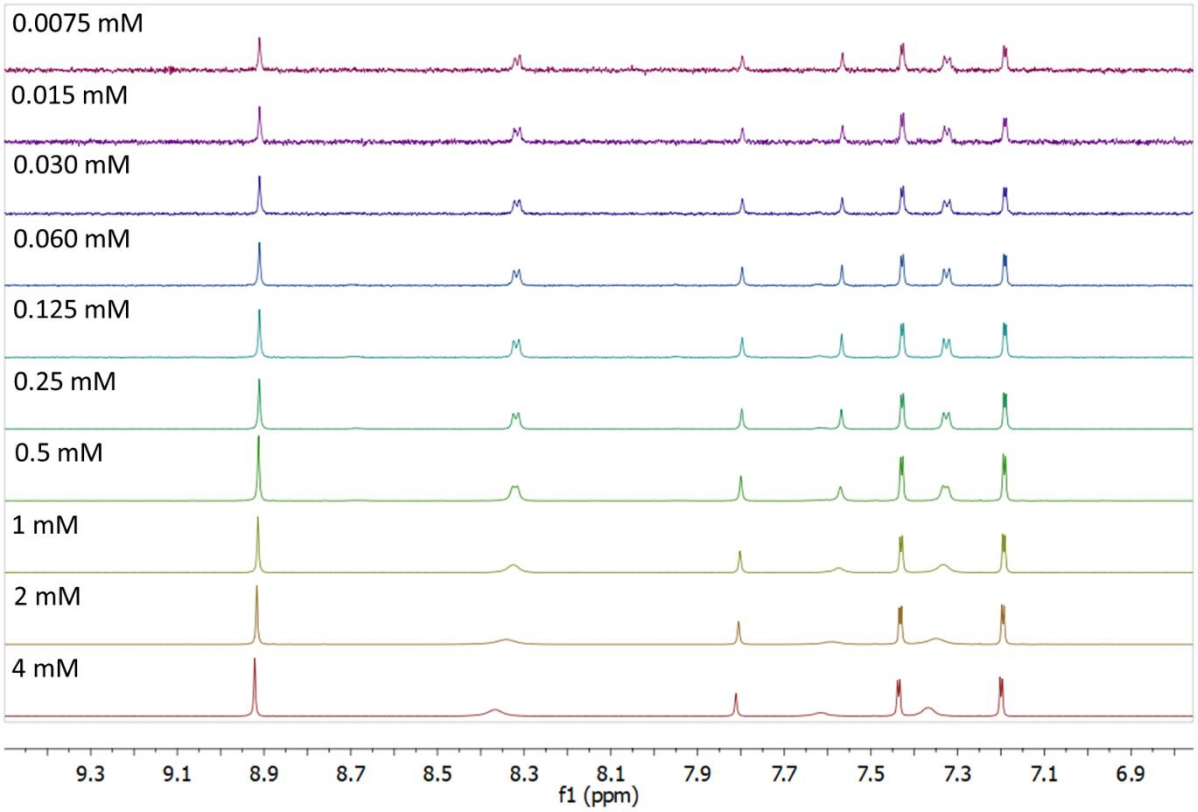

*Figure S41: Variable concentration NMR spectra of cage **1** (500 MHz, CD_2Cl_2, 298 K). Focus on aromatic area. Please note that the intensity of the individual spectra has been adjusted.*

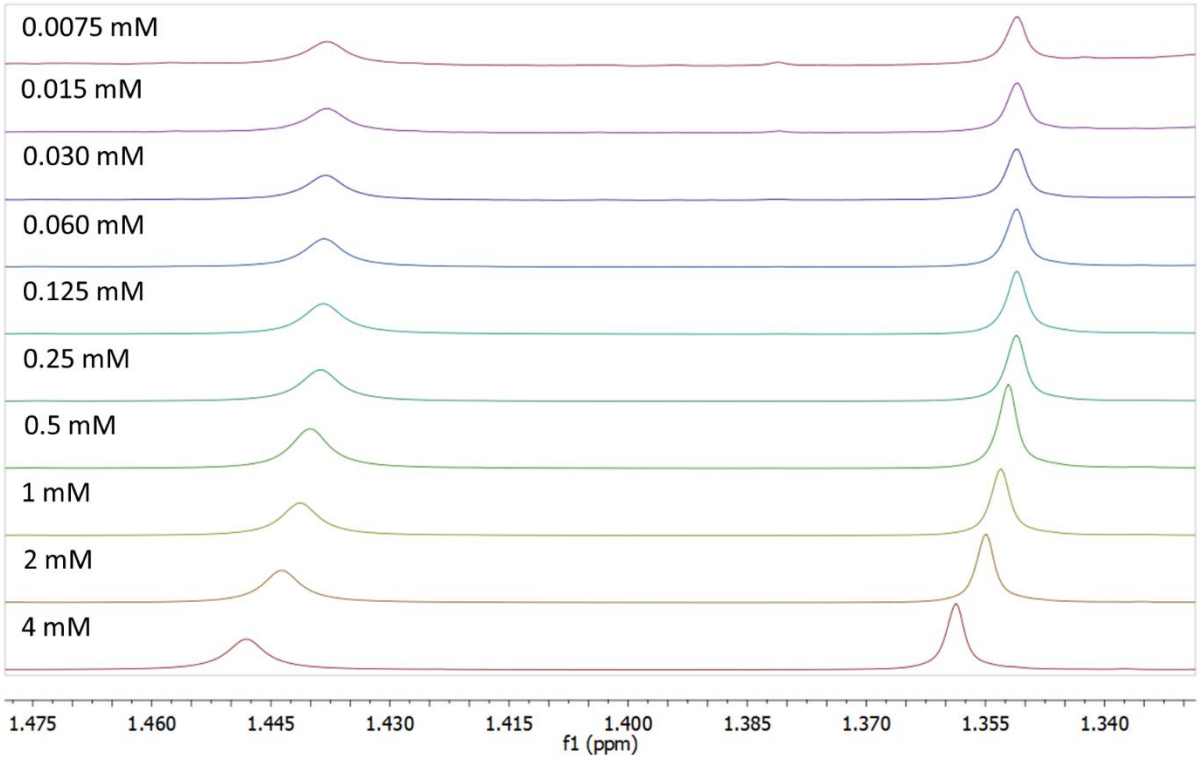

*Figure S42: Variable concentration NMR spectra of cage **1** (500 MHz, CD_2Cl_2, 298 K). Focus on aliphatic area. Please note that the intensity of the individual spectra has been adjusted.*

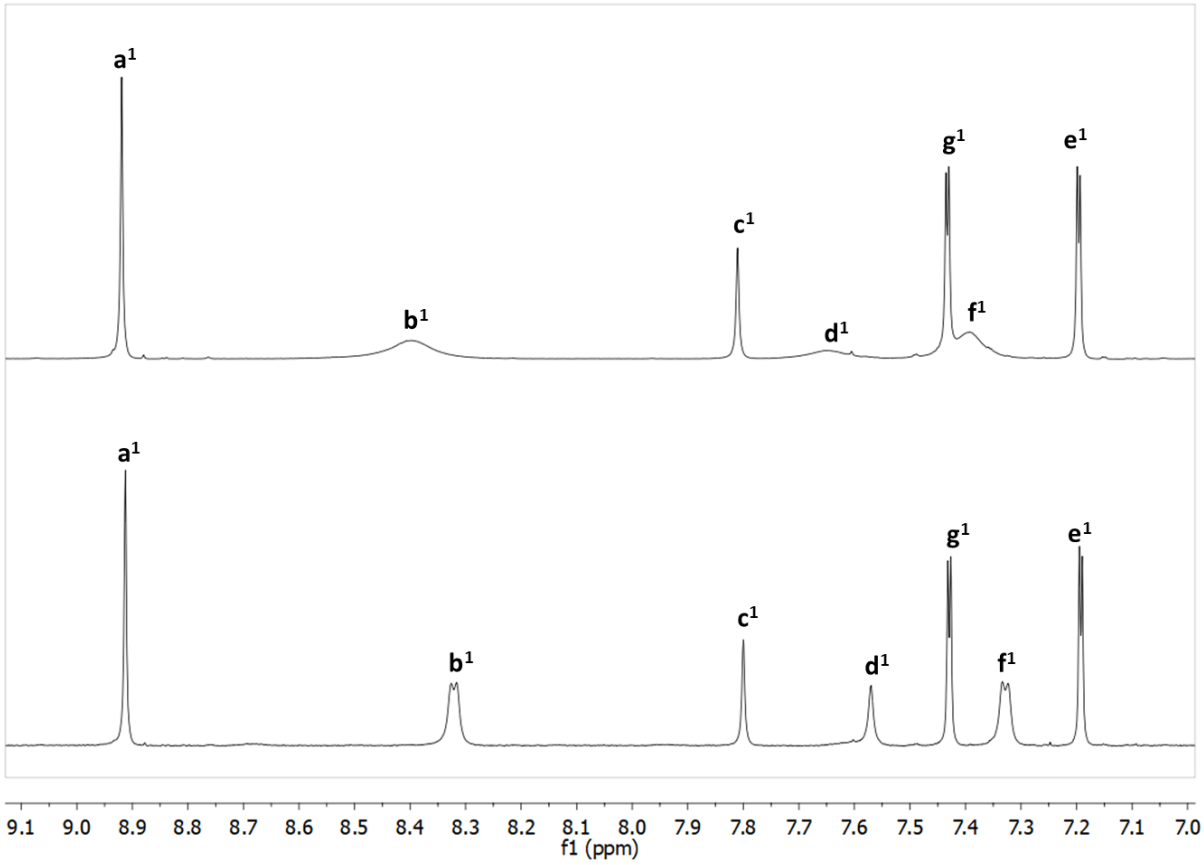

*Figure S43: ^{1}H NMR spectra of cage **1** assembly with excess of **A** (3 equivalents) **[**2.0 mM] (top) and ^{1}H NMR spectra of cage **1** with **Zn_2L** (4 equivalents) (bottom) [2.0 mM] (500 MHz, CD_2Cl_2, 298 K). To be noted that peaks **b^1**, **d^1**, and **f^1** shift and broaden.*

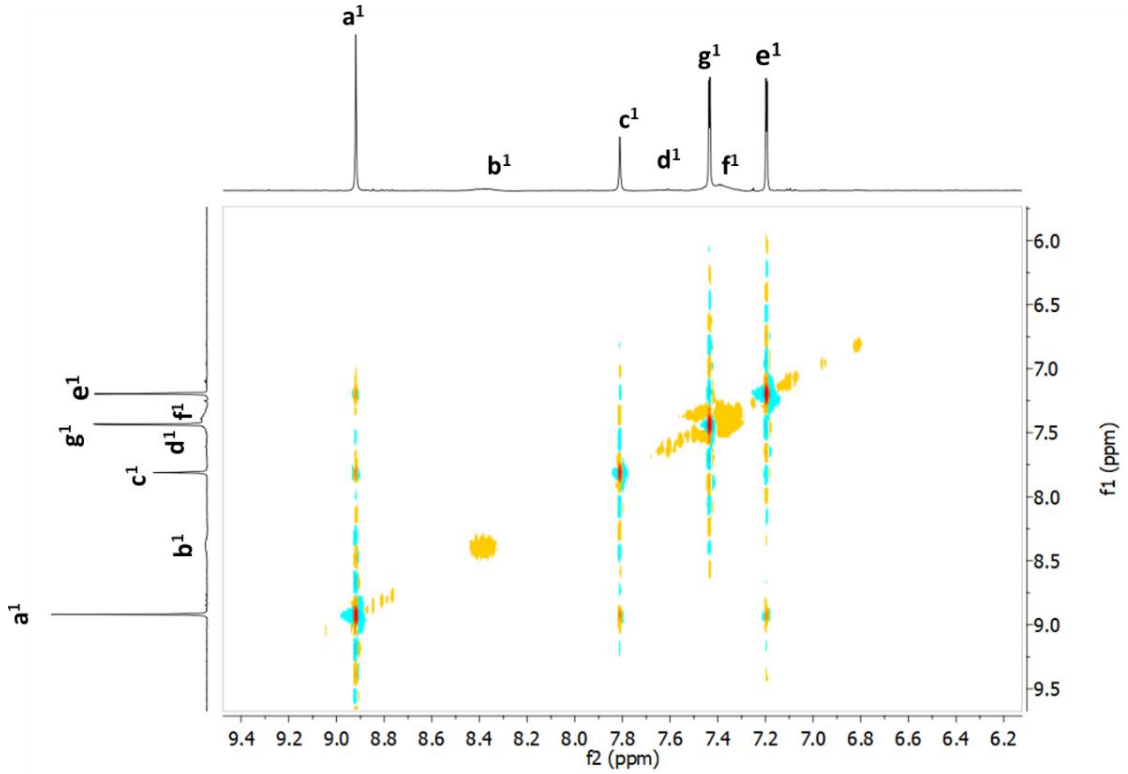

*Figure S44: Zoom into aromatic region of the EXSY NMR spectrum of cage **1** with excess of **A** (1 equivalent) [1 mM] (600 MHz, CD_2Cl_2, 298 K).*

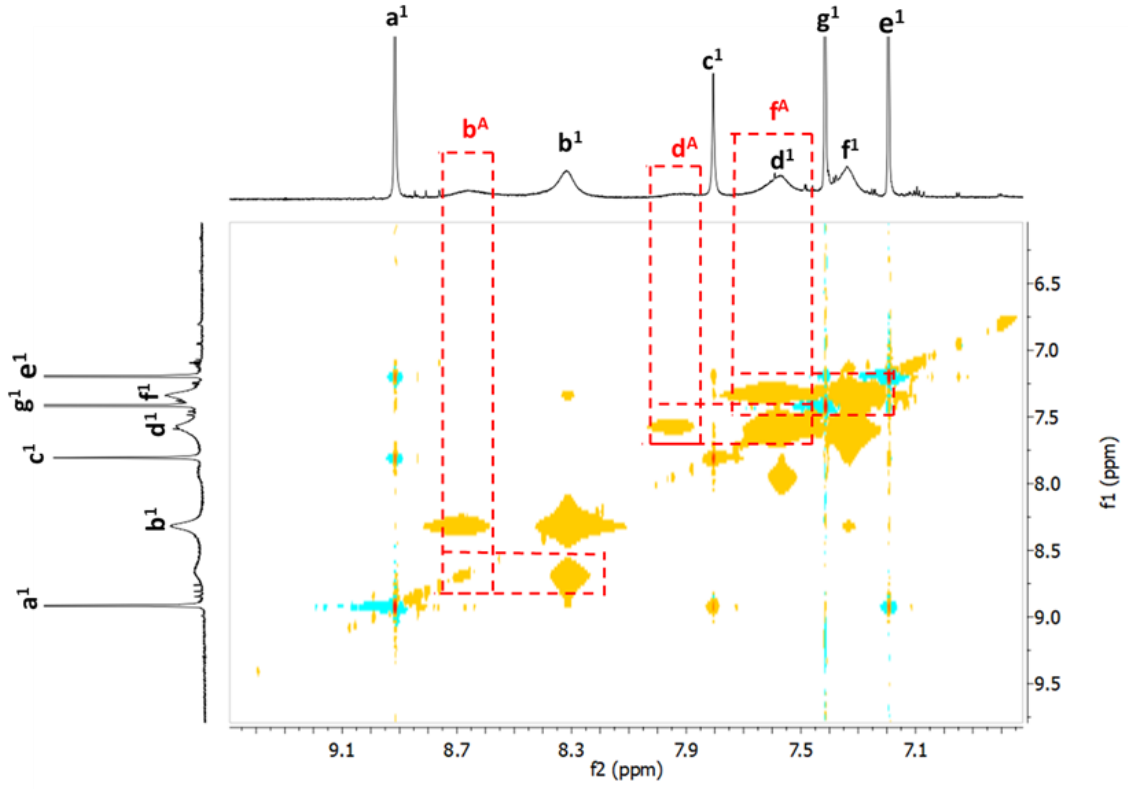

*Figure S45: Zoom into aromatic region of the EXSY NMR spectrum of cage **1** with excess of **A** (1 equivalent) [1 mM] (1000 MHz, CD_2Cl_2, 278 K).*

4.2. Dilution series cage 2

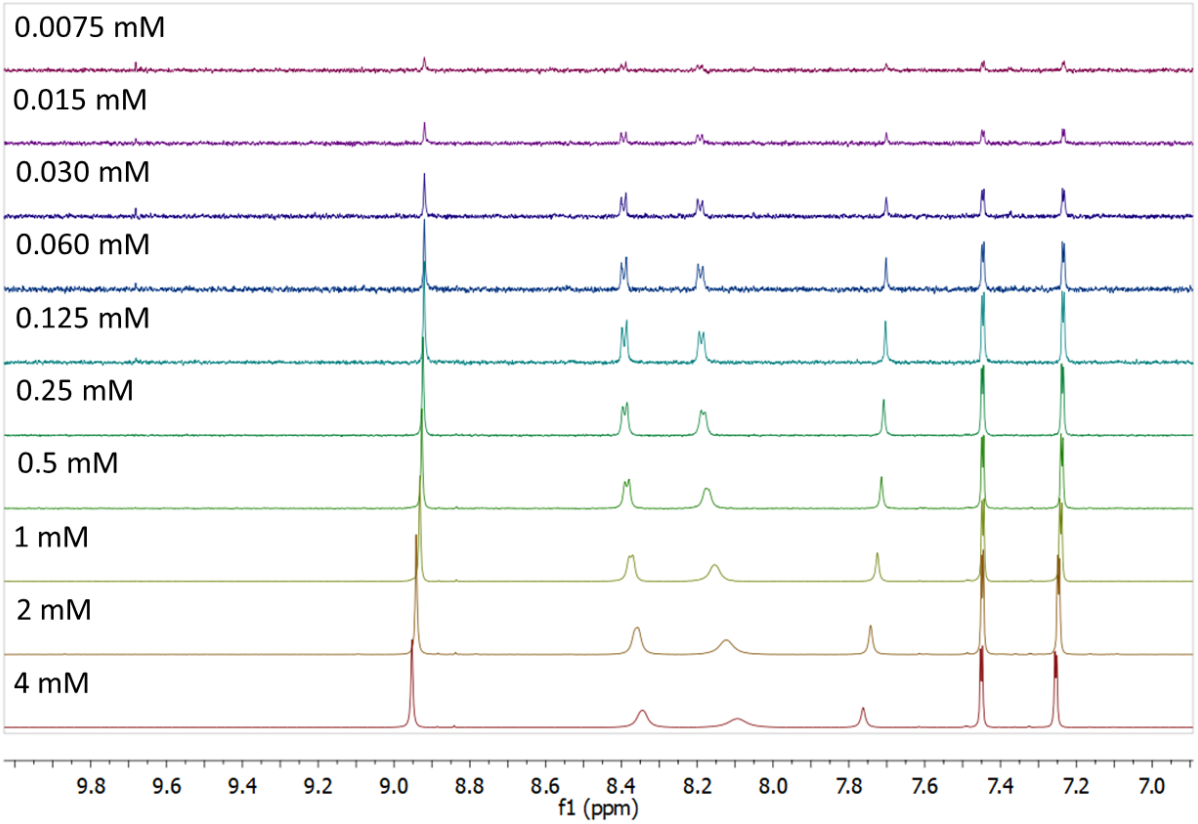

*Figure S46: Variable concentration NMR spectra of cage **2** (500 MHz, CD_2Cl_2, 298 K). Zoom into aromatic area. Please note that the intensity of the individual spectra has been adjusted.*

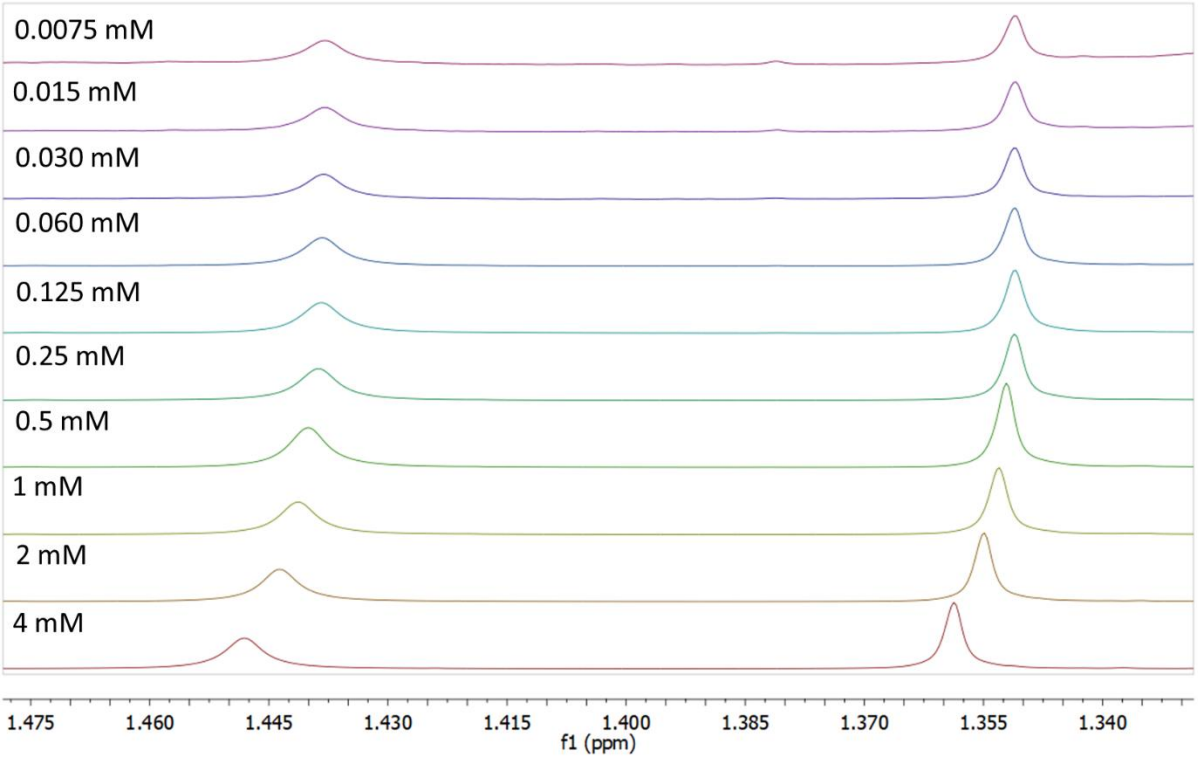

*Figure S47: Variable concentration NMR spectra of cage **2** (500 MHz, CD_2Cl_2, 298 K). Focus on aliphatic area. Please note that the intensity of the individual spectra has been adjusted.*

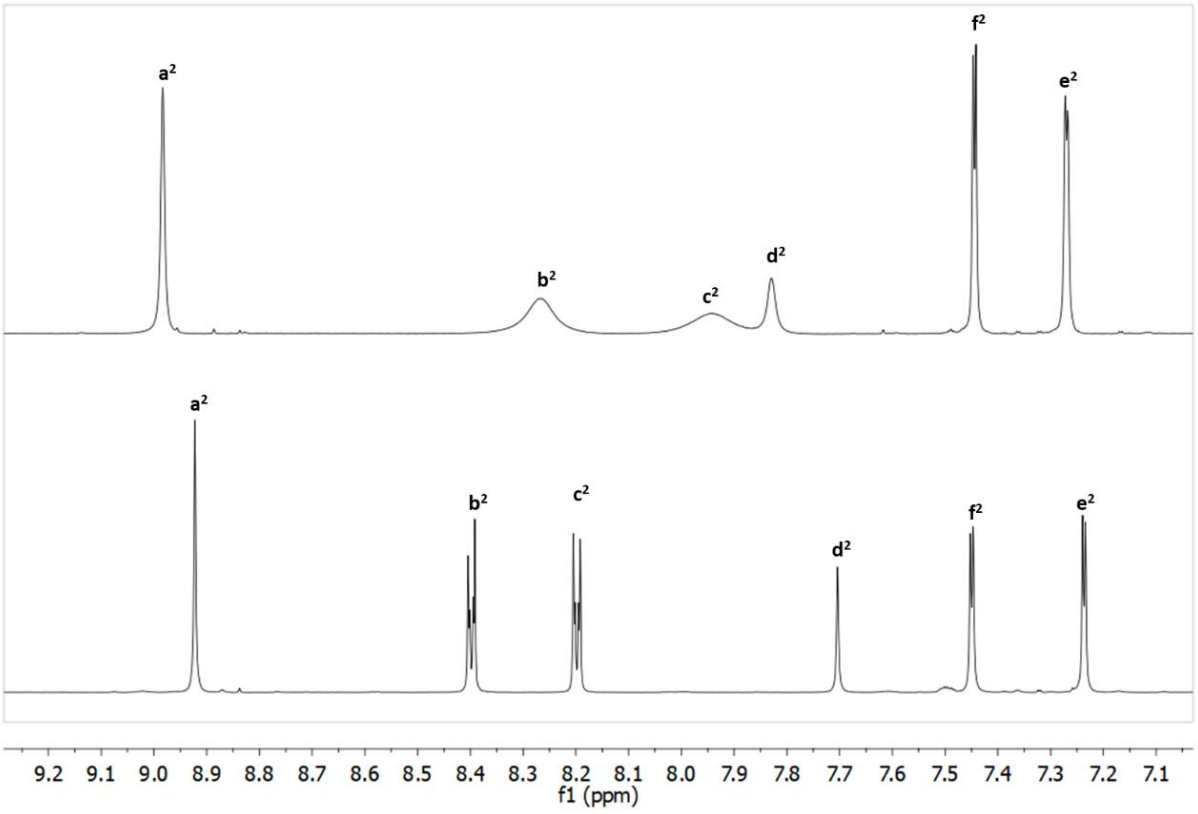

*Figure S48: ^{1}H NMR spectra of cage **2** assembly with excess of **B** (3 equivalents) [2.0 mM] (top) and ^{1}H NMR spectra of cage **2** with **Zn_2L** (4 equivalents) (bottom) [2.0 mM] (500 MHz, CD_2Cl_2, 298 K).*

5. Optical studies

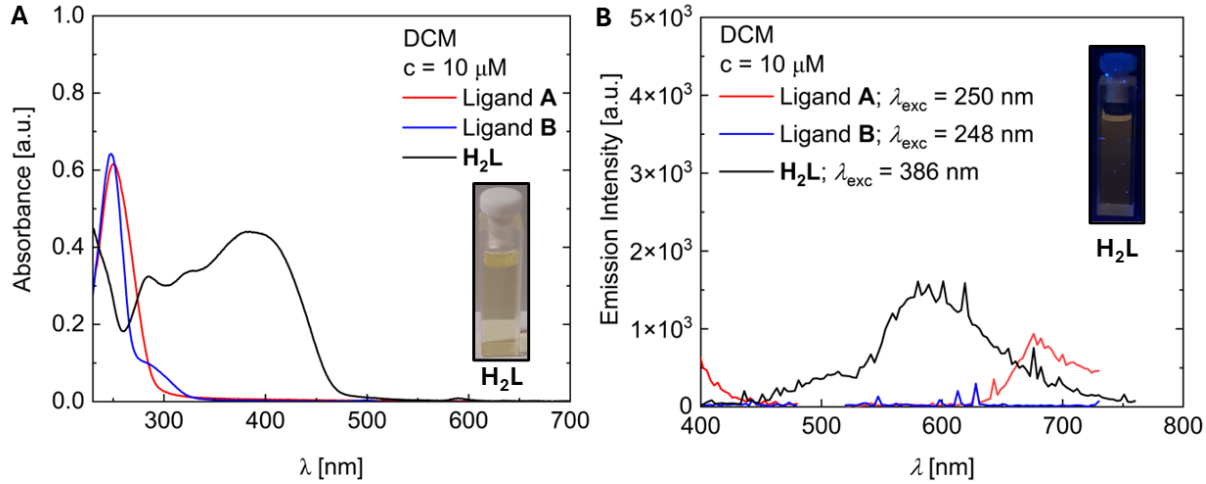

*Figure S49: Absorbance (**A**) and emission (**B**) spectra of **A**, **B**, and **H_2L** in DCM (c = 10 μM, 10mm cuvette). The emission measurements were performed with the same parameters than utilized for the emission measurement of **Zn_2L** and cage **1**. Please note that the scale in B is 10^3, while for the other emission spectra it is 10^5.*

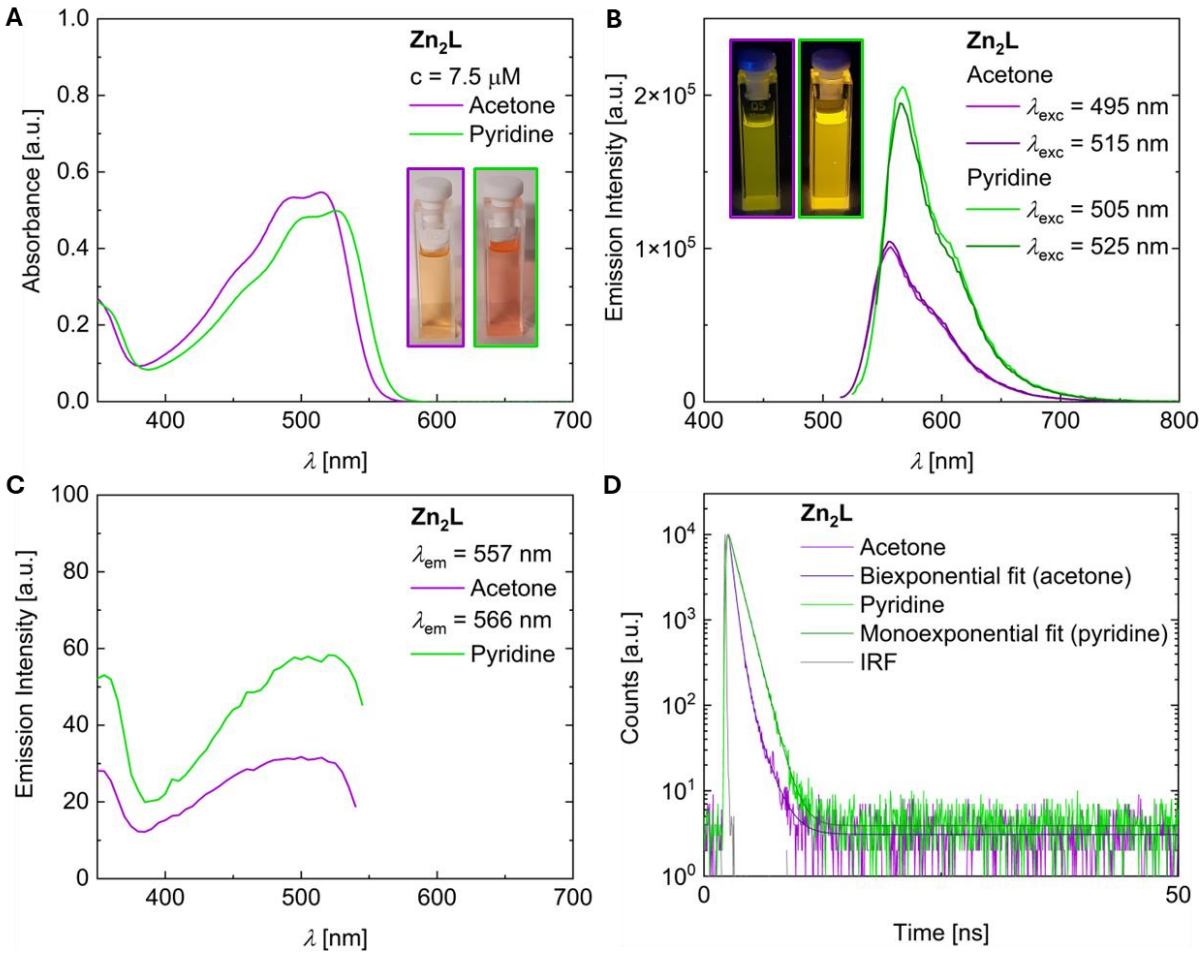

*Figure S50: Absorbance (**A**), emission (**B**), fluorescence excitation (**C**) spectra of **Zn_2L** in acetone and pyridine (c = 7.5 μM, 10mm cuvette). TCSPC detected fluorescence decays of **Zn_2L** in acetone and pyridine (**D**) (IRF = instrumental resolution file).*

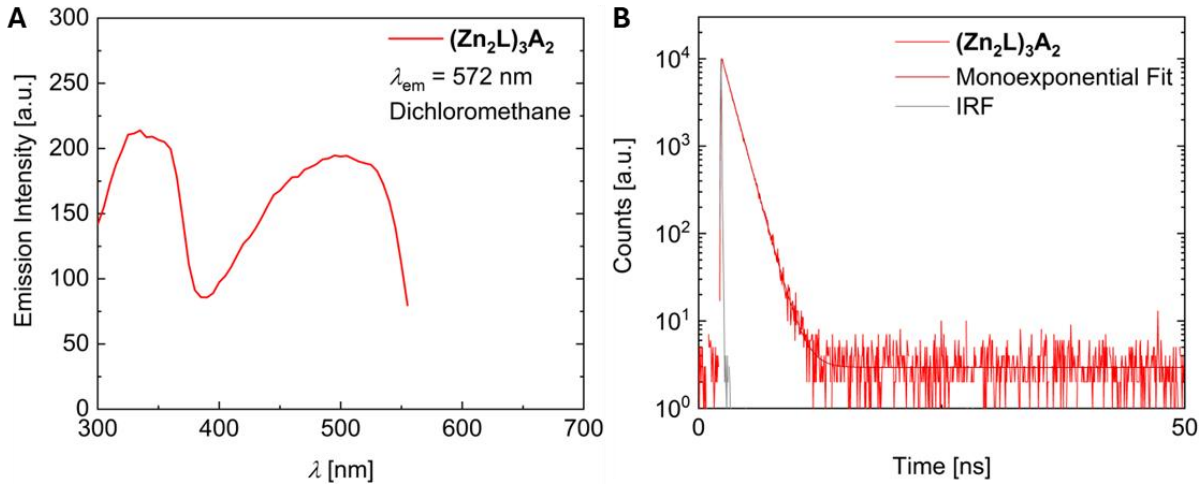

*Figure S51: Fluorescence excitation (**A**) spectrum of cage **1** in DCM (c = 16 μM, 2mm cuvette). TCSPC detected fluorescence decays of cage **1** in dichloromethane (**B**) (IRF = instrumental resolution file).*

*Table S2: Absorbance maxima, extinction, and extinction coefficients of **Zn_2L**, cage **1**, and cage **2**. Please note that the **Zn_2L** solutions were measured in a cuvette with 10mm diameter, while the cage solutions were measured in a 2mm cuvette.*

Compound	Solvent	λ_{max} [nm]	E [a.u.]	ε [$M^{-1}\cdot cm^{-1}$]
Zn_2L	Acetone	492	0.53	71000
		515	0.55	73000

	Pyridine	335	0.29	38000
		503	0.48	64000
		525	0.50	66000
Cage **1**	DCM	330	0.27	85000
		500	0.44	138000
Cage **2**	DCM	328	0.37	116000
		495	0.55	173000

* Absorbance band at 330 nm could not be determined for acetone due to self-absorption of the solvent.

Table S3: PL lifetimes in ns (λ_{exc}= 355 nm) and amplitudes of the biexponential fit components recorded at the respective maximum detection wavelengths.

Compound	Solvent	τ_1 [ns]; (amplitude ratio [%])	τ_2 [ns]; (amplitude ratio [%])
Zn_2L	Acetone	1.25 (7%)	0.44 (93%)
	Pyridine	0.97 (100%)	
Cage **1**	DCM	1.07 (100%)	

6. Mixed assemblies

Mixed assemblies were carried out by reacting **A** and **B** in different ratios (in total 2 eq) with three equivalents of complex **Zn_2L** in dichloromethane for 3h at room temperature. The ratios of **A** and **B** are highlighted in the ^{1}H NMR stacked spectra in Figures S45 and S46.

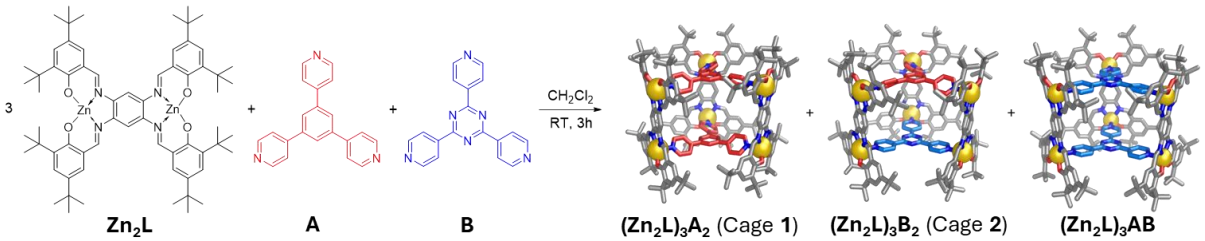

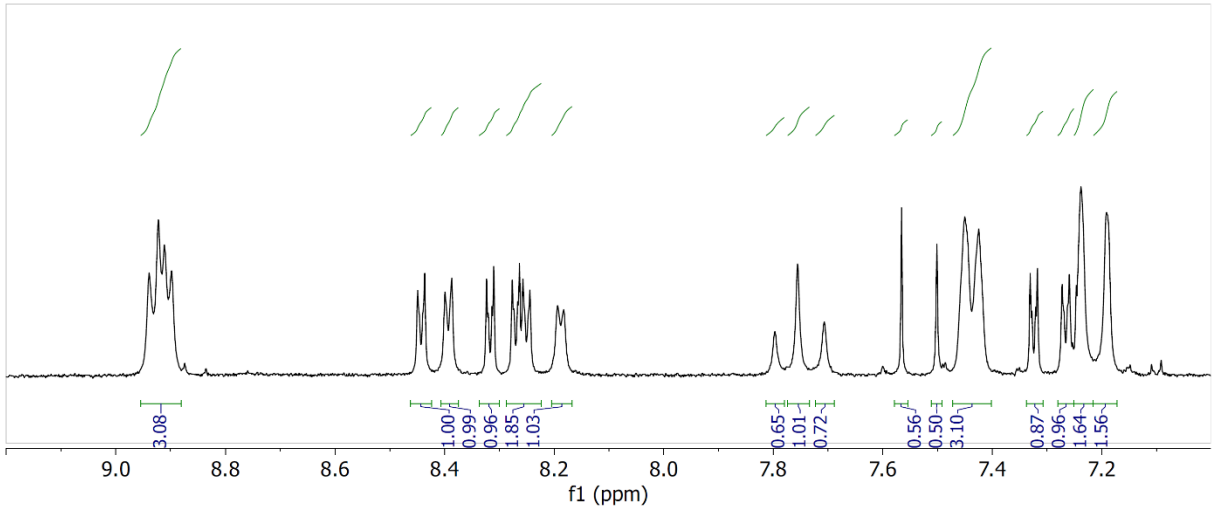

*Figure S52: ^{1}H NMR spectrum of the mixed assembly **A**:**B** 1:1 assembly [0.5 mM] (500 MHz, CD_2Cl_2, 298 K).*

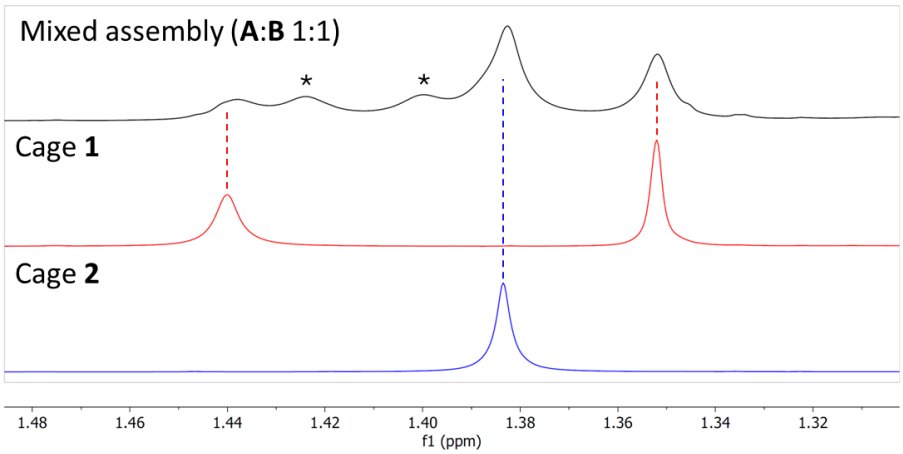

*Figure S53: Stacked ^{1}H NMR of mixed assembly with cage **1** [0.5 mM] and cage **2** [0.5 mM] (500 MHz, CD_2Cl_2, 298 K). Asterisks indicating new signals belonging to the mixed cage **$(Zn_2L)_3AB$**. Focus on the aliphatic area.*

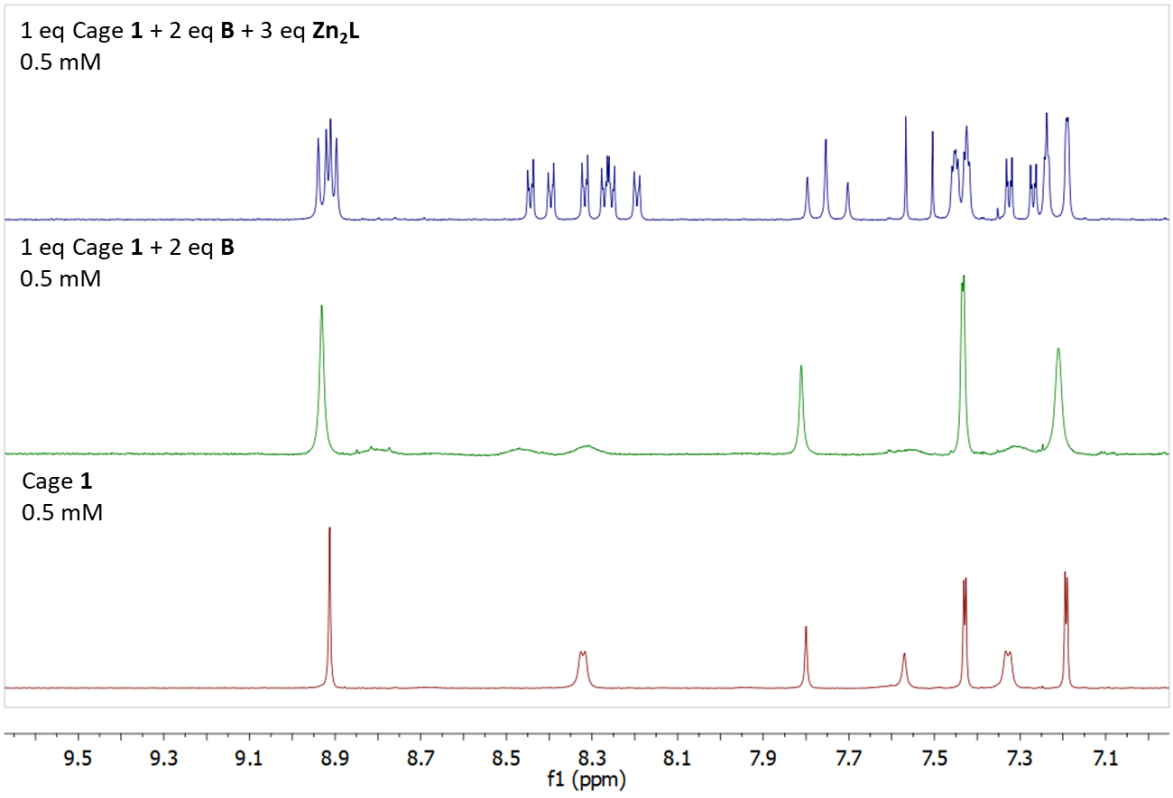

*Figure S54: Exchange experiment of cage **1** with **B**. To a solution of cage **1** [1.6 mM], were added 2 eq **B** (0.5 mg, 1.6 µmol). Due to the broadness of signals, 3 eq **Zn_2L** (2.7 mg, 2.4 µmol) were added to clarify whether the mixed cage assembly forms. ^{1}H NMR spectra of the diluted solutions [0.5 mM] are given (500 MHz, CD_2Cl_2, 298 K).*

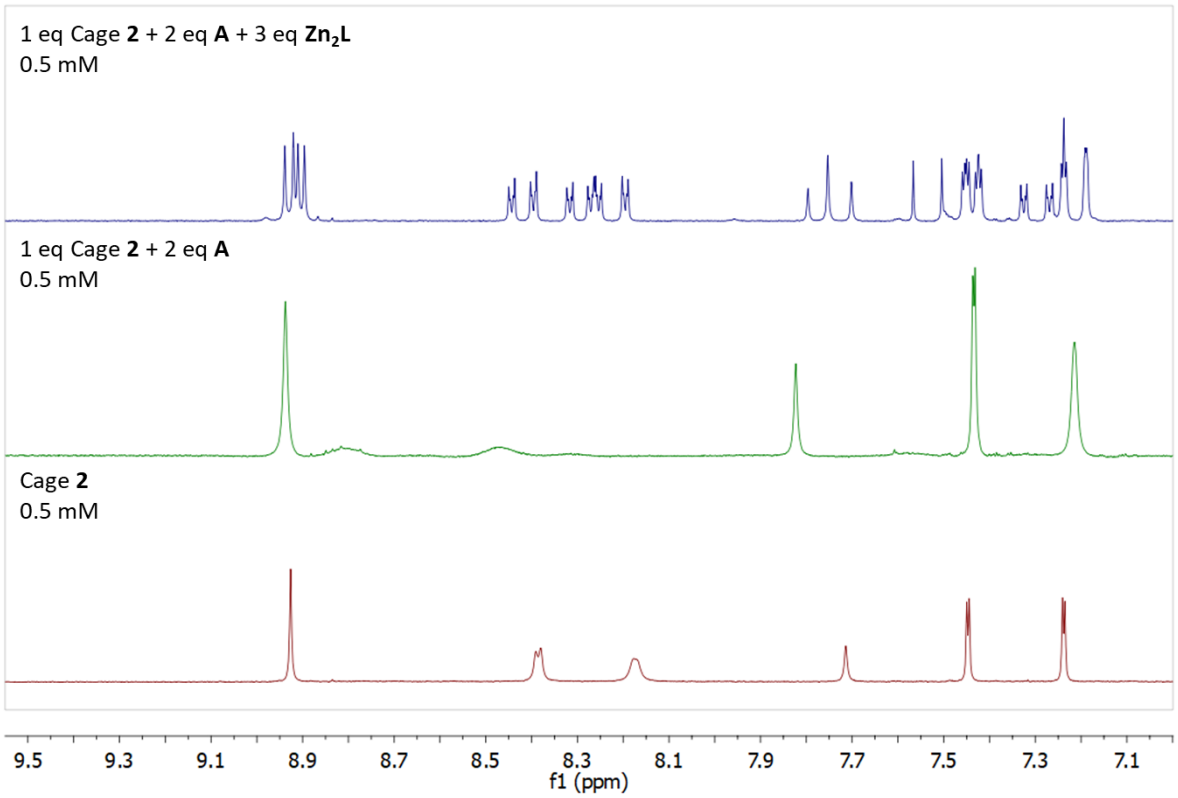

*Figure S55: Exchange experiment of cage **2** with **A**. To a solution of cage **2** [1.6 mM], were added 2 eq **A** (0.5 mg, 1.6 µmol). Due to the broadness of signals, 3 eq **Zn$_2$L** (2.7 mg, 2.4 µmol) were added to clarify whether the mixed cage assembly forms. ^{1}H NMR spectra of the diluted solutions [0.5 mM] are given (500 MHz, CD_2Cl_2, 298 K).*

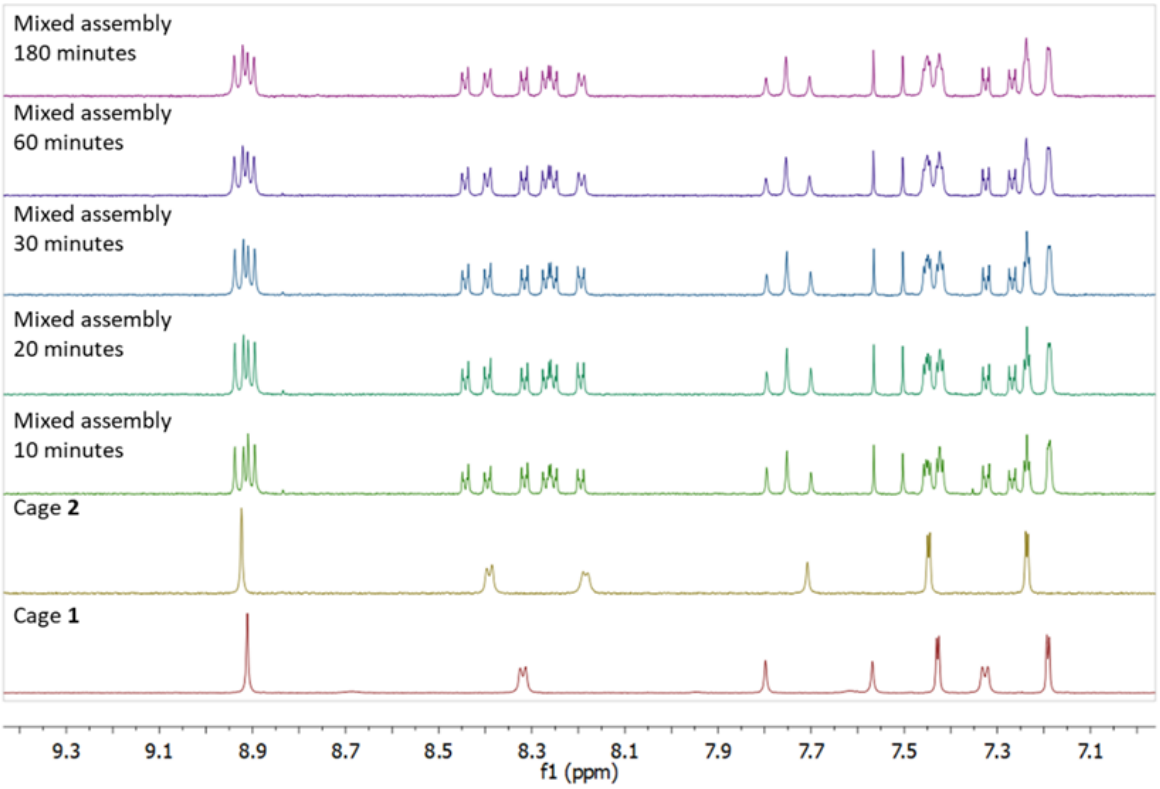

Figure S56: Time-dependent ^{1}H NMR spectra of the mixed cage assembly (500 MHz, CD_2Cl_2, 298 K). The assembly was carried out at 3 mM. Aliquots of the reaction solution were removed after the respective time intervals and diluted to 0.5 mM prior to the ^{1}H NMR experiment. The poor solubility of the educts prevents any measurement prior to 10 minutes.

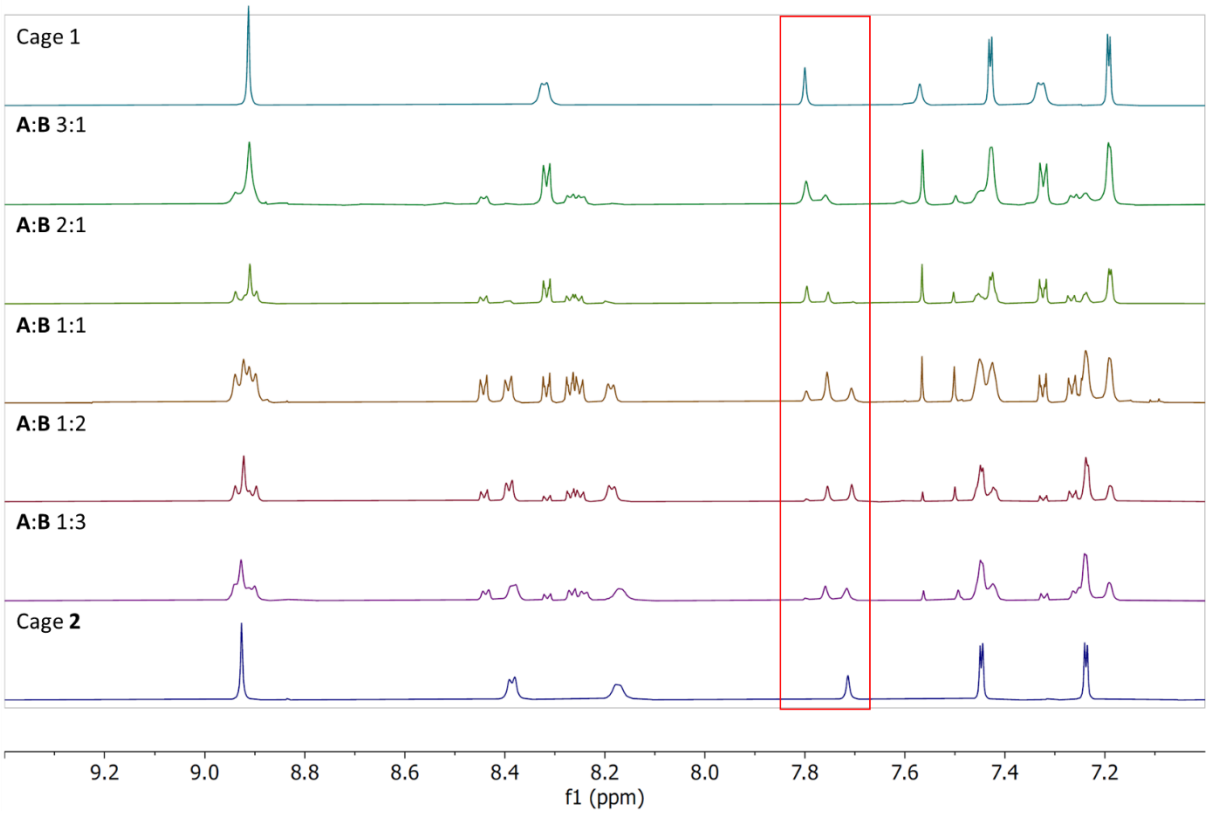

*Figure S57: Stacked ^{1}H NMR spectra of cages assemblies with different **A** and **B** ratios forming the respective cages in the same exact ratio. [0.5 mM] of total cage concentration (500 MHz, CD_2Cl_2, 298 K). Focus on aromatic area.*

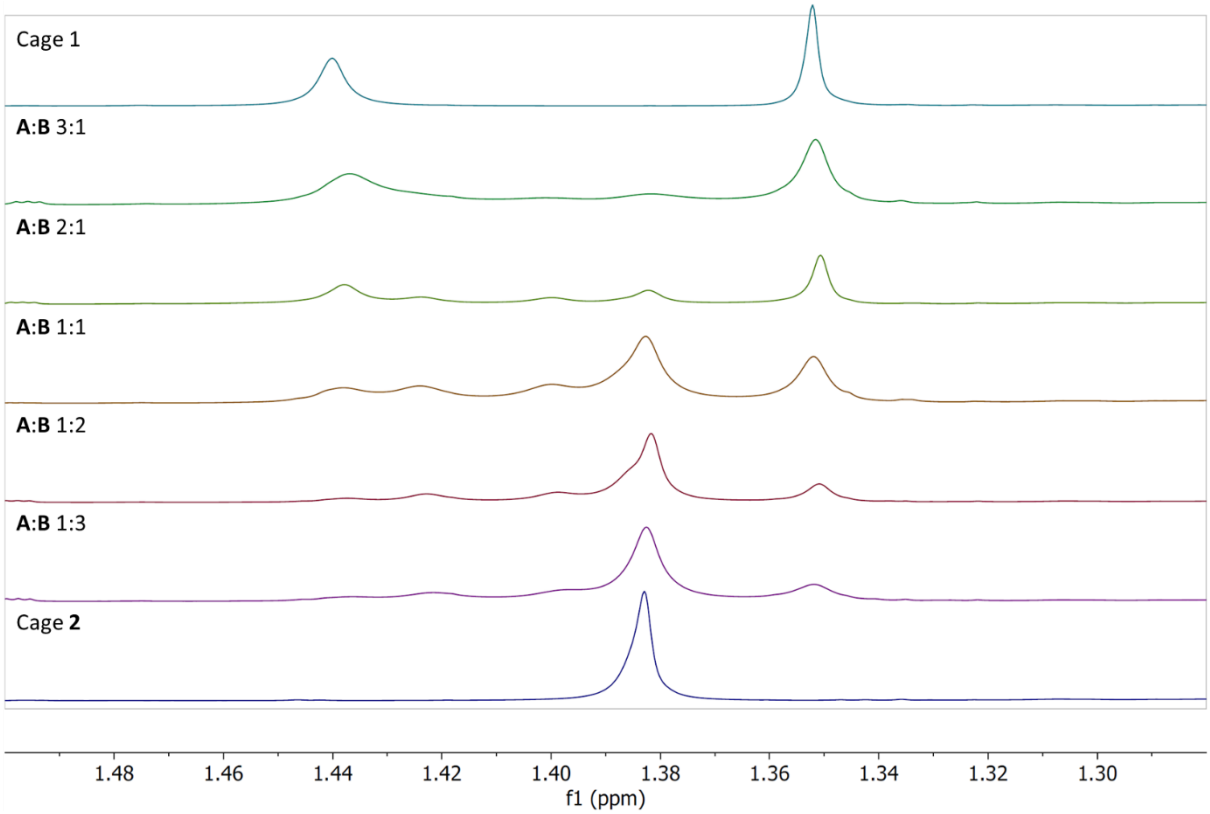

*Figure S58: Stacked ^{1}H NMR spectra of cages assemblies with different **A** and **B** ratios forming the respective cages in the same exact ratio [0.5 mM] of total cage concentration (500 MHz, CD_2Cl_2, 298 K). Focus on aliphatic area.*

*Table S4: Determination of the ratio of cage **1** $(Zn_2L)_3A_2$, mixed cage $(Zn_2L)_3AB$, and cage **2** $(Zn_2L)_3B_2$ within the self-assemblies of cages with varying **A**:**B** ratio. Proton 1 corresponds to cage **1**, proton 2 to the mixed cage and proton 3 to cage **2**. The percentages were calculated by dividing the respective integral against the sum of the integrals of the three signals.*

Sample	Integral 1 7.80 ppm (Cage **1**)	Integral 2 7.76 (mixed Cage)	Integral 3 7.71 (Cage **2**)	Sum of integrals 1-3	Cage **1** [%]	Mixed Cage (%)	Cage **2** (%)
A:**B** 2:1	1.25	0.88	0.15	2.28	55	39	7
A:**B** 1:1	0.18	0.4	0.24	0.82	22	49	29
A:**B** 1:2	0.06	0.28	0.33	0.67	9	42	49

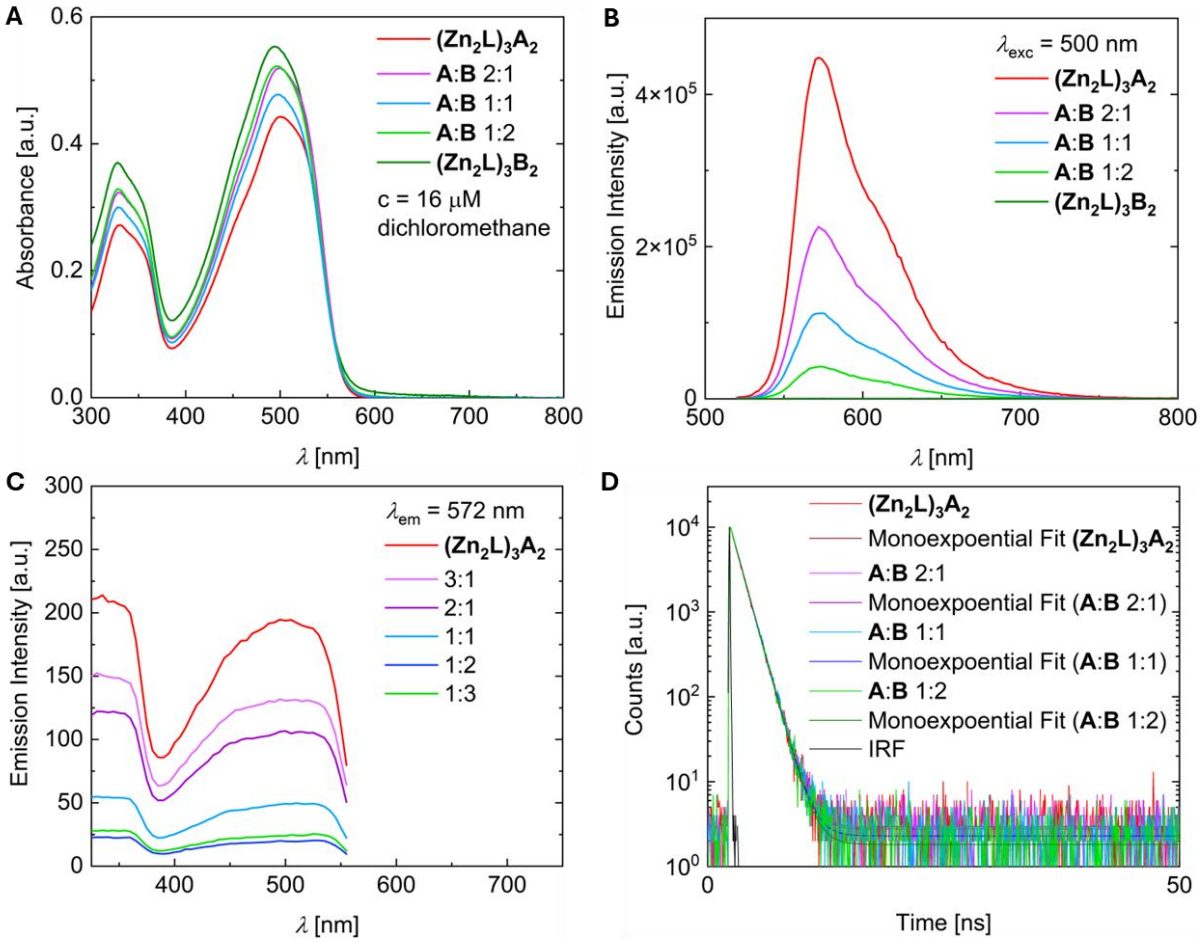

*Figure S59: Absorbance (**A**), emission (**B**), fluorescence excitation (**C**) spectra of mixed cage assemblies with varying **A:B** ratios in dichloromethane (c = 16 μM, 2mm cuvette). TCSPC detected fluorescence decays of mixed cage assemblies (**D**) (IRF = instrumental resolution file).*

*Table S5: Determination of normalized emission intensity in mixed cage series with different **A:B** ratios. PL lifetimes in ns (λ_{exc}= 355 nm) detected at the emission maximum λ_{det} = 574 nm. The data was fitted with a monoexponential decay function.*

Compound	Emission intensity at $\lambda_{Em,max}$ = 574 nm, [Counts]	Normalized emission intensity [%]	τ_1 [ns]
Cage **1**	448393	100	1.066
A:**B** 2:1	226026	50	1.067
A:**B** 1:1	112376	25	1.074
A:**B** 1:2	42095	9	1.068
Cage **2**	0	0	(non-emissive)

7. Host-guest chemistry

Molovol 1.2.0[7] has been used to calculate the cavity volume and shape of both cages from its crystal structure. The "Probe-occupied volume" (V_{occ}) has been obtained via calculation using the "two-probe mode". The parameters used for the calculation are:

Small probe radius: 2.4 Å
Large probe radius: 4.0 Å
Grid resolution: 0.1 Å
Optimization depth: 5
Element radii: Zn = 2.39 Å, C = 1.77 Å, H = 1.20 Å, N = 1.66 Å, O = 1.50 Å
Based on the calculations the interior volume of cage **1** is 933 Å^3, and that of cage **2** is 1277 Å^3.

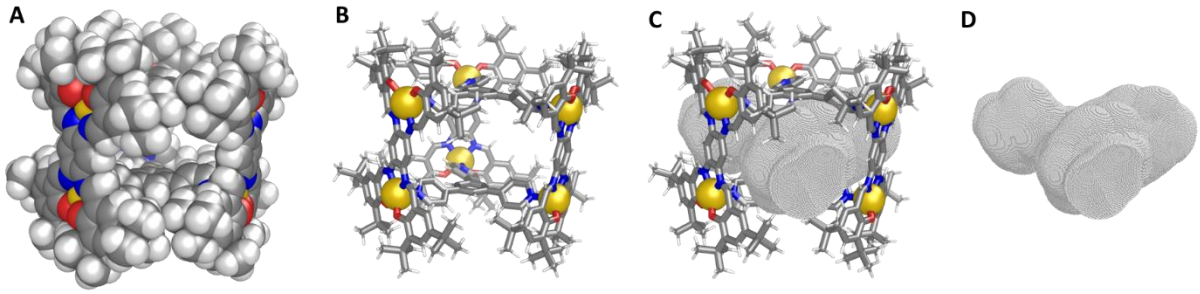

*Figure S60: MM2 models of cage **1**. Color code: C (grey), H (white), N (blue), O (red), and Zn (yellow). **A** spacefill model, **B** stick model, **C** stick model with cavity volume, and **D** cavity volume of cage **1**.*

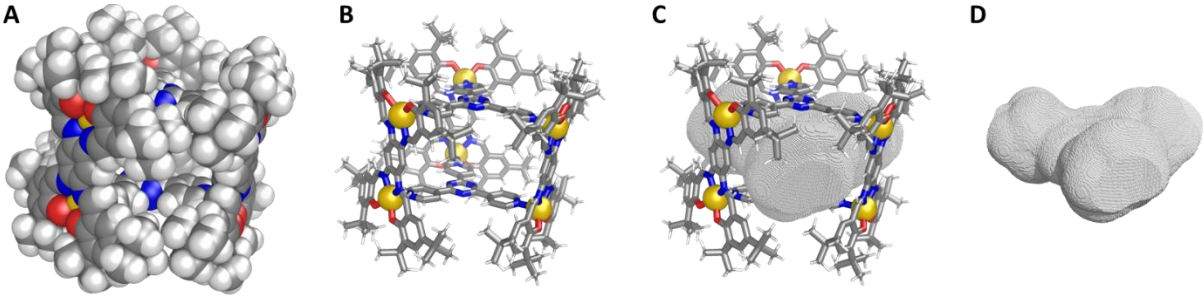

*Figure S61: MM2 models of cage **2**. Color code: C (grey), H (white), N (blue), O (red), and Zn (yellow). **A** spacefill model, **B** stick model, **C** stick model with cavity volume, and **D** cavity volume of cage **2**.*

NMR host-guest studies were carried out in NMR tubes using a 0.5 mM DCM-d_2 solution of the respective cage. Cage solutions were titrated with the guest of interest until no significant shifts were observed in the NMR spectra.

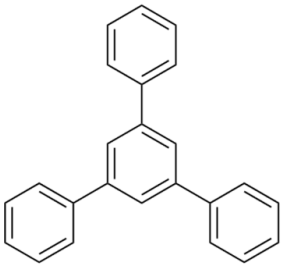

1,3,5-Triphenylbenzene (**G1**)

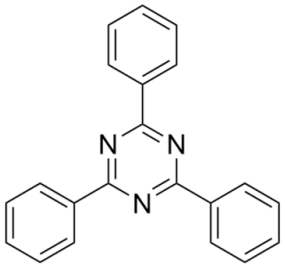

1,3,5-Triphenyltriazine (**G2**)

Screening was performed on two guests with similar geometry and sterics. Given the planar structure of the tritopic pyridyl panels composing the cage, the two cages were screened for planar guests with different electronic and steric properties. Guest volumes were calculated using Molovol[7] (Single probe radius: 1.2 Å, grid resolution: 0.1, optimization depth: 4). Guest **G1** resulted in a volume of 542 Å^3, and **G2** 521 Å^3. These guests satisfy Rebek's 55% rule[8].

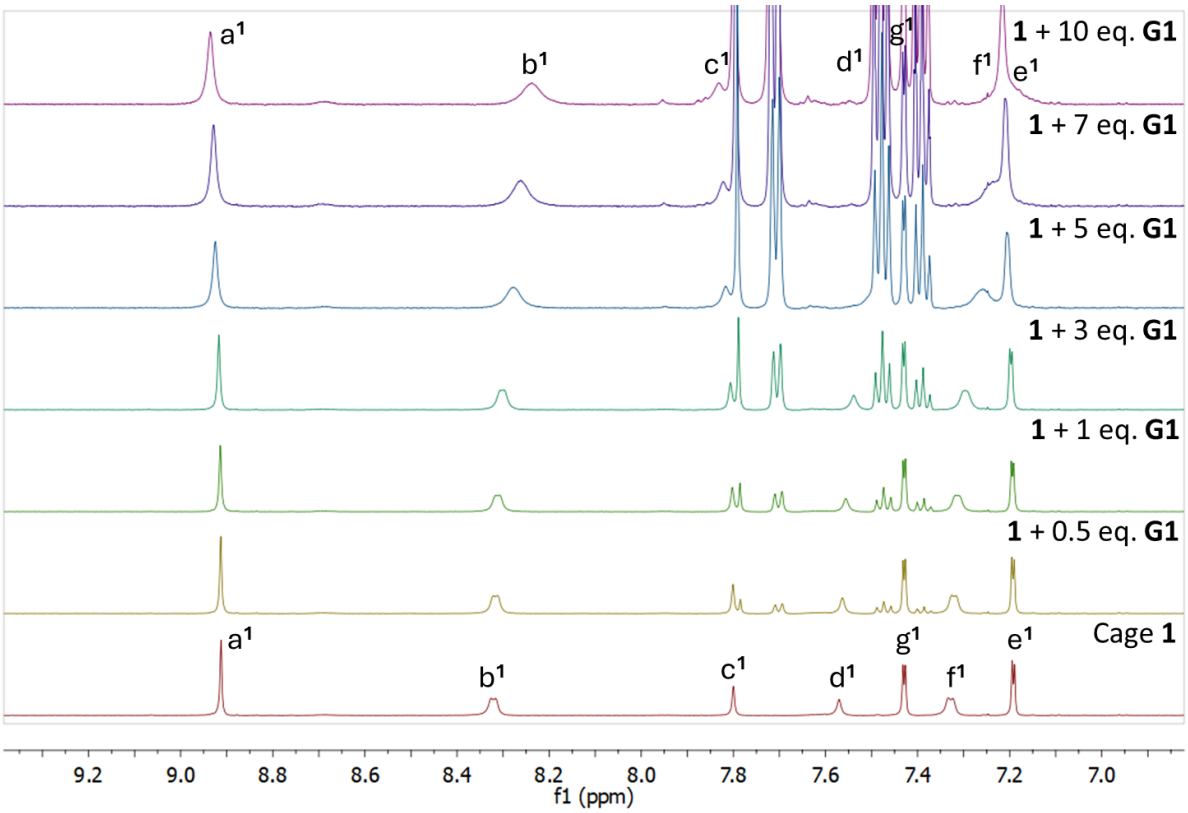

*Figure S62: Stack plot showing changes in the ^{1}H NMR spectrum upon the addition of guest **G1** in a stock solution of cage **1**. Focus on aromatic area.*

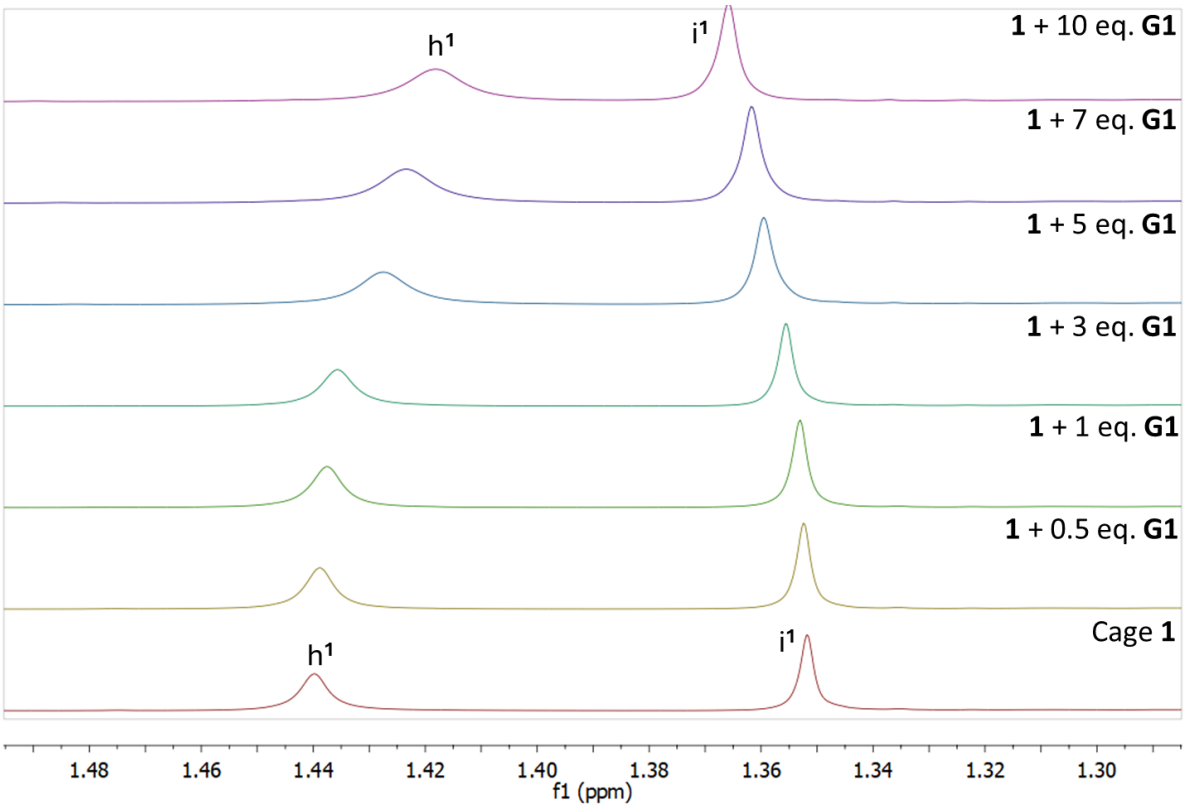

*Figure S63: Stack plot showing changes in the ^{1}H NMR spectrum upon the addition of guest **G1** in a stock solution of cage **1**. Focus on aliphatic area.*

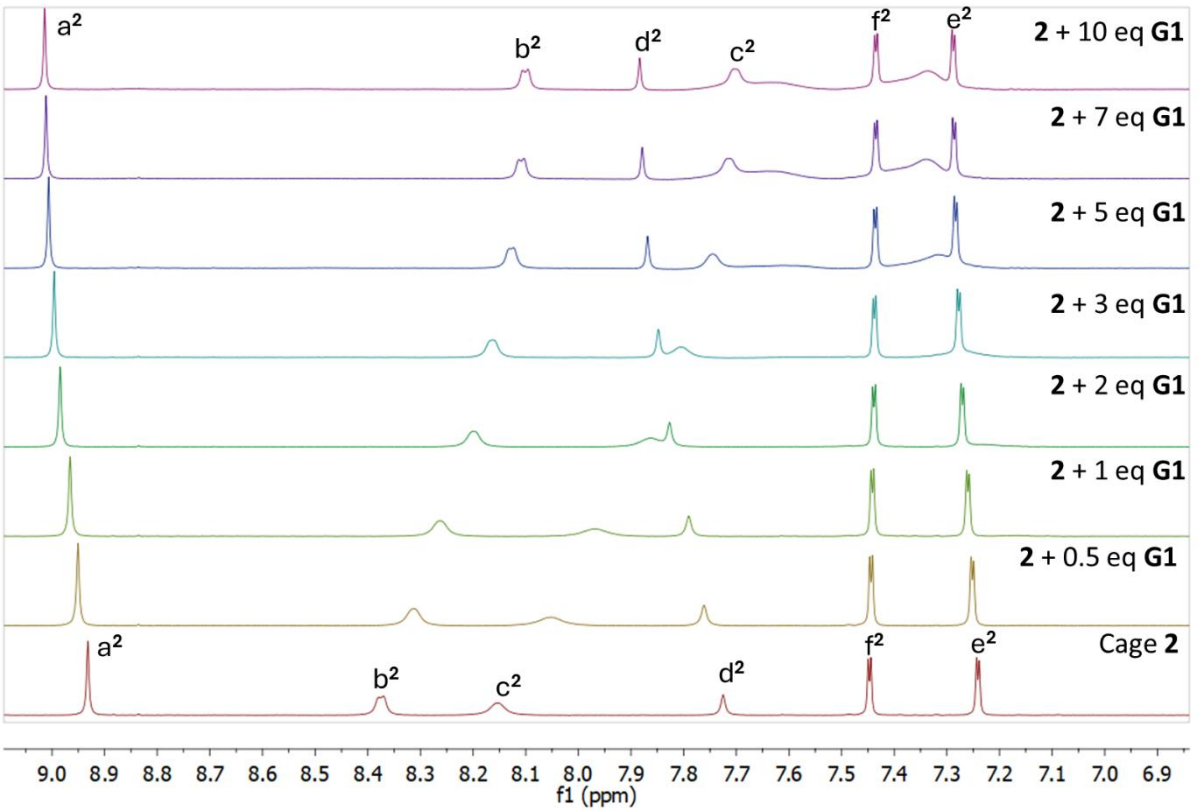

*Figure S64: Stack plot showing changes in the ^{1}H NMR spectrum upon the addition of guest **G1** in a stock solution of cage **2**. Focus on aromatic area.*

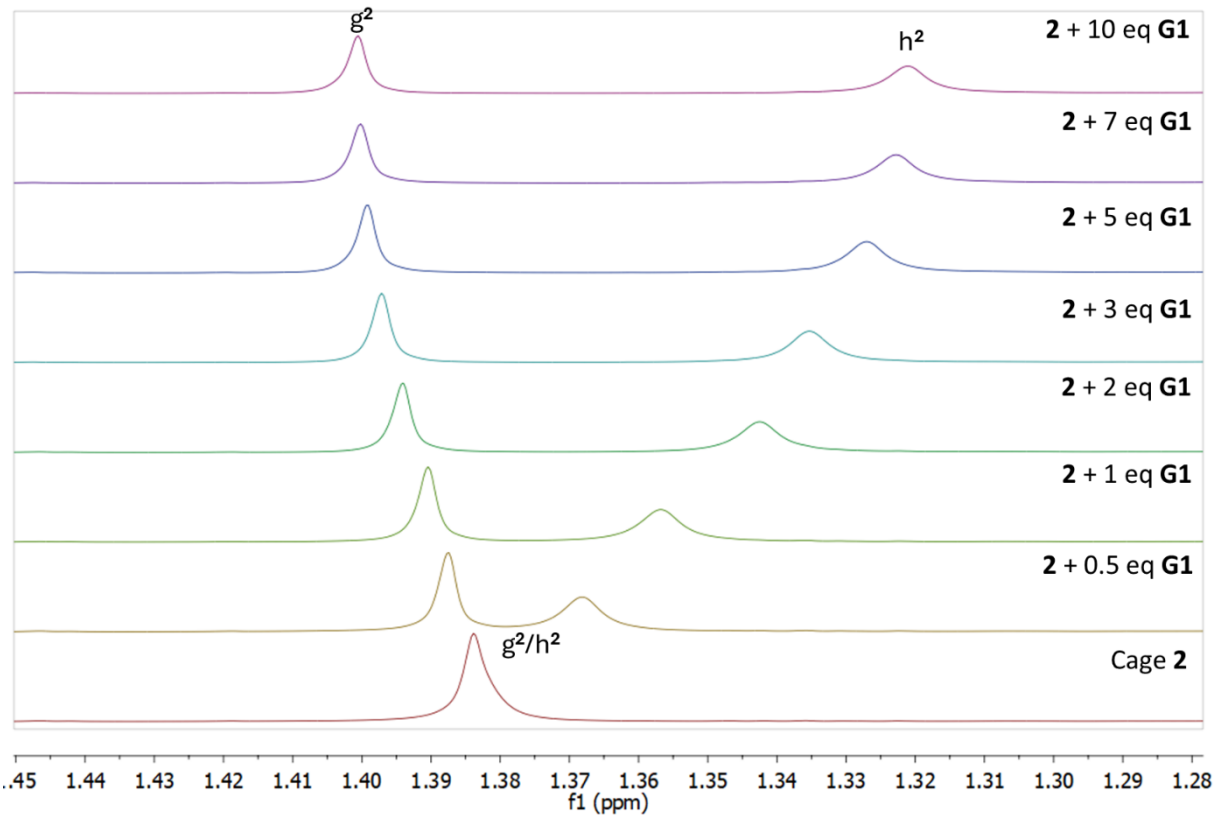

*Figure S65: Stack plot showing changes in the ^{1}H NMR spectrum upon the addition of guest **G1** in a stock solution of cage **2**. Focus on aliphatic area.*

The method of continuous variation (Job plot) allows for the confirmation of the stoichiometry of the binding event. It confirmed the 1:1 host-guest stoichiometry in accordance with the MM2 studies (Figures S60 and S61). We only analysed the binding of cage **2** + **G1** since it was the only host-guest combination that did not result in partly decomposition of the respective cage. Ten ^{1}H NMR samples with different molar fractions of cage **2** and **G1** (χ) were prepared (total concentration c_t = 0.5 mM; see Figure S66).

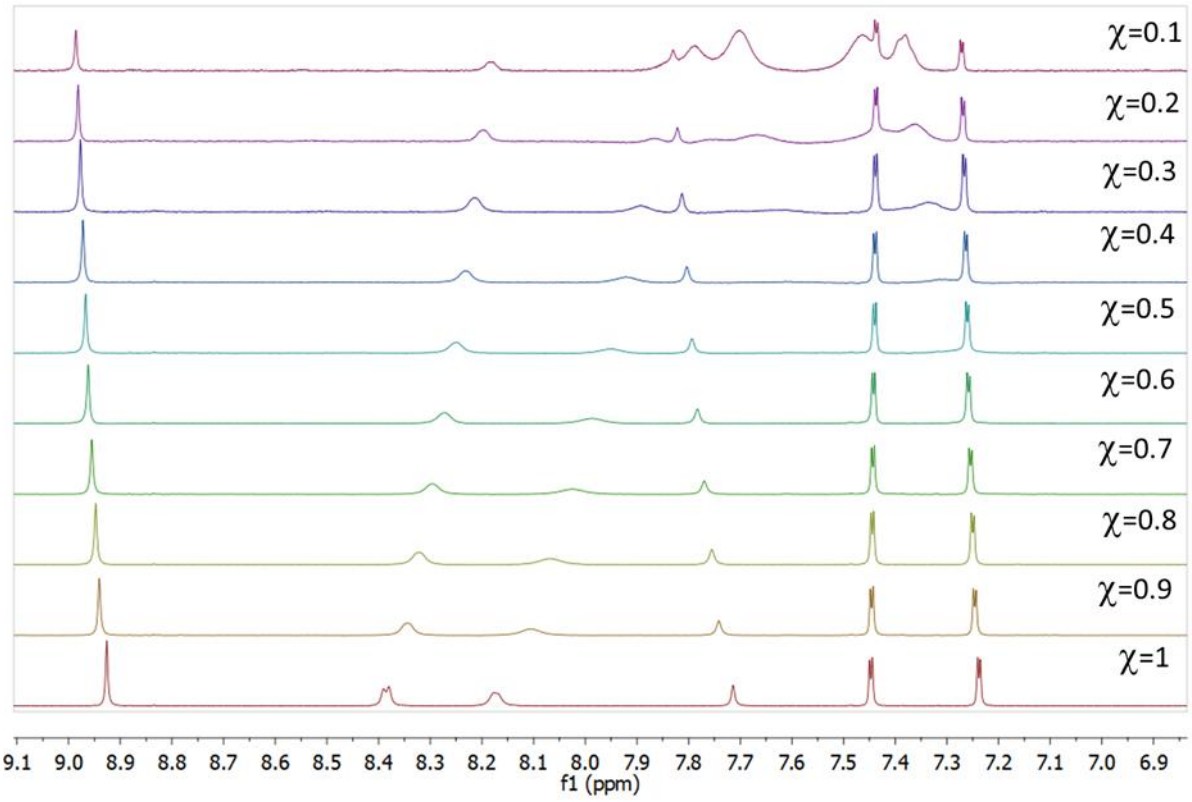

*Figure S66: ^{1}H NMR spectra of molar Cage **2** + **G1** solutions in different molar fractions.*

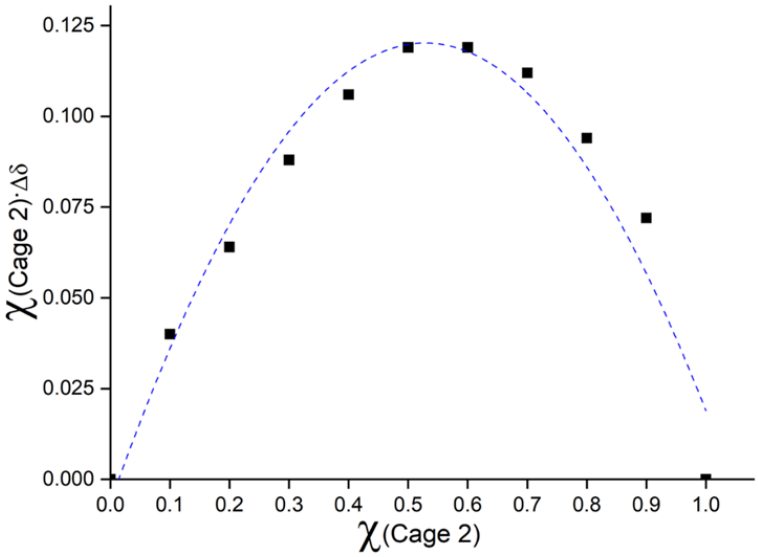

*Figure S67: Job plot for determining the binding stoichiometry of cage **2** and **G1**, produced using ^{1}H NMR shifts of signal c^2.*

Based on the maximum of the Job plot being at approximately χ = 0.5, the 1:1 stoichiometry is confirmed for the cage **2**:**G1** host-guest system. This is coherent with the internal cage **2** volume not being sufficient for encapsulating two guest molecules (see Figure S61).

The Binding analysis was carried out using the Hill equation, where the fractional occupancy (θ) denotes the fraction of bound cages, which can be approximated by the following expression:

$$\Theta = \frac{[bound\ cages]}{[total\ cages]} = \frac{\Delta\delta}{\delta_{saturated\ cages} - \delta_{free\ cage}} \qquad (1)$$

The Hill-Langmuir equation can be expressed with equation (2):

$$log\left(\frac{\theta}{1-\theta}\right) = n_H log[\boldsymbol{G1}] - log(K_a) \qquad (2)$$

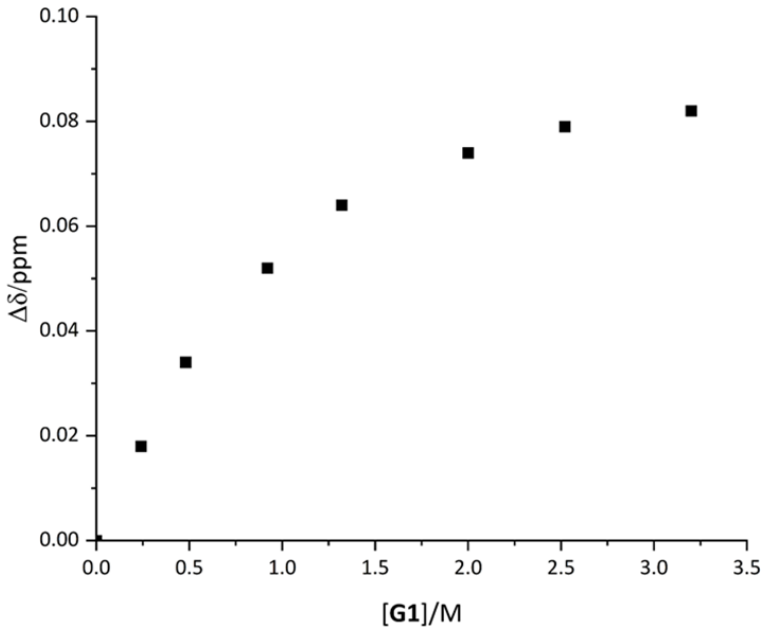

*Figure S68: Binding curve based on the chemical shift of proton **a²** of the ¹H NMR titration series of cage **2** with **G1**.*

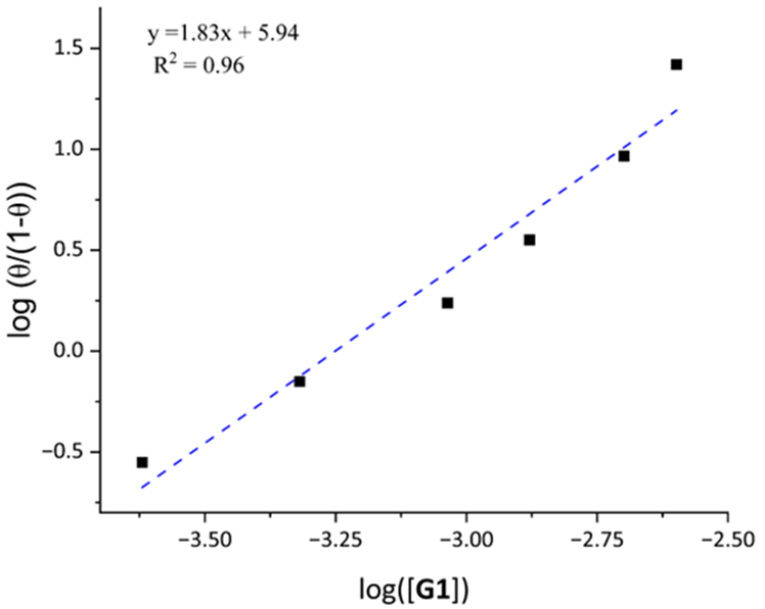

*Figure S69: Fit based on the Hill equation of ¹H NMR titration of cage **2** with **G1**. Chemical shifts of proton **a²** were considered for constructing of the graph.*

Based on the fitting of the Scatchard plot, the obtained values for the Hill coefficient (n_H) and binding constant (K_a) are:

- n_H = 1.83
- K_a = 1.77 x 10^3 M^{-1}

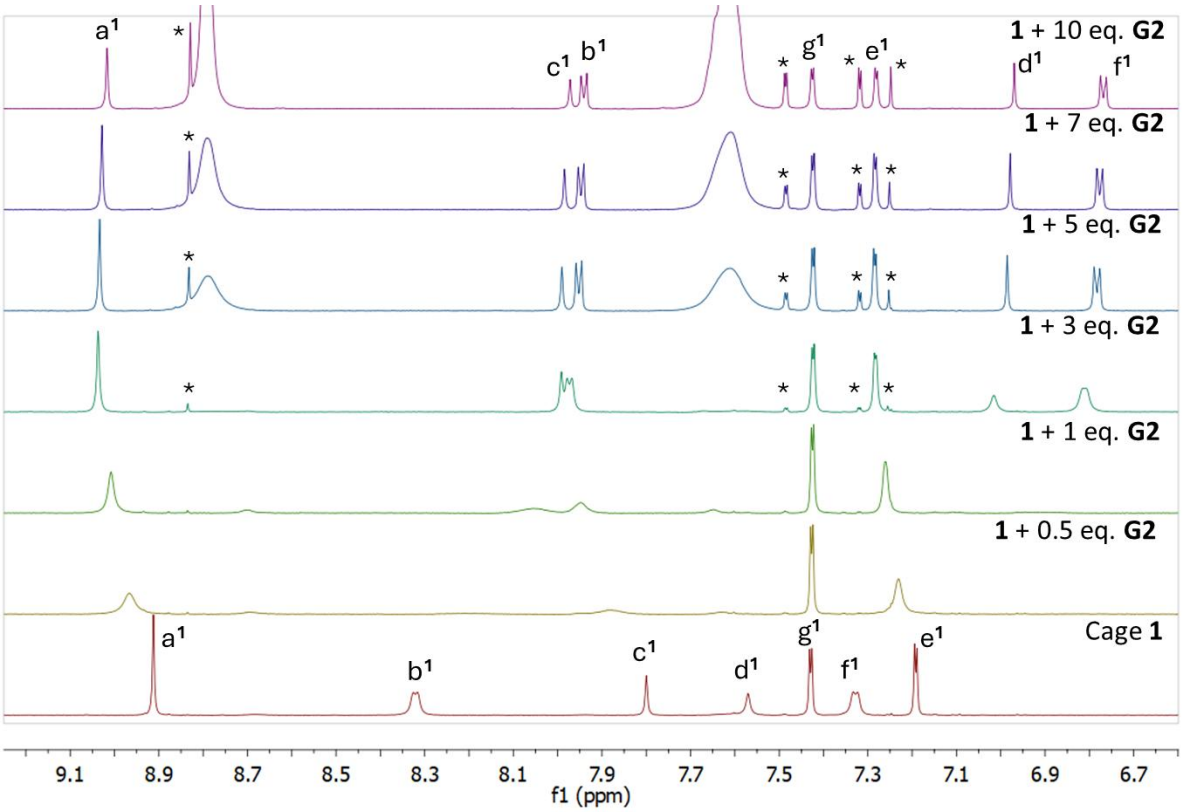

*Figure S70: Stack plot showing changes in the ^{1}H NMR spectrum upon the addition of guest **G2** in a stock solution of cage **1**. Focus on aromatic area.*

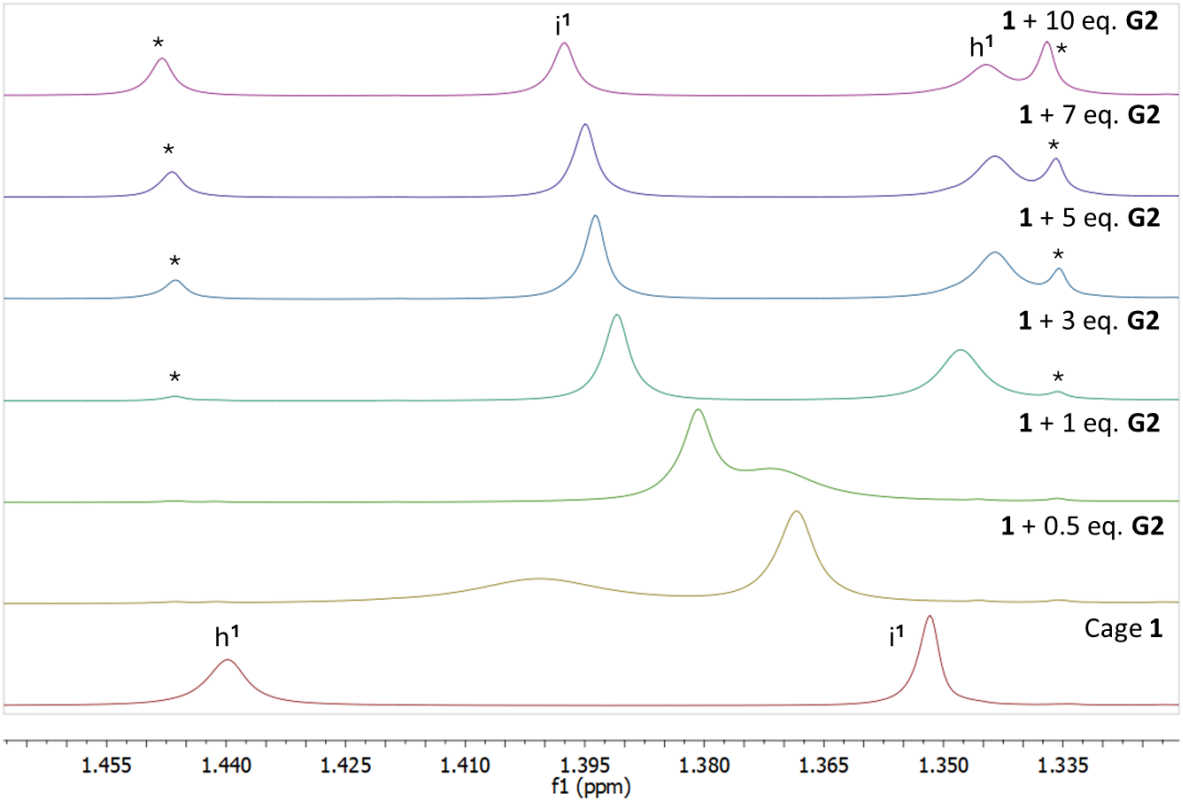

*Figure S71: Stack plot showing changes in the ^{1}H NMR spectrum upon the addition of guest **G2** in a stock solution of cage **1**. Focus on aliphatic area.*

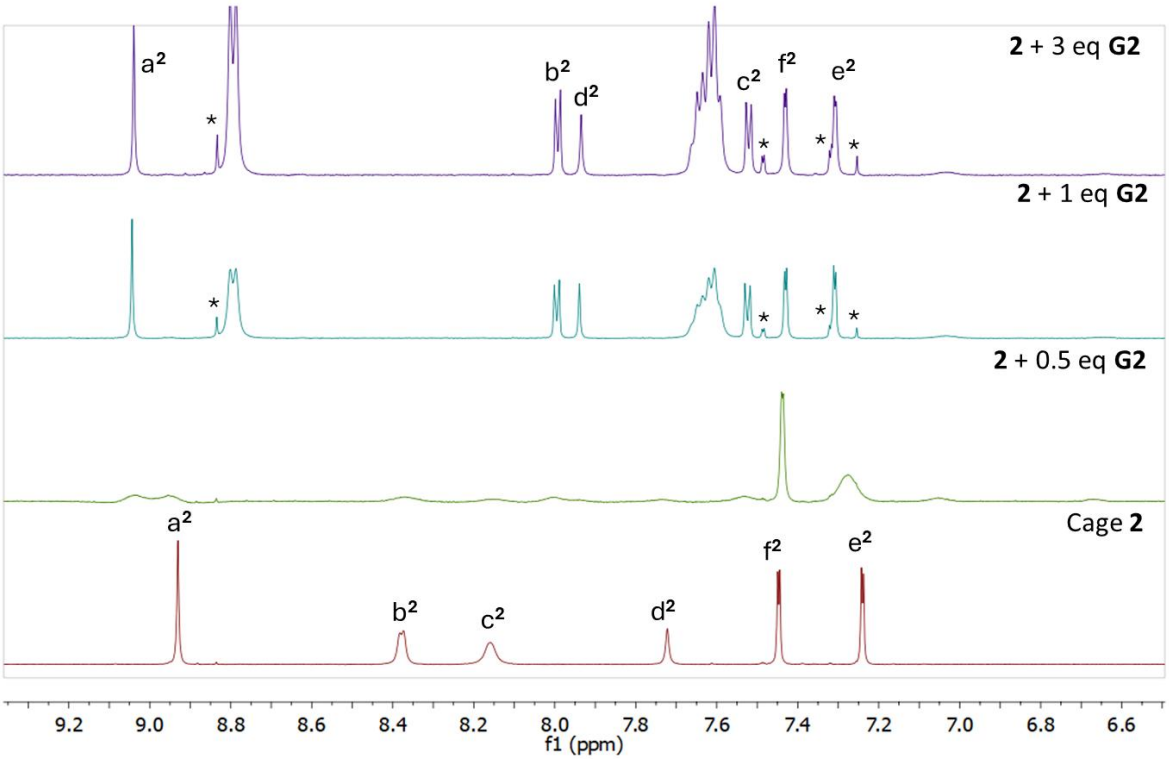

*Figure S72: Stack plot showing changes in the ^{1}H NMR spectrum upon the addition of guest **G2** in a stock solution of cage **2**. Focus on aromatic area.*

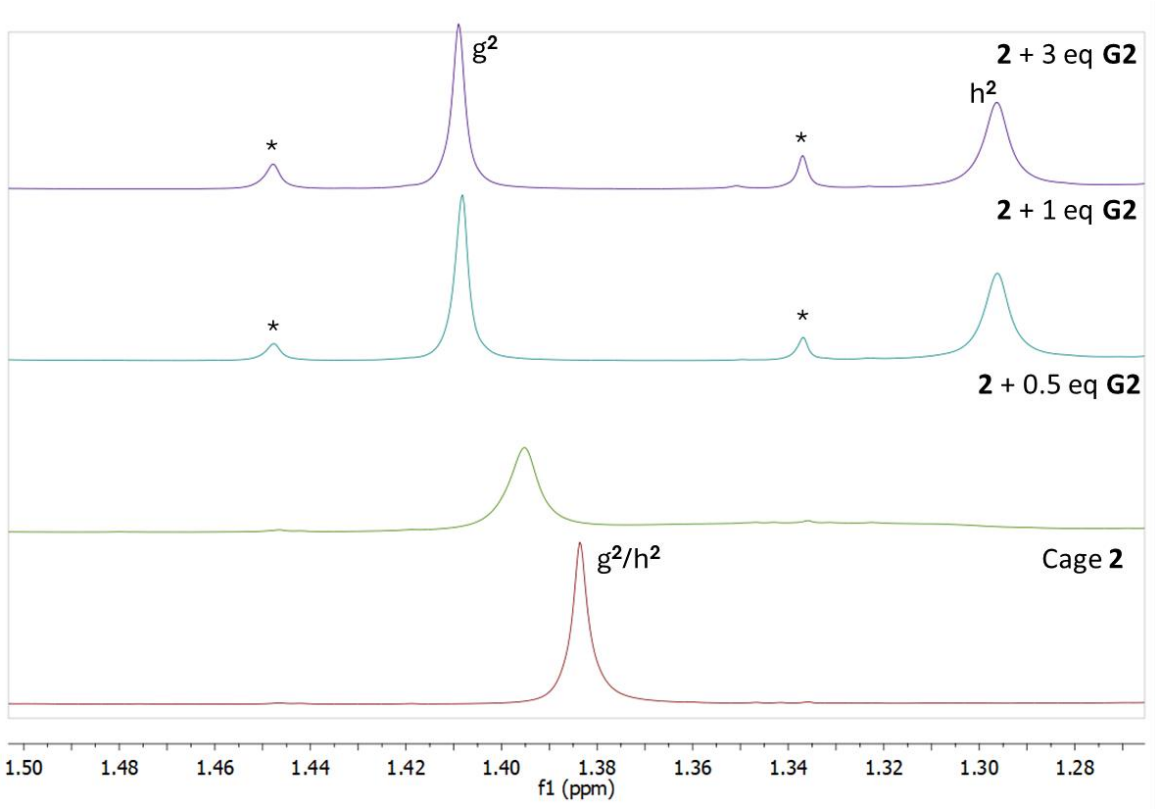

*Figure S73: Stack plot showing changes in the ^{1}H NMR spectrum upon the addition of guest **G2** in a stock solution of cage **2**. Focus on aliphatic area.*

8. References

1 D. H. Wu, A. D. Chen and C. S. Johnson, *J. Magn. Reson. A*, 1995, **115**, 260–264.
2 A. Jerschow and N. Müller, *J. Magn. Reson.*, 1997, **125**, 372–375.
3 E. O. Stejskal and J. E. Tanner, *J. Chem. Phys.*, 1965, **42**, 288–292.
4 G. M. Sheldrick, *Acta Crystallogr. Sect. Found. Adv.*, 2015, **71**, 3–8.
5 G. M. Sheldrick, *Acta Crystallogr. A*, 2008, **64**, 112–122.
6 A. W. Kleij, M. Kuil, D. M. Tooke, M. Lutz, A. L. Spek and J. N. H. Reek, *Chem. Eur. J.*, 2005, **11**, 4743–4750.
7 J. B. Maglic and R. Lavendomme, *J. Appl. Crystallogr.*, 2022, **55**, 1033–1044.
8 S. Mecozzi and J. Rebek Jr., *Chem. Eur. J.*, 1998, **4**, 1016–1022.